Dynamics of a 2D Bose-Einstein Condensate With an Impurity

Jonas Rønning

Thesis submitted for the degree of
Master of Science in Theoretical Physics

Institute of Physics
University of Oslo

15/05/2020

Abstract

In this project we have studied the hydrodynamic forces that are acting on a small impurity submerged into a two-dimensional Bose-Einstein condensate at finite temperature. The condensate is modeled by the damped Gross-Pitaevskii equation which we have coupled to a repulsive Gaussian potential to model the interaction with the impurity. We have considered a weakly coupled impurity in an untrapped condensate. The perturbations away from the condensates ground-state, both the ones caused by the particle and those that are not, are assumed to be small. We therefore use linear perturbation analysis to find expressions for the hydrodynamic forces and compare these expressions to the classical Maxey-Riley equation. We find that the force caused by the perturbations that were in the fluid in the absence of the particle are proportional to the local condensate acceleration. This is analogous to the inertial term in the Maxey-Riley equation. The force due to the perturbations that were caused by the impurity takes, for slowly moving impurities in the steady-state, the form of the Stokes' drag. The obtained expressions are then compared to numerical simulations.

Acknowledgments

I must first thank my supervisor Associate Professor Luiza Angheluta for guiding me through the project with great knowledge and an infectious enthusiasm. I have truly enjoyed working with her and feel like I have learned a lot during the process. I would also thank Dr. Audun Skaugen, Prof. Emilio Hernández-García and Prof. Cristóbal López for great discussions and insight. I also want to thank John Kristian Aasen for lending me his server. Finally I would like to thank my friends, family and chair for their great support.

Contents

List of Figures

Chapter 1

Introduction

One thing that characterises the fluids we are interacting with on a daily basis is that they have some resistance to flow due to internal friction between fluid layers. This is the fluids viscosity [1]. This is the property we normally think about as the fluids thickness, where thicker fluids like honey have higher viscosity than thin fluids like water [2]. In some exotic fluids there are no internal friction. These fluids are called superfluids. Some examples of superfluids are helium below 2.17K, cold dilute alkali gasses, polariton condensates and dilute solutions of bacteria [3, 4, 5, 6, 7, 8]. Of these the first three experience superfluidity due to quantum effects, while the solution of bacteria experience superfluidity due to the colective motion of the bacteria. Superfluids exhibit many fasinating properties like dissipationless flow, quantized vortices and the fountain effect [3, 9]. The property of dissipationless flow makes it possible for the fluid to maintain persistence flows, and it results in a vanishing drag force.

Superfluidity was first discovered in liquid helium in 1938 by P. Kapitza [10, 3], when he measured that the viscosity of liquid helium dropped by a factor of at least 1500 when cooled below 2.17K. This is called the λ-point, because the curve for specific heat is shaped like the letter λ at the transition temperature. He suggested that the helium below the λ-point entered a new state with vanishing viscosity that he called a superfluid in analogy to superconduction. A phenomenological description, and the link between superfluidity and the quantum properties of helium was established by L. Landau in the 1940s[3]. The model he developed separates the helium into a superfluid and a normal fluid component. Where the normal fluids and the superfluids velocity fields are independent and described by hydrodynamic equations. This is called the two fluid model, and it gives a good description of the superfluidity of liquid helium.

To describe the superfluidity in dilute alkali gasses one uses that they undergo Bose-Einstein condensation at sufficiently low temperatures [11]. A Bose-Einstein condensate is a phase that emerge in Bose fluids when the thermal wavelength of the particles starts to overlap, making the quantum mechanical properties of the particles important [12]. One can describe the condensate at zero temperature by the Gross-Pitaevskii equation [13], which was derived independently by Gross and Pitaevskii in the 1960s[14, 15]. This is a mean-field equation describing the collective wavefunction of the atoms that

are in the ground-state. The Gross-Pitaevskii equation can be modified to describe the condensate at finite temperature by adding noise and damping terms [16, 17, 18], or only a damping term. The equation we get when adding the damping term is called the damped Gross-Pitaevskii equation. It can also be modified to describe polariton condensates by adding pumping and damping terms [6].

There have been many studies on the interactions between Bose-Einstein condensates and impurities. Experimentally one have among others studied how a polariton condensate interact with a defect in the non-linear media, the effect of stirring a condensate of dilute alkali atoms with lasers, and the effect of putting different types of particles like neutral atoms, ions or electrons into the condensate [19, 20, 21, 22, 23]. There are many ways of modeling this systems that are suited for answering different types of questions. One approach that is suitable for studying the effect of an obstacle on the superfluid flow is to model the condensate with the Gross-Pitaevskii equation and add the condition that the density vanishes on the impurity's boundary [24]. This approach is however not fit for finding the coupled impurity-condensate dynamics, and the boundary conditions introduces non-linearities that can't be dealt with analytically. An approach that can be used for finding the impurity-condensate dynamics is to model the interaction with the impurity as condensate particles scattering on a potential [25, 26, 27, 28, 29]. The forces on the particle is then found by applying the Erhenfest theorem [30]. This model have been used to study the forces in the steady state limit in condensates at zero temperature described by the Gross-Pitaevski equation [25, 26, 31], and in driven non-equilibrium condensates [27]. These studies have mostly been concerned on the criteria for superfluidity in a condensate that is stirred by an impurity at constant velocity in the steady-state. For the condensates at zero temperature one gets that the drag force vanish if the relative velocity between the condensate and the impurity is below a critical velocity. Above the critical velocity the forces are non-zero, but bear little resemblance with the classical Stokes' drag.

In this thesis we are studying the interaction between a Bose-Einstein condensate of weakly interacting particles and an impurity at finite temperature. We want to see if the forces that are acting on the impurity bear any resemblance with the classical hydrodynamic forces that are acting on a sphere placed in a classical fluid. We use the damped Gross-Pitaevskii equation to model the condensate at finite temperature and couple it to a repulsive Gaussian potential to model the interaction with the impurity. We consider weakly coupled impurities and uses perturbation theory to find analytical expressions for the forces. The expressions are then simplified to find in what limit they look similar to the analog classical equations. We then test these equations by numerically integrating the damped Gross-Pitaevskii equation coupled to the impurity and calculate the force given by Ehrenfest's theorem. The resulting forces are compared with the forces given by the analytical expressions we found.

The outline of the thesis is as follows. In chapter 2 we discuss the concept of Bose-Einstein condensation. We derive the Gross-Pitaevskii equation and use it to find and motivate some of the properties of the condensate. In chapter 3 we discuss the criteria for superfluidity following the arguments of Landau. We then use this criteria to show that a weakly interacting Bose-Einstein condensate at zero temperature is a superfluid.

We also find the dispersion relation for the condensate and look at the effects that finite temperatures have on the exitations in the condensate. We then turn our attention to the equations of motion for a small particle submerged in a classical incompresible fluid in chapter 4, and look at simplifications of it. Chapter 5 deals with a condensate that is stirred by an impurity at zero temperature. We find the drag force on the impurity and use it to find the heating of the condensate. We also discuss qualitatively the wave pattern that is created by the particle. In chapter 6 we present the numerical setup and the methods that are used to test the theoretical predictions we make in chapter 7. Chapter 7 contains the main results obtained during this project. It starts with the derivation of analytical expressions for the forces that are acting on the particle. The obtained equations are then compared with the classical forces that where presented in chapter 4. We then compare the expressions with numerical simulations. The thesis is concluded in chapter 8 and we present an outlook for further studies. As a result of this project there was written a paper that is submitted in ref. [32]. The latest submitted version(per 15/05) of this paper is attached in the appendix.

Chapter 2

Bose-Einstein Condensaton

In this chapter we discus the concept of Bose-Einstein condensation within the framework of the mean-field approximation. In section 2.1 we start by defining the Bose-Einstein distribution and shows how it leads to a condensation in momentum space for an ideal Bose gas. In section 2.2 we discus condensation of interacting bosons in 2D. We then derive the Gross-Pitaevskii equation in section 2.3 and in the following sections we use it to define concepts that are useful when discussing the condensate, and extend it to describe a condensate at finite temperature.

2.1 Condensation of an Ideal Bose Gas

An ideal Bose gas is a gas of non-interacting bosons. The characteristic property of bosons is that multiple particles can occupy the same quantum state simultaneously. The occupation of a single particle state is given by the Bose-Einstein distribution [11]

$$f_{BE}(\epsilon) = \frac{1}{e^{\beta(\epsilon-\mu)} - 1}. \tag{2.1}$$

Where ϵ is the energy of the state, μ is the chemical potential and $\beta = \frac{1}{k_B T}$ where k_B is the Boltzmann constant. The ideal Bose gas undergo a phase transition when cooled below a critical temperature T_c, creating a Bose-Einstein condensate (BEC). The transition happens when a macroscopic number of particles are occupying the single particle ground state. What is interesting with this phase transition is that it is not caused by the particles interactions(obviously its a non-interacting gas), but by their statistics.

The particle density of an ideal Bose gas in the thermodynamic limit, N and V goes to infinity while the ratio stays fixed, is given by the Bose-Einstein distribution as [11, 33]

$$\rho = \frac{1}{V}\frac{1}{e^{-\beta\mu} - 1} + \int_0^\infty \frac{g(\epsilon)}{e^{\beta(\epsilon-\mu)} - 1}. \tag{2.2}$$

Where

$$g(\epsilon) = \frac{m^{3/2}}{\sqrt{2}\pi^2\hbar^3}\epsilon^{1/2} \tag{2.3}$$

is the density of states in three dimensions. The first term in eq. (2.2) is the density in the $\epsilon = 0$ state, while the second is the density in the exited states. One have to consider the ground state separately before taking the continuum limit, because it will not be counted in the integral. Since $V \to \infty$ the density of the ground state is zero unless the occupation diverges, i.e becomes macroscopic. One can carry out the integration in eq. (2.2) and get that the density of the exited states is [11, 33]

$$\rho_{ex} = \left(\frac{mk_BT}{2\pi\hbar^2}\right)^{3/2} g_{3/2}(z). \tag{2.4}$$

We have here introduced the fugacity $z = e^{\beta\mu}$, and the polylogathrimic function

$$g_{3/2}(z) = \sum_{p=1}^{\infty} \frac{z^p}{p^{3/2}}. \tag{2.5}$$

The series in eq. (2.5) converges if $|z| < 1$ and diverges for $|z| > 1$. When $z = 1$ the series converge, but have an infinite derivative. We see that the function $g_{3/2}(z)$ is increasing for $z > 0$. This means that there is a maximal particle density in the exited states given by

$$\rho_{ex}^{max} = \left(\frac{mk_BT}{2\pi\hbar^2}\right)^{3/2} g_{3/2}(1) \approx 2.612\lambda^{-3}. \tag{2.6}$$

Where λ is the thermal de Broglie wavelength. Since this function is proportional to $T^{3/2}$ with no constant term we can for any non zero density ρ lower the temperature so that $\rho > \rho_{ex}^{max}$. The remaining density have to be the ground state density. Since we are considering the thermodynamic limit this means that the ground state occupation number diverges. At zero temperature the maximal occupation of the exited states vanish. This means that all particles are in the ground-state. The critical temperature is given as the temperature where the ground state gets a macroscopic occupation, i.e when $\rho_c = 2.612\lambda^{-3}$. This means that the quantum statistics becomes important when the wavelengths of the particles starts to overlap. The explicit expression for the critical temperature is

$$T_c = \frac{2\pi\hbar^2}{k_B m}\left(\frac{\rho}{2.612}\right)^{2/3}. \tag{2.7}$$

The first BEC was realised in liquid helium in the 1930s when it was cooled below 2.17K [11]. The condensation of the liquid helium is however not a good test of the model described above, since the interactions between the helium atoms in the fluid are not weak. The first example of a condensate of weakly interacting particles was not realised before 1995, in trapped gasses of alkali metals [4, 5]. Figure 2.1 shows the velocity distribution of a dilute gas of rubidium right before and after it condense. The temperature is decreasing to the right in the figure. To the left we see the thermal cloud right before the gas condenses. When the temperature decreases a spike is forming. This spike is the atoms that are almost stationary, indicating a macroscopic occupation of the ground-state. Reducing the temperature further almost all of the atoms are in the ground-state with only a small occupation of the exited states.

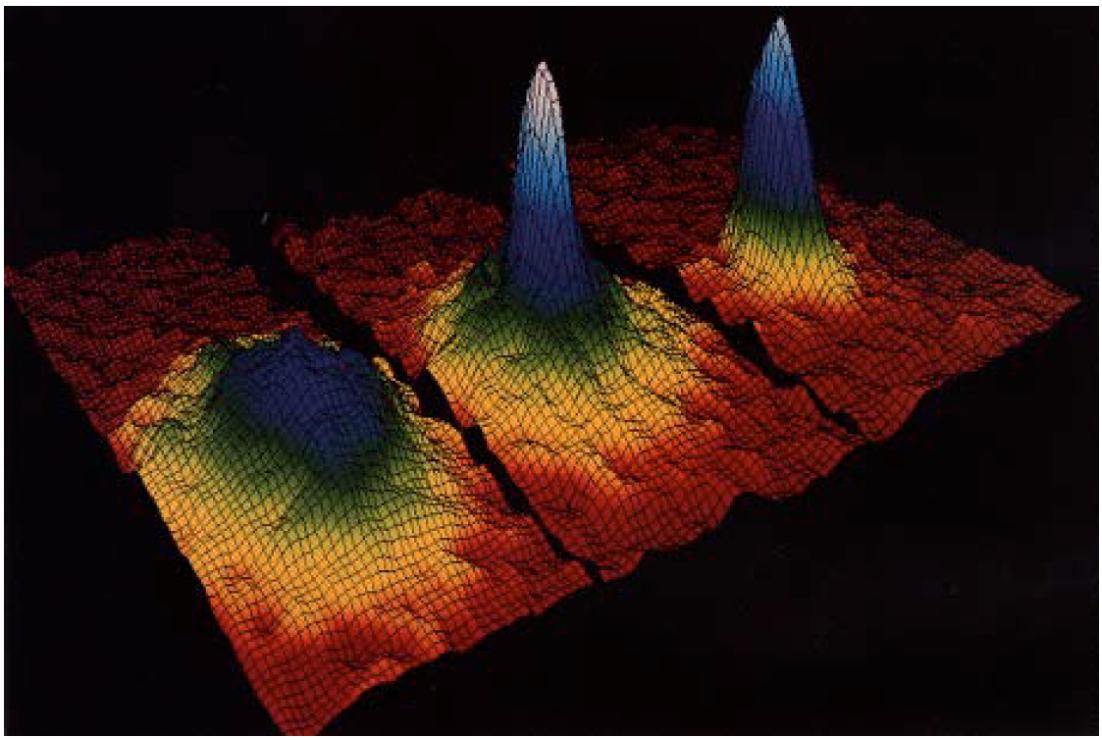

Figure 2.1: Velocity distribution of a trapped dilute alkali gas. To the left we see the distribution right before the appearance of the condensate. In the middle we see the gas when the condensate appears. We can see the coexistence of the thermal cloud and the condensate. On the right we have the condensate at lower temperatures, where the thermal cloud is almost gone. Figure from [34] with data from [4].

2.2 2D Interacting Bose-Einstein Condensate

Above we showed that the formation of a three dimensional BEC in a weakly interacting Bose gas is due to the particles statistics and not their interactions. In two dimensions the picture is different. An untrapped weakly interacting two dimensional Bose gas is a true condensate at $T = 0$, but any non-zero temperature will destroy it [35]. Even if there is no true condensate in two dimensions one have a transition to a quasicondensate state below a critical temperature T_{BKT}. This is called the Berezinkii-Kosterlitz-Thouless(BKT) transition [36].

The quasicondensate state is a condensate with fluctuating phase [37, 38]. There is a formation of local condensates in the system that can be described by local wavefunctions. Above the transition temperature the correlation of the phases of the local wavefunctions is exponentially decaying with distance, while below there is a power law decay. Since the correlation of the phases in the quasicondensate is decaying it is not possible to describe the whole system with one wavefunction. However since the decay is slow there exist a scale R_c so that if we are considering a cell of size $L << R_c$ we can

treat it as a true condensate and describe it with one wavefunction [37]. There is also a smallest scale the correlation length ξ, which is the typical length scale of distortion in the condensate.

The mechanism behind this change in the long range behaviour of the condensate at the critical temperature is due to the behaviour of the vortices in the condensate [38, 39]. As will be discussed in section 2.9 vortices are phase defects that caries the circulation of the BEC [40]. They are characterised by having zero density at their core and carry a continuous phase rotation of $2\pi n$ around it. The most relevant vortices are the single charged ones $n = \pm 1$, since the others are unstable and will split up into single charged ones [39]. In the condensate one can observe two forms of vortices, free vortices and bound vortex-antivortex pairs. This two forms have different effects on the coherence of the condensate. The vortex-antivortex pairs cancel each other and have little effect on the phase of the condensate, while the free vortices ruins the phase coherence. The BKT transition happens because the free vortices can only be found above the critical temperature. Below the transition temperature we have only vortex-antivortex pairs, such that the only contribution to the decay in the coherence is due to the thermally exited phonons [39].

2.3 The Gross-Pitaevskii Equation

The second quantized Hamiltonian describing a dilute Bose gas is given by [13]

$$H = \int d^3\mathbf{r}\big[-\frac{\hbar^2}{2m}\hat{\Psi}^\dagger(\mathbf{r})\nabla^2\hat{\Psi}(\mathbf{r})+\hat{\Psi}^\dagger(\mathbf{r})\mathcal{U}(\mathbf{r})\hat{\Psi}(\mathbf{r})+\frac{1}{2}\int d^3\mathbf{r}'\hat{\Psi}^\dagger(\mathbf{r})\Psi^\dagger(\mathbf{r}')\mathcal{U}_{int}(\mathbf{r}-\mathbf{r}')\hat{\Psi}(\mathbf{r}')\hat{\Psi}(\mathbf{r})\big] \tag{2.8}$$

Here $\hat{\Psi}(\mathbf{r})$ and $\hat{\Psi}^\dagger(\mathbf{r})$ are the annihilation and creation operators for particles at position $\mathbf{r}$. They can be written as $\hat{\Psi}(\mathbf{r}) = \sum_\alpha \Psi_\alpha(\mathbf{r})\hat{a}_\alpha$, where $\Psi_\alpha(\mathbf{r})$ is a single-particle wavefunction and $\hat{a}_\alpha$ is the annihilation operator for the single-particle α state. $\mathcal{U}(\mathbf{r})$ is an external potential, and $\mathcal{U}_{int}(\mathbf{r}-\mathbf{r}')$ is an interacting potential. For a dilute gas one approximate the interaction as point particle collisions and set the effective interaction potential as $\mathcal{U}_{int}(\mathbf{r}-\mathbf{r}') = g\delta(\mathbf{r}-\mathbf{r}')$. Where $g = \frac{4\pi\hbar^2 a_s}{m}$ and a_s is the s-wave scattering length [13]. The Hamiltonian then becomes

$$H = \int d^3\mathbf{r}\big[-\frac{\hbar^2}{2m}\hat{\Psi}^\dagger(\mathbf{r})\nabla^2\hat{\Psi}(\mathbf{r}) + \hat{\Psi}^\dagger(\mathbf{r})\mathcal{U}(\mathbf{r})\hat{\Psi}(\mathbf{r}) + \frac{1}{2}g\hat{\Psi}^\dagger(\mathbf{r})\hat{\Psi}^\dagger(\mathbf{r})\hat{\Psi}(\mathbf{r})\hat{\Psi}(\mathbf{r})\big]. \tag{2.9}$$

We find the time evolution of $\hat{\Psi}$ by using the Heisenberg equation

$$i\hbar\partial_t\hat{\Psi} = [\hat{\Psi}, H]. \tag{2.10}$$

Using that $[\hat{\Psi}(\mathbf{r}), \hat{\Psi}^\dagger(\mathbf{r}')] = \delta(\mathbf{r}-\mathbf{r}')$, and $\big[\hat{\Psi}, \nabla^2\hat{\Psi}\big] = 0$ the time dependence of the field becomes

$$i\hbar\partial_t\hat{\Psi}(\mathbf{r}) = -\frac{\hbar^2}{2m}\nabla^2\hat{\Psi}(\mathbf{r}) + \mathcal{U}(\mathbf{r})\hat{\Psi}(\mathbf{r}) + g\hat{\Psi}^\dagger(\mathbf{r})\hat{\Psi}(\mathbf{r})\hat{\Psi}(\mathbf{r}). \tag{2.11}$$

We then decomposes the operator as $\hat{\Psi} = \hat{\psi} + \hat{\phi}$. Here $\hat{\psi}$ is the annihilation operator for the ground state and $\hat{\phi}$ is for the exited states. As discussed above a BEC is formed when the occupation of the ground state N_0 becomes macroscopic. This means that the fraction of particles in the ground state $\frac{N_0}{N}$ is finite even in the thermodynamic limit when $N \to \infty$. Since the fraction is finite we must have that $N_0 \to \infty$, meaning that the states with occupation number N_0 and $N_0 \pm 1$ is the same physical configuration. We can therefore treat $\hat{a}_0$ and $\hat{a}_0^\dagger$ as complex numbers, and $\hat{\psi}$ becomes a classical field. If the occupation of the exited states is low, e.g at zero temperature, we can neglect the $\hat{\phi}$ and get

$$i\hbar\partial_t\psi(\mathbf{r}) = -\frac{\hbar^2}{2m}\nabla^2\psi(\mathbf{r}) + \mathcal{U}(\mathbf{r})\psi(\mathbf{r}) + g|\psi(\mathbf{r})|^2\psi(\mathbf{r}). \tag{2.12}$$

This is the Gross-Pitaevskii equation(GPE). It can also be obtained by using a variation procedure [13]

$$i\hbar\partial_t\psi = \frac{\delta H}{\delta\psi^*}. \tag{2.13}$$

Here H is the Hamiltonian for the classical field

$$H = \int d^3\mathbf{r}\left[\frac{\hbar^2}{2m}|\nabla\psi|^2 + \mathcal{U}|\psi|^2 + \frac{g}{2}|\psi|^4\right]. \tag{2.14}$$

It is common to transform the GPE to the comoving frame $\psi \to \psi e^{-i\frac{\mu}{\hbar}t}$, since the ground state oscillates with the chemical potential $\mu = \frac{\partial E}{\partial N}$ [13]. This gives an extra $-\mu\psi$ on the right, such that the GPE becomes

$$i\hbar\partial_t\psi(\mathbf{r}) = -\frac{\hbar^2}{2m}\nabla^2\psi(\mathbf{r}) + [\mathcal{U}(\mathbf{r}) - \mu + g|\psi(\mathbf{r})|^2]\psi(\mathbf{r}). \tag{2.15}$$

As for eq. (2.12) we can obtain this equation by a variation principle [13, 41]

$$i\hbar\partial_t\psi = \frac{\delta\mathcal{H}}{\delta\psi^*}. \tag{2.16}$$

With $\mathcal{H} = H - \mu N_0$ as the Hamiltonian. It is given by

$$\mathcal{H} = \int d^3\mathbf{r}\left[\frac{\hbar^2}{2m}|\nabla\psi|^2 + \mathcal{U}|\psi|^2 + \frac{\mu^2}{2g}(\frac{g}{\mu}|\psi|^2 - 1)^2\right]. \tag{2.17}$$

Where we have completed the square for $\frac{g}{2}|\psi|^4 - \mu|\psi|^2$ and ignored a constant energy term[41]. This Hamiltonian will conserve energy as long as the potential is time independent. We can see this by taking the time derivative, which gives [41]

$$\begin{aligned}\partial_t\mathcal{H} &= \int d^3\mathbf{r}\left(\frac{\delta\mathcal{H}}{\delta\psi}\partial_t\psi + \frac{\delta\mathcal{H}}{\delta\psi^*}\partial_t\psi^* + \frac{\delta\mathcal{H}}{\delta\mathcal{U}}\partial_t\mathcal{U}\right) \\ &= \int d^3\mathbf{r}\left(\frac{\delta\mathcal{H}}{\delta\psi}\frac{1}{i\hbar}\frac{\delta\mathcal{H}}{\delta\psi^*} - \frac{\delta\mathcal{H}}{\delta\psi^*}\frac{1}{i\hbar}\frac{\delta\mathcal{H}}{\delta\psi} + \frac{\delta\mathcal{H}}{\delta\mathcal{U}}\partial_t\mathcal{U}\right) = \int|\psi|^2\partial_t\mathcal{U}d^3\mathbf{r}.\end{aligned} \tag{2.18}$$

And it is clear that if we have a time independent potential the energy is conserved.

2.4 The Thomas-Fermi Ground State

When working with the BEC it is convenient to know what the ground state of the system is. We will use it as a starting point for perturbation theories when studying the condensate analytically, and when doing numerics we will use it to find an initial wavefunction. We can find the ground state of the GPE by looking at stationary solutions to eq. (2.15) [40]. In the steady-state the equation takes the form

$$\mu\psi = \left[-\frac{\hbar^2}{2m}\nabla^2 + \mathcal{U} + g|\psi|^2\right]\psi. \tag{2.19}$$

This is the time-independent Gross-Pitaevskii equation. If we set $g = 0$ this becomes the time-independent Schrödinger equation, with the energy replaced by the chemical potential. When considering non-zero interactions between the bosons this equation becomes non-linear and hard to solve analytically. We can make it simpler by considering a large number of particles in a nearly uniform condensate with repulsive interactions ($g > 0$). In this case the particles are pressed towards the edge of the condensate [40, 13], making it flat and increasing its radius. The density fare from the edge is then slowly varying, so that the kinetic energy of the ground state is small compared to the interaction energy and it can be neglected. This is the Thomas-Fermi approximation. The wavefunction in this approximation is

$$|\psi_{TF}|^2 = \frac{\mu - \mathcal{U}}{g} \tag{2.20}$$

when $\mu > \mathcal{U}$ and zero else. If we have a spherical harmonic magnetic trap $\mathcal{U} = \frac{1}{2}m\omega_{ho}^2 r^2$ we find that the size of the condensate is given by the Thomas-Fermi radius

$$R_{TF}^2 = \frac{2\mu}{m\omega_{ho}^2}. \tag{2.21}$$

Rewriting the ground state in terms of this we get

$$|\psi_{TF}|^2 = \frac{\mu}{g}\left(1 - \frac{r^2}{R_{TF}^2}\right). \tag{2.22}$$

We can see from this that the Thomas-Fermi approximation breaks down near the edges of the condensate due to large variations when r comes close to R_{TF}.

2.5 Reduction of Dimensionality

The effective dimension of the BEC can be controlled by adjusting the trapping potential. We can see this by considering a condensate that is trapped in a pancake formed harmonic oscillator potential

$$\mathcal{U}(\mathbf{r}) = \frac{1}{2}m(\omega_r^2(x^2 + y^2) + \omega_z^2 z^2). \tag{2.23}$$

The GPE eq. (2.15) can then be reduced to an effective two dimensional equation[40] by making sure that the frequency ratio ω_r/ω_z and the harmonic oscillator length $a_{ho,z} \equiv \sqrt{\hbar/(m\omega_z)}$ are sufficiently small. Under this assumptions we can decompose the wavefunction in a component in the xy-plane and the axial component. We are therefore looking for solutions of the form

$$\psi(\mathbf{r}, t) = \psi(x, y, t)\phi(z). \tag{2.24}$$

The axial component $\phi(z)$ is because of the tight confinement approximately given as the wavefunction for a harmonic oscillator and it satisfy the equation

$$\frac{\hbar^2}{2m}\partial_z^2\phi(z) - \frac{1}{2}m\omega_z^2 z^2\phi(z) + \mu\phi(z) = 0. \tag{2.25}$$

Since the trapping frequency is so large the exited states are suppressed. The axial component is therfore the ground state wavefunction of the harmonic oscillator

$$\phi(z) = \pi^{-1/4}a_{ho,z}^{-1/2}e^{-(z^2/2a_{ho,z}^2)}. \tag{2.26}$$

Inserting this wavefunction into eq. (2.15) multiplying with ϕ^* and integrating out the axial dependence we get the two dimensional GPE given by

$$i\hbar\partial_t\psi(\mathbf{r}_{2D}) = -\frac{\hbar^2}{2m}\nabla_\perp^2\psi(\mathbf{r}_{2D}) + \big[\mathcal{U}_{2D}(\mathbf{r}_{2D}) - \mu + g_{2D}|\psi(\mathbf{r}_{2D})|^2\big]\psi(\mathbf{r}_{2D}). \tag{2.27}$$

Where $g_{2D} = g/(\sqrt{2\pi}a_{ho,z})$ is the effective 2D coupling constant, $r_{2D}^2 = x^2 + y^2$, $\mathcal{U}_{2D}(\mathbf{r}_{2D}) = \frac{1}{2}m\omega_r^2 r_{2D}^2$ and $\nabla_\perp^2 = \partial_x^2 + \partial_y^2$. We will drop the subscripts since we are mostly working in 2D. The exception is chapter 4 which is in three dimensions.

2.6 Dissipation

At finite temperature the ground state is not fully populated and there is some population in the exited states. The interaction between particles in the condensate and the exited states can be modeled by adding a dissipative term to the GPE [41]. This results in energy dissipation from the condensate into the exited states. The GPE then becomes the damped Gross-Pitaevskii equation (dGPE)

$$i\hbar\partial_t\psi(\mathbf{r}) = (1 - i\gamma)\big[-\frac{\hbar^2}{2m}\nabla^2\psi(\mathbf{r}) - \mu\psi + V(\mathbf{r})\psi(\mathbf{r}) + g|\psi(\mathbf{r})|^2\psi(\mathbf{r})\big]. \tag{2.28}$$

Where the dimensionless parameter γ is a function of temperature, chemical potential and the energy of the thermal cloud [17, 18]. It is typically very small, around 10^{-4} in typical experiments with rubidium. The dGPE can be derived from the stochastic Gross-Pitaevskii equation, which is obtained via a microscopic reservoir theory [17, 18]. In this theory one defines an energy cutoff ϵ_c. The particles with energy above the cutoff are treated as thermalized, while the particles below are the ones that are described by the condensate wavefunction. The interactions between the thermalized particles and

the atoms in the condensate creates damping and noise terms. We can neglect the noise at sufficiently low temperatures, leaving us with the dGPE[18].

One can see that the effect of the parameter γ is to remove energy from the condensate by considering the change in energy of the condensate, which is now given by [41]

$$\begin{aligned}\partial_t \mathcal{H} &= \int d^2\mathbf{r} \left(\frac{\delta \mathcal{H}}{\delta \psi} \partial_t \psi + \frac{\delta \mathcal{H}}{\delta \psi^*} \partial_t \psi^* + \frac{\delta \mathcal{H}}{\delta \mathcal{U}} \partial_t \mathcal{U} \right) \\ &= \int d^2\mathbf{r} \left(\frac{\delta \mathcal{H}}{\delta \psi} \frac{1-i\gamma}{i\hbar} \frac{\delta \mathcal{H}}{\delta \psi^*} - \frac{\delta \mathcal{H}}{\delta \psi^*} \frac{1+i\gamma}{i\hbar} \frac{\delta \mathcal{H}}{\delta \psi} + \frac{\delta \mathcal{H}}{\delta \mathcal{U}} \partial_t \mathcal{U} \right) = -\frac{2\gamma}{\hbar} \int d^2\mathbf{r} |\frac{\delta \mathcal{H}}{\delta \psi^*}|^2 + \int |\psi|^2 \partial_t \mathcal{U} d^2\mathbf{r}.\end{aligned} \tag{2.29}$$

Since the first term is negative its clear that the effect of it is to dissipate energy out of the system. If one have a time dependent potential one can balance out this effect by adding the same amount of energy that is dissipated.

2.7 Dimensionless Units

To make the analytical and numerical work easier we can introduce dimensionless units. As the unit for speed we use the speed of sound in the condensate $c^2 = \mu/m$, see section 3.2. As the unit for length we use the healing length $\xi = \hbar/mc = \hbar/\sqrt{m\mu}$. Which sets the length for typical distortions in the condensate. We can see this from the fact that a distortion over a distance ξ is accompanied by a rise in the kinetic energy of order $\hbar^2/m\xi^2$ [41]. This is allowed as long as the increase in the energy is not larger than the chemical potential. The unit for time is then given by $\tau = c/\xi = \hbar/\mu$. The unit for energy is the chemical potential μ. Rescaling the dGPE according to these units it becomes

$$i\partial_t \psi(\mathbf{r}) = (1-i\gamma)\big[-\frac{1}{2}\nabla^2\psi - \psi + V\psi + \frac{g}{\mu}|\psi|^2\psi \big]. \tag{2.30}$$

We rescale the wavefunction to $\psi \to \psi\sqrt{\mu/g}$. Note that $\sqrt{\mu/g}$ is the Thomas-Fermi ground state for an uniform condensate. Which is very convenient when considering perturbation theories. The dimensionless equation is then

$$\partial_t \psi(\mathbf{r}) = (i+\gamma)\big[\frac{1}{2}\nabla^2\psi + (1 - V - |\psi|^2)\psi \big]. \tag{2.31}$$

So that the only adjustable parameter is the thermal drag γ. As mentioned the size of this thermal drag is of order 10^{-4} in typical experiments, but we will consider drags of the size 10^{-2} to see its effect clearer. Note that there is an other convention for units that is commonly used, for example in [42], where the half in front of the Laplacian is removed.

2.8 Hydrodynamics

We want to show that the dGPE can be transformed into a hydrodynamical description of the condensate. To do this we first take the Madelung transform $\psi(\mathbf{r}) =$

$\sqrt{\rho(\mathbf{r})}e^{i\Phi(\mathbf{r})}$[41, 17]. Here $\rho = |\psi|^2$ is the particle density, while Φ is a complex phase. The current density of ρ is given by

$$\mathbf{J} = \frac{\hbar}{2mi}(\psi^*\nabla\psi - \psi\nabla\psi^*) = \frac{\hbar}{2mi}(\sqrt{\rho}\nabla\rho + \rho i\nabla\Phi - \sqrt{\rho}\nabla\rho + \rho i\nabla\Phi) = \frac{\hbar}{m}\rho\nabla\Phi = \rho\mathbf{v}. \tag{2.32}$$

We have here identified the superfluid velocity as $\mathbf{v} = \frac{\hbar}{m}\nabla\Phi$. Inserting the Madelung transformation into eq. (2.28) and multiplying with ψ^* we get the two equations

$$\partial_t\rho + \nabla\cdot(\rho\mathbf{v}) = \frac{2\gamma\rho}{\hbar}(\mu - \mathcal{U}_{eff}), \tag{2.33}$$

and

$$\hbar\partial_t\Phi = \mu - \mathcal{U}_{eff} + \frac{\hbar\gamma}{2\rho}\nabla\cdot(\rho\mathbf{v}). \tag{2.34}$$

From the real and the imaginary part. Notice that eq. (2.33) gives that the particle number is only conserved when $\mathcal{U}_{eff} = \mu$. This term is driving the condensate into particle number equilibrium with the thermal cloud [17]. The effective potential is given by

$$\mathcal{U}_{eff} = \frac{m\mathbf{v}^2}{2} + \mathcal{U} + g\rho - \frac{\hbar^2}{2m}\frac{\nabla^2\sqrt{\rho}}{\sqrt{\rho}}. \tag{2.35}$$

The last term in the effective potential is the quantum pressure. It is typically very small unless the density ρ is changing rapidly [41, 17]. If we now take the gradient of eq. (2.34) we get

$$\hbar\partial_t\nabla\Phi = -\nabla\frac{m\mathbf{v}^2}{2} - \nabla(\mathcal{U} + \rho g) + \frac{\hbar\gamma}{2}\nabla\frac{\nabla\cdot(\rho\mathbf{v})}{\rho} + \frac{\hbar^2}{2m}\nabla\frac{\nabla^2\sqrt{\rho}}{\sqrt{\rho}}. \tag{2.36}$$

Using the product rule on the second to last term and assuming that we are far away from vortices so that we can neglect terms that includes the curl of the velocity this equation becomes

$$\partial_t\mathbf{v} + \mathbf{v}\cdot\nabla\mathbf{v} = -\frac{1}{m}\nabla(\mathcal{U} + g\rho) + \frac{\hbar\gamma}{2m}\nabla^2\mathbf{v} + \frac{\hbar^2}{2m^2}\nabla\frac{\nabla^2\sqrt{\rho}}{\sqrt{\rho}} + \frac{\hbar\gamma}{2m}\nabla(\nabla(\ln\rho)\cdot\mathbf{v}). \tag{2.37}$$

Assuming that the condensate is slowly varying we can remove the two last terms and get

$$\partial_t\mathbf{v} + \mathbf{v}\cdot\nabla\mathbf{v} = -\frac{1}{m}\nabla(\mathcal{U} + g\rho) + \frac{\hbar\gamma}{2m}\nabla^2\mathbf{v}. \tag{2.38}$$

This is a quantum Navier-Stokes equation where $(\mathcal{U} + g\rho)$ is the pressure term and the dynamical viscosity is given by $\nu_q = \frac{\hbar\gamma}{2m}$ or $\nu_q = \frac{\gamma}{2}$ in the dimensionless units [17]. It is clear that under these assumptions the condensate behave as an inviscid fluid at $T = 0$, and follows a quantum Euler equation. It is in other words a superfluid, we will discuss this in more dept in the next chapter. The finite viscosity at $T > 0$ is caused by the interaction between the thermal cloud and the condensate. We are therefore sometime referring to γ as the thermal drag or the thermal viscosity.

2.9 Vortices

As mentioned in section 2.2 the vortices in a BEC are phase defects that carries the circulation. Something that characterises the flow in a BEC is that the circulation is quantized. We can see this directly from the Madelung transformation. Since the wavefunction of the condensate is single valued the circulation around any closed curve C is given by

$$\Gamma = \oint_C \mathbf{v} \cdot d\mathbf{l} = \frac{\hbar}{m} \oint_C \nabla\Phi \cdot d\mathbf{l} = 2\pi \frac{\hbar}{m} n. \tag{2.39}$$

Where n is an integer, the circulation of the fluid is therefore quantized in units of $2\pi\frac{\hbar}{m}$ [40]. We now consider a condensate where the phase is continuous everywhere except at some point. We place a closed curve in the condensate and change it continuously without letting it pass through this point [42]. The circulation around the curve can then only change continuously because the phase is continuous. However the circulation is quantized so it has to be constant. If the circulation is non-zero and we deform the curve in this way until it becomes a point, then the gradient of the phase at that point has to be infinite [42]. This point with circulation $2\pi\hbar/m \cdot n$ and singular phase is a quantized vortex with charge n. Since the energy of the vortex should not be infinite the density has to vanish. The vortices therefore have a core with zero density. The size of the vortex core is characterised by the healing length [40]. Knowing that the circulation is due to point like defects we can find the velocity profile around one vortex from eq. (2.39) as

$$\mathbf{v} = n\frac{\hbar}{mr}\hat{\theta}. \tag{2.40}$$

Where $\hat{\theta}$ is the azimuthal unit vector and r is the distance from the vortex. We have here assumed azimuthal symmetry and that the net flux into the vortex is zero, i.e the vortex is neither a sink nor a source. An effect of the quantization of the circulation is that single charged vortices are stable. This is because the circulation around an isolated vortex can't gradually decrease. Vortices can be removed from the condensate by vortex-antivortex collisions, where two vortices with opposite charge annihilates each other.

Chapter 3

Superfluidity.

In this chapter we discus the superfluidity of a BEC. We start by discussing the criteria for superfluidity, and then we proceed to show that the BEC fulfils this criteria at zero temperature. We also find the dispersion relations for small exitations in the condensate.

3.1 Landau's Criteria for Superfluidity

A superfluid is characterised by its ability to flow without friction when flowing under a critical velocity. This behavior was first observed in liquid helium below 2.17K [3]. The superfluidity observed in helium is a quantum effect that is caused by the discretisation of excitations in the fluid. When a fluid flowing past an obstacle experience friction part of its kinetic energy is converted into thermal energy[3]. If the fluid heats up it means that it makes a transition into an exited state. Since the energy of the excited states are quantized we can't excite the fluid if the velocity is below a critical velocity, and therefore we get a frictionless flow. This is illustrated in figure 3.1 which shows the heating caused by a moving laser in a superfluid and a thermal gas.

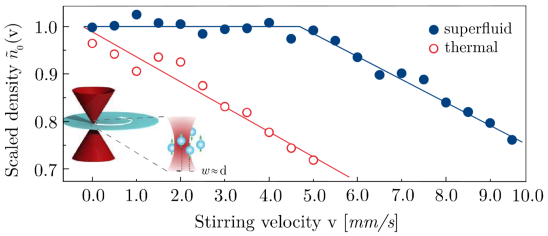

Figure 3.1: The figure shows the density of superfluid and a thermal gas after they have been stirred by a laser. A decrease in density indicates heating. For the superfluid (blue, whole) there is no heating below a critical speed, while the thermal cloud (red, hollow) experiences heating for any stirring velocity. The critical velocity of the superfluid can be found from a bilinear fit. Figure from [20].

When the fluid is heated to the lowest exited state an excitation is created. Consider

a fluid flowing past an obstacle with velocity $\mathbf{v}$, creating excitations. Let the energy and momentum of the excitation in the frame moving with the fluid be $\epsilon(p)$ and $\mathbf{p}$ respectively. The energy in the frame of the obstacle is then changed by[3]

$$\epsilon(p) + \mathbf{p} \cdot \mathbf{v}. \tag{3.1}$$

This change of energy have to be smaller than zero in order for the transition to be energetically favorable. We see that the second term is smallest when the momentum of the excitation is opposite of the flow velocity. The condition for creating an excitation is then

$$v > \frac{\epsilon(p)}{p}. \tag{3.2}$$

It is sufficiently that this condition is fulfilled at the minimum of the ratio, so that the critical velocity becomes

$$v_c = \min_p \frac{\epsilon(p)}{p}. \tag{3.3}$$

This is the Landau critical velocity [3]. If this critical velocity is non-zero the fluid flows without friction at velocities below this, and we call it a superfluid.

3.2 Dispersion Relation and Critical Velocity.

Let us look at how small excitation's behave in a weakly interacting Bose-Einstein condensate described by the dGPE eq. (2.28). We write the wavefunction on the form

$$\psi = \psi_h + \delta\psi_0. \tag{3.4}$$

Where ψ_h is the ground state and $\delta\psi_0$ are small perturbations. Linearising the dGPE with respect to $\delta\psi_0$ gives [40]

$$i\hbar\partial_t\delta\psi_0 = (1 - i\gamma)\left[-\frac{\hbar^2}{2m}\nabla^2\delta\psi_0 + (\mathcal{U} + 2g|\psi_h|^2 - \mu)\delta\psi_0 + g|\psi_h|^2\delta\psi_0^*\right]. \tag{3.5}$$

We write the perturbation as $\delta\psi_0 = u(\mathbf{r})e^{-i\omega t} + v^*(\mathbf{r})e^{i\omega^* t}$ and consider an uniform gas with $\mathcal{U} = 0$. For a uniform gas the Thomas-Fermi ground state eq. (2.20) gives that $\mu = g\rho_h$. Inserting this into eq. (3.5) we get

$$\left[\hbar\omega u(\mathbf{r}) + (1 - i\gamma)\left(\frac{\hbar^2}{2m}\nabla^2 u(\mathbf{r}) - g\rho_h u(\mathbf{r}) - g\rho_h v(\mathbf{r})\right)\right] e^{-i\omega t} \tag{3.6}$$

$$+\left[-\hbar\omega^* v^*(\mathbf{r}) + (1 - i\gamma)\left(\frac{\hbar^2}{2m}\nabla^2 v^*(\mathbf{r}) - g\rho_h v^*(\mathbf{r}) - g\rho_h u^*(\mathbf{r})\right)\right] e^{i\omega^* t} = 0. \tag{3.7}$$

Since $e^{-i\omega t}$ and $e^{i\omega^* t}$ are rotating independently in time the coefficients in front of them have to be zero. We therefore get two equations for u and v. Transforming to Fourier space the equations read

$$\begin{bmatrix} \hbar\omega - (1 - i\gamma)\left[\frac{\hbar^2 k^2}{2m} + g\rho_h\right] & -(1 - i\gamma)g\rho_h \\ -(1 + i\gamma)g\rho_h & -\hbar\omega - (1 + i\gamma)\left[\frac{\hbar^2 k^2}{2m} + g\rho_h\right] \end{bmatrix} \begin{bmatrix} \tilde{u}(k) \\ \tilde{v}(k) \end{bmatrix} = 0. \tag{3.8}$$

This can only give non-zero solutions if the determinant of the matrix vanishes. This leads to the equation

$$(\hbar\omega)^2 + 2i\gamma\hbar\omega\left[\frac{\hbar^2k^2}{2m} + g\rho_h\right] - (1+\gamma^2)\frac{\hbar^2k^2}{2m}\left[\frac{\hbar^2k^2}{2m} + 2g\rho_h\right] = 0. \tag{3.9}$$

We then find the following dispersion relation for the exitations

$$\hbar\omega = -i\gamma\left[g\rho_h + \frac{\hbar k^2}{2m}\right] + \sqrt{\frac{\hbar^2k^2}{2m}\left[\frac{\hbar^2k^2}{2m} + 2g\rho_h\right] - \gamma^2(g\rho_h)^2}. \tag{3.10}$$

From the decomposition of the perturbation $\delta\psi_0$ we see that the imaginary part of the dispersion relation corresponds to exponential damping, while the real part corresponds to rotation in the complex plane i.e oscillations. The imaginary part grows quadratic with the wavenumber, such that high frequency exitations are damped faster than the low frequency ones. The damping rate is proportional to the thermal drag and vanish at zero temperature. The group and phase velocities of the waves can be found from the real part of the dispersion relation. The group velocity is given as $d\mathrm{Re}(\omega)/dk$. It is the velocity of a single wavepacket [1]. The phase velocity is defined as $\mathrm{Re}(\omega)/k$. This is the propagation velocity of the waves phase. In the limit of small wavenumber the group and phase velocities are

$$v_g = \frac{\frac{g\rho_h}{m}\hbar k}{\sqrt{\frac{g\rho_h}{m}\hbar^2k^2 - \gamma^2(g\rho_h)^2}} \tag{3.11}$$

and

$$v_p = \sqrt{\frac{g\rho_h}{m} - \frac{\gamma^2(g\rho_h)^2}{\hbar^2k^2}} \tag{3.12}$$

respectively. When $k \to 0$ it seams like these velocities becomes imaginary. This happens when $\gamma^2(g\rho_h)^2 > \hbar^2k^2(g\rho_h)/m$. This is not the case since the dispersion relation also becomes purely imaginary for these values of k. This means that the exitations with wavenumbers $k^2 \leq \gamma^2(g\rho_h m)/\hbar^2$ don't propagate in the condensate.

In the limit of $\gamma = 0$ the dispersion relation becomes

$$(\hbar\omega)^2 = \frac{\hbar^2k^2}{2m}\left(\frac{\hbar^2k^2}{2m} + 2g\rho_h\right). \tag{3.13}$$

Which is caled the Bogoliubov Spectrum [40]. In the limit of small momenta we get a linear dispersion relation $\omega = ck$. In this case the group and phase velocity coincides as $c = \sqrt{g\rho_h/m}$ which we identified as the sound speed in section 2.7. In the other limit with large momentum the dispersion relation reads $\hbar\omega = \hbar^2k^2/2m$ which is the same as the relation for free particles.

The amplitudes $u(\mathbf{r})$ and $v(\mathbf{r})$ are then plane waves proportional to $e^{i\mathbf{k}\cdot\mathbf{r}}$ [40]. The specific form of the proportionality constants are not needed to show that the momentum of the exitations are $\hbar k$ and that the energy spectrum is given by

$$\epsilon(p) = \frac{p}{\sqrt{2m}}\sqrt{\left(\frac{p^2}{2m} + 2g\rho_h\right)}, \tag{3.14}$$

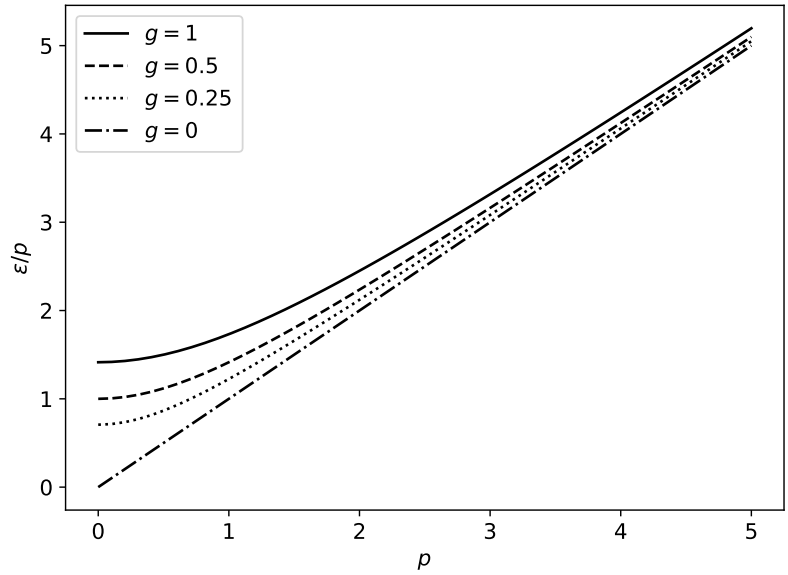

Figure 3.2: Plot of the energy spectrum divided by the momentum for different interaction strengths g. We can see that the minimum is decreasing with g, and when $g = 0$ it vanishes. This is equivalent to saying that an ideal BEC is not a superfluid.

which follows directly from the momentum operator $-i\hbar\nabla$ and the dispersion relation. Eq. (3.3) tells us that the critical velocity is given as the minimum of the ratio $\epsilon(p)/p$. From the spectrum we see that the minimum of this ratio is $v_c = \sqrt{g\rho_h/m}$ at $p = 0$. In reality the critical velocity can be lower due to the nucleation of quantised vortices [11]. In figure 3.2 we plot this ratio for different values of g. We have here set $2m = \rho_h = 1$, so the critical velocity is given as $\sqrt{2g}$. In the high momentum limit the graphs joins the line $p/2m$. At low momentum they split from this line and crosses the ϵ/p-axis at the critical velocity. The height of this crossing are dependent on g, and for a non-interacting condensate, $g \to 0$, it crosses at the origin making the critical velocity vanish. This means that an ideal Bose-Einstein condensate is not a superfluid.

Chapter 4

Hydrodynamics

In this chapter we discuss the classical analogue to the impurity submerged in a BEC. In section 4.1 we introduce the Navier-Stokes equation, and in section 4.2 we use it to find the equation of motion for a small sphere in the fluid. The systems discussed in this chapter are in three dimensions.

4.1 The Navier-Stokes Equation

The equation that describes the flow of an incompressible fluid is the Navier-Stokes equation [1]

$$\partial_t \mathbf{v} + (\mathbf{v} \cdot \nabla)\mathbf{v} = -\frac{1}{\rho}\nabla p + \nu \nabla^2 \mathbf{v} + \mathbf{f}. \tag{4.1}$$

Together with the incompressibility condition

$$\nabla \cdot \mathbf{v} = 0. \tag{4.2}$$

Here $\mathbf{v}(\mathbf{x}, t)$ is the fluids velocity field, $p(\mathbf{x}, t)$ is the pressure, $\rho(\mathbf{x}, t)$ is the density, $\nu = \mu/\rho$ is the kinematic viscosity and μ is the dynamic viscosity. $\mathbf{f}$ is here some external force e.g gravity $\mathbf{g}$. We will assume that there are no external forcing for the rest of this section. The Navier-Stokes equation is in general hard to solve, but for some special cases it can be simplified. We can do this by considering the Reynolds number[1] of the flow. The Reynolds number is dimensionless and defined by

$$Re = \frac{ul}{\nu}. \tag{4.3}$$

Where u is the velocity of the main stream and l is a characteristic length. The Reynolds number characterises a flow. If the Reynolds number is large we have a turbulent flow, while if it is low the flow is laminar. We can simplify the Navier-Stokes equation by changing the unit of length to l and the unit of velocity to u. The advection term $(\mathbf{v}\cdot\nabla)\mathbf{v}$ is then of the magnitude u^2/l. The term $\nu\nabla^2\mathbf{v}$ is of magnitude $\nu u/l^2$. The ratios of these magnitudes is the Reynolds number. So if we have a low Reynolds number we

can neglect the advection term and the Navier-Stokes equation reduces to the Stokes equation

$$\partial_t \mathbf{v} = -\frac{1}{\rho}\nabla p + \nu \nabla^2 \mathbf{v}. \tag{4.4}$$

This equation is relevant for flow with low velocity, small lengths or high viscosity.

If however the Reynolds number is large we can neglect the viscous term and the Navier-Stokes equation reduces to the Euler equation

$$\partial_t \mathbf{v} + (\mathbf{v} \cdot \nabla)\mathbf{v} = -\frac{1}{\rho}\nabla p. \tag{4.5}$$

This equation is relevant for flow with high velocity, large lengths or low viscosity. This is the equation that is used to describe non-viscous ideal fluids [1].

4.2 The Maxey-Riley Equation

The equation of motion for a small sphere in a nonuniform incompresible fluid in the low Reynolds number limit was derived by Maxey and Riley in 1983 [43]. Here is a summary of their derivation.

The problem they considered was a small sphere of radius a, mass m_p and position $r_p(t)$ placed in a fluid that in the absence of the particle have the flow $\mathbf{v}^{(0)}$, and the goal is to find the equation of motion expressed in terms of this undisturbed flow. The present of the particle changes the flow to $\mathbf{v} = \mathbf{v}^{(0)} + \mathbf{v}^{(1)}$, where $\mathbf{v}^{(1)}$ is the flow perturbations caused by the sphere. The modified flow $\mathbf{v}$ and the undisturbed flow $\mathbf{v}^{(0)}$ are described by the Navier-Stokes equation (4.1) with gravity as the external force and the incompressibility condition eq. (4.2). The boundary conditions are the non-slip boundary conditions and that the modified flow should reduce to the undisturbed flow far away from the sphere. The equation of motion for the sphere is given by

$$m_p \frac{d}{dt} V_{p,i} = m_p g_i + \oint_s \sigma_{ij} n_j dS. \tag{4.6}$$

Where the integral is taken over the surface of the sphere, $\mathbf{n}$ is the surface vector and the time derivative is given by $d/dt = \partial_t + \mathbf{V}_p \cdot \nabla$. The problem is therefore to find the stress tensor which is given as

$$\sigma_{ij} = -p\delta_{ij} + \mu\left(\partial_j v_i + \partial_i v_j\right). \tag{4.7}$$

Since the equation of motion requires us to evaluate an integral on the sphere it is convenient to transform to the frame comoving with it. The new variables are $\mathbf{z} = \mathbf{r} - \mathbf{r}_p(t)$, and $\mathbf{w} = \mathbf{v} - \mathbf{V}_p$. The Navier-Stokes and the boundary conditions are in this reference frame

$$\rho\big[\partial_t \mathbf{w} + (\mathbf{w} \cdot \nabla)\mathbf{w}\big] = \rho(\mathbf{g}_i - \frac{d}{dt}\mathbf{V}_p) - \nabla p + \mu \nabla^2 \mathbf{w}, \tag{4.8}$$

$$\mathbf{w}(|\mathbf{z}| = a, t) = \mathbf{\Omega} \times \mathbf{z}, \tag{4.9}$$

$$\mathbf{w}(|\mathbf{z}| \to \infty, t) = \mathbf{v}^{(0)} - \mathbf{V}_p. \tag{4.10}$$

Where $\mathbf{\Omega}$ is the particles angular velocity. The velocity field in the new frame can also be decomposed into the velocity field in the absence of the particle $\mathbf{w}^{(0)}$ and the perturbations caused by it $\mathbf{w}^{(1)}$. We decompose the pressure p and the stress tensor σ_{ij} in a similar way. The force is then naturally decomposed as

$$F_i = m_p g_i + F_i^{(0)} + F_i^{(1)} = m_p g_i + \oint_s \sigma_{ij}^{(0)} n_j dS + \oint_s \sigma_{ij}^{(1)} n_j dS. \tag{4.11}$$

The force caused by the unperturbed flow $\mathbf{F}^{(0)}$ as a function of $\mathbf{v}^{(0)}$ can be found easily from this. The unperturbed force is given as

$$F_i^{(0)} = \oint_s \left[-p^{(0)}\delta_{ij} + \mu \left(\partial_j w_i^{(0)} + \partial_i w_j^{(0)} \right) \right] n_j dS. \tag{4.12}$$

By applying the divergence theorem the integral reads

$$F_i^{(0)} = \int \partial_j \left[-p^{(0)}\delta_{ij} + \mu \left(\partial_j w_i^{(0)} + \partial_i w_j^{(0)} \right) \right] dV = \int dV \left[-\partial_i p^{(0)} + \mu \partial_j \partial_j w_i^{(0)} \right]. \tag{4.13}$$

Where we have used the incompresibility condition. To solve this integral we assume that the pressure gradient is nearly uniform inside the sphere and that we can express the velocity as

$$w_i^{(0)}(\mathbf{z}, t) = w_i^{(0)}(0, t) + z_j \partial_j w_i^{(0)}|_{\mathbf{z}=0} + z_j z_k \partial_j \partial_k w_i^{(0)}|_{\mathbf{z}=0} \tag{4.14}$$

inside the sphere. This approximation is valid if the sphere is small compared to the length scale of variations in the undisturbed flow. The force is then

$$F_i^{(0)} = \frac{4}{3}\pi a^3 \left(-\partial_j p + \mu \nabla_z^2 w_i^{(0)} \right)_{\mathbf{z}=0}. \tag{4.15}$$

Using that $\mathbf{w}^{(0)}$ and $p^{(0)}$ fulfils eq. (4.8) the force reads

$$F_i^{(0)} = -m_f g_i + m_f \left(\frac{d}{dt} V_{p,i} + \partial_t w_i^{(0)} + w_j^{(0)} \partial_j w_i^{(0)} \right)_{\mathbf{z}=0}. \tag{4.16}$$

Here we have introduced $m_f = \frac{4}{3}\pi a^3 \rho$, which is the mass of the fluid displaced by the particle. Transforming this into the original frame we get

$$F_i^{(0)} = -m_f g_i + m_f \frac{D v_i^{(0)}}{Dt}|_{\mathbf{r}=\mathbf{r}_p}. \tag{4.17}$$

Were we have introduced the material derivative $D/Dt = \partial_t + \mathbf{v}^{(0)} \cdot \nabla$. The term containing the material derivative is the inertial term and it gives the sphere an acceleration proportional to that of a small fluid sphere at the same position. The first term on the right hand side is the buoyancy force. The equation of motion is now given by

$$m_p \frac{d}{dt} V_{p,i} = (m_p - m_f) g_i + m_f \frac{D v_i^{(0)}}{Dt}|_{\mathbf{r}=\mathbf{r}_p} + F_i^{(1)}. \tag{4.18}$$

To find the force caused by the disturbance flow we use that $\mathbf{w}$ and $\mathbf{w}^{(0)}$ satisfies eq. (4.8), and find that the equation of motion for $\mathbf{w}^{(1)}$ is

$$\rho\left(\partial_t w_i^{(1)} + w_j^{(1)}\partial_j w_i^{(1)} + w_j^{(0)}\partial_j w_i^{(1)} + w_j^{(1)}\partial_j w_i^{(0)}\right) = -\frac{\partial p^{(1)}}{\partial z_i} + \mu\partial_j\partial_j w_i^{(1)}. \tag{4.19}$$

If we consider flows with low Reynolds number we can do the same dimension analysis as in the previous section and we see that this reduces to the Stokes equation

$$\rho\partial_t w_i^{(1)} = -\partial_i p^{(1)} + \mu\nabla^2 w_i^{(1)}. \tag{4.20}$$

With the boundary conditions

$$\mathbf{w}^{(1)}(|\mathbf{z}| = a, t) = -\mathbf{w}^{(0)} + \mathbf{\Omega}\times\mathbf{z}, \tag{4.21}$$

$$\mathbf{w}^{(1)}(|\mathbf{z}\to\infty|, t) = 0, \tag{4.22}$$

and the incompresibility condition eq. (4.2). One can then find the force by taking the Laplace transform, and exploiting the symmetry

$$\oint dS n_j\left(\tilde{w}_i^{(0)}\tilde{\sigma}_{ij}^{(1)} - \tilde{w}_i^{(1)}\tilde{\sigma}_{ij}^{(0)}\right) = \int dV\left[w_i^{(0)}(\mathbf{z},0)\tilde{w}_i^{(1)}(\mathbf{z},s) - w_i^{(1)}(\mathbf{z},0)\tilde{w}_i^{(0)}(\mathbf{z},s)\right], \tag{4.23}$$

for the two unsteady Stokes flow $\mathbf{w}^{(0)}$ and $\mathbf{w}^{(1)}$. This is used to make the disturbance force $\mathbf{F}^{(1)}$ depend on the undisturbed flow $\mathbf{w}^{(0)}$ instead of the disturbance flow $\mathbf{w}^{(1)}$. One can then show that the force due to the disturbance flow is in the original frame given as

$$\begin{aligned}\mathbf{F}^{(1)} = -6\pi a\mu&\left(\mathbf{V}_p - \mathbf{v}^{(0)}(\mathbf{r}_p(t),t) - \frac{1}{6}a^2\nabla^2\mathbf{v}^{(0)}|_{\mathbf{r}_p(t)}\right)\\ &- \frac{1}{2}m_f\left(\frac{d}{dt}\mathbf{V}_p(t) - \frac{D}{Dt}\mathbf{v}^{(0)}|_{\mathbf{r}_p(t)} - \frac{1}{10}a^2\frac{D}{Dt}\nabla^2\mathbf{v}^{(0)}|_{\mathbf{r}_p(t)}\right)\\ &- 6\pi a^2\mu\int_0^t d\tau\frac{d/d\tau\left[\mathbf{V}_p(\tau) - \mathbf{v}^{(0)}(\mathbf{r}_p(\tau),\tau) - \frac{1}{6}a^2\nabla^2\mathbf{v}^{(0)}|_{\mathbf{r}_p(\tau)}\right]}{\sqrt{\pi\nu(t-\tau)}}.\end{aligned} \tag{4.24}$$

When doing the calculation one will find that the time derivative in front of the undisturbed flow $\mathbf{v}^{(0)}$ is given as d/dt and not D/Dt as we have written here. This is because the difference between these derivatives vanishes in the limit of low Reynolds number [43, 44]. The use of D/Dt has on physical grounds been established as more correct, since it corresponds to the force being a result of the local accelerating in the undisturbed fluid. The terms containing the Laplacian are the so called Faxén correction [43]. These can be neglected for a small sphere. The first term on the right hand side is the Stokes' drag. Ignoring the Faxén correction we see that this is a viscous force proportional to the relative velocity between the sphere and the undisturbed fluid, acting in the opposite direction. The second term is the added mass term [44]. This is the force that is caused by the fluid the sphere have to move when accelerating. The

last term is the Basset-history integral. It is a viscous force that resists the unsteady motion of the particle [45]. The full equation of motion for the sphere is then

$$\begin{aligned} m_p\frac{d}{dt}\mathbf{V}_p(t) = (m_p - m_f)\mathbf{g} - 6\pi a\mu\left(\mathbf{V}_p - \mathbf{v}^{(0)}(\mathbf{r}_p(t),t) - \frac{1}{6}a^2\nabla^2\mathbf{v}^{(0)}|_{\mathbf{r}_p(t)}\right) + m_f\frac{D}{Dt}\mathbf{v}^{(0)}|_{\mathbf{r}_p(t)} \\ - \frac{1}{2}m_f\left(\frac{d}{dt}\mathbf{V}_p(t) - \frac{D}{Dt}\mathbf{v}^{(0)}|_{\mathbf{r}_p(t)} - \frac{1}{10}a^2\frac{D}{Dt}\nabla^2\mathbf{v}^{(0)}|_{\mathbf{r}_p(t)}\right) \\ - 6\pi a^2\mu\int_0^t d\tau\frac{d/d\tau\left[\mathbf{V}_p(\tau) - \mathbf{v}^{(0)}(\mathbf{r}_p(\tau),\tau) - \frac{1}{6}a^2\nabla^2\mathbf{v}^{(0)}|_{\mathbf{r}_p(\tau)}\right]}{\sqrt{\pi\nu(t-\tau)}}. \end{aligned} \tag{4.25}$$

This is called the Maxey-Riley equation. This equation is hard to solve numerically. We can simplify it by considering a sphere that is sufficiently small, so that we can neglect the Faxén correction and the Basset history integral [46]. The equation of motion is then

$$(m_p + \frac{1}{2}m_f)\frac{d}{dt}\mathbf{V}_p(t) = (m_p - m_f)\mathbf{g} - 6\pi a\mu(\mathbf{V}_p(t) - \mathbf{v}^{(0)}(\mathbf{r}_p(t),t)) + \frac{3}{2}m_f\frac{D}{Dt}\mathbf{v}^{(0)}|_{\mathbf{r}_p(t)}. \tag{4.26}$$

This form of the Maxey-Riley equation and modifications of it is used to study the dynamics of inertial particles in classical flows. It is for example used to study the dynamics of biogenic particles (e.g plankton) and feeding jellyfish [47, 48].

Chapter 5

Dissipasion Near an Impurity

In this chapter we discus the effect of an obstacle in the BEC at zero temperature. First we discuss the steady-state force on a small obstacle, then we discuss the heating this force is causing in the condensate. In the last section we discuss the waves that are created by an impurity that is moving at a constant velocity.

5.1 Potential Force

Ehrenfest's theorem states that the equations for the mean of position, momentum and force in a quantum mechanical system are the same as the classical equations of motion [49]. The force on the condensate due to a potential $\mathcal{U}$ is then

$$\langle \mathbf{F} \rangle = -\langle \nabla \mathcal{U} \rangle. \tag{5.1}$$

If the potential is due to an impurity then the force acting on the impurity from the condensate is

$$\mathbf{F}_p = \int d^2\mathbf{r} \nabla \mathcal{U}_p \rho. \tag{5.2}$$

Doing an integration by parts it becomes

$$\mathbf{F}_p = -\int d^2\mathbf{r} \mathcal{U}_p \nabla \rho. \tag{5.3}$$

In the dimensionless units that we discused in section 2.7 the force is $\mathbf{F}_p = \frac{\mu^2 \xi}{g} \mathbf{F}'_p$. From here on all calculations are done in the dimensionless units and the primes are removed.

We now want to find an expression for the force on an impurity that is moving linearly in the condensate at $T = 0$. To model the impurity we use the Gaussian potential

$$\mathcal{U}_p(\mathbf{r} - \mathbf{r}_p(t)) = \frac{g_p}{2\pi a^2} e^{-(\mathbf{r}-\mathbf{r}_p(t))^2/2a^2} \tag{5.4}$$

Here a is the size of the particle, $\mathbf{r}_p(t)$ is the position and g_p is the coupling constant between the impurity and the condensate. We will consider a weakly interacting impurity with $g_p << 1$ that is moving with a constant speed $\mathbf{V}_p$, such that the position is

given by $\mathbf{r}_p(t) = \mathbf{V}_p t$. We will follow the derivation of the drag force from the papers [26, 25]. Notice that [26] is using a different convention for the units than we are.

We consider an impurity that is suspended in an uniform BEC. Since we consider a weakly interacting impurity we can write the wavefunction as $\psi = \psi_0 + g_p \delta\psi_1$. Where ψ_0 is the wavefunction of the condensate without the impurity and $\delta\psi_1$ is the perturbations due to the interaction with the impurity. In this section we will assume that we have an uniform condensate where all perturbations are due to the impurity. This means that the wavefunction without the impurity is given by the Thomas-Fermi ground state $\psi_0 = 1$. The density of the condensate to linear order in g_p is then given by $\rho = 1 + g_p \delta\rho_1$, where $\delta\rho_1 = \delta\psi_1 + \delta\psi_1^*$. The force due to the density perturbations in the condensate becomes

$$\mathbf{F}^{(1)} = -g_p \int d^2\mathbf{r} \mathcal{U}_p \nabla \delta\rho_1. \tag{5.5}$$

Notice that since $\mathcal{U}_p$ is linear in g_p this force is quadratic in g_p. To find the density perturbation $\delta\psi_1$ we insert the wavefunction into eq. (2.31) with $\gamma = 0$ and neglecting terms that is of order $O(g_p^2)$. It becomes

$$i\partial_t \delta\psi_1 = -\frac{1}{2}\nabla^2 \delta\psi_1 + \frac{1}{2\pi a^2} e^{-(\mathbf{r}-\mathbf{r}_p)^2/2a^2} + \delta\psi_1^* + \delta\psi_1. \tag{5.6}$$

We now do a Galilean transformation into the frame that is comoving with the particle. The transformation laws are given by

$$\begin{aligned} \mathbf{z} &= \mathbf{r} - \mathbf{r}_p & t' &= t \\ \partial_t &= \partial_{t'} - \mathbf{V}_p \cdot \nabla_{\mathbf{z}} & \nabla &= \nabla_{\mathbf{z}} \end{aligned} \tag{5.7}$$

Using these laws eq. (5.6) is transformed into

$$i(\partial_{t'} - \mathbf{V}_p \cdot \nabla_{\mathbf{z}})\delta\psi_1' = -\frac{1}{2}\nabla_{\mathbf{z}}^2 \delta\psi_1' + \frac{1}{2\pi a^2} e^{-z^2/2a^2} + \delta\psi_1'^* + \delta\psi_1'. \tag{5.8}$$

From this point we are removing the primes. We want to look for solutions that are in the steady state in the frame comoving with the particle. We then have

$$-i\mathbf{V}_p \cdot \nabla_{\mathbf{z}} \delta\psi_1 = -\frac{1}{2}\nabla_{\mathbf{z}}^2 \delta\psi_1 + \frac{1}{2\pi a^2} e^{-z^2/2a^2} + \delta\psi_1^* + \delta\psi_1. \tag{5.9}$$

This equation can be solved for $\delta\psi_1$ by transforming it into Fourier space. Taking the Fourier transform and doing a complex conjugation we get the two equations

$$\begin{aligned} [-2\mathbf{V}_p \cdot i\mathbf{k} + i(k^2+2)]\delta\tilde{\psi}_1(\mathbf{k}) + 2i\delta\tilde{\psi}_1^*(-\mathbf{k}) &= -2ie^{-k^2a^2/2}, \\ [-2\mathbf{V}_p \cdot i\mathbf{k} - i(k^2+2)]\delta\tilde{\psi}_1^*(-\mathbf{k}) - 2i\delta\tilde{\psi}_1(\mathbf{k}) &= 2ie^{-k^2a^2/2}. \end{aligned} \tag{5.10}$$

We use the first equation to find an expression for $\delta\psi_1^*(-\mathbf{k})$. Inserting it into the second equation we get that the Fourier modes of the perturbed wavefunction are

$$\delta\tilde{\psi}_1(\mathbf{k}) = e^{-k^2a^2/2} \frac{4\mathbf{V}_p \cdot \mathbf{k} + 2k^2}{4(\mathbf{V}_p \cdot \mathbf{k})^2 - k^2(k^2+4)}. \tag{5.11}$$

We can now turn our attention to the force. Using the convolution theorem on eq. (5.5) in the comoving frame we get that the force on the impurity is given by

$$\mathbf{F}^{(1)} = -\frac{g_p}{(2\pi)^2}\int d^2\mathbf{k} i\mathbf{k}\tilde{\mathcal{U}}_p(-\mathbf{k})(\delta\tilde{\psi}_1(\mathbf{k}) + \delta\tilde{\psi}_1^*(-\mathbf{k})). \tag{5.12}$$

Inserting the expression for $\delta\tilde{\psi}_1(\mathbf{k})$ the force becomes

$$\mathbf{F}^{(1)} = -\frac{g_p^2}{(2\pi)^2}\int d^2\mathbf{k}\frac{4k^2 i\mathbf{k}}{4(\mathbf{V}_p\cdot\mathbf{k})^2 - k^2(k^2+4)}e^{-k^2a^2}. \tag{5.13}$$

We now consider the component that is parallel to the velocity of the impurity, since the tangential component vanishes due to symmetry. In polar coordinates this component becomes

$$F_\parallel^{(1)} = -\frac{g_p^2}{(2\pi)^2}\int_0^\infty\int_0^{2\pi}\frac{4ik^2\cos\theta}{4V_p^2\cos^2\theta - (k^2+4)}e^{-k^2a^2}d\theta dk. \tag{5.14}$$

We see that if $V_p < 1$ the integral is zero because of the cosine. This is consistent with the critical velocity we found in chapter 3.2. If $V_p > 1$ the integrand have poles, so we have to take some extra care. We see that for $k > 2\sqrt{V_p^2 - 1} = k_{max}$ the integral over θ is trivial. For $V_p > 1$ we therefore change the limits and consider the integral

$$F_\parallel^{(1)} = -\frac{g_p^2}{(2\pi)^2}\int_0^{k_{max}}\int_0^{2\pi}\frac{4ik^2\cos\theta}{4V_p^2\cos^2\theta - (k^2+4)}e^{-k^2a^2}d\theta dk. \tag{5.15}$$

We first want to do the integration over θ. We start by doing a change of variables to $x = \cos\theta$, such that the integral becomes

$$F_\parallel^{(1)} = \frac{2g_p^2\rho_e}{\pi^2}\int_0^{k_{max}}\int_{-1}^{1}\frac{ik^2xe^{-k^2a^2}dxdk}{[4V_p^2x^2 - (4\rho_e + k^2)]\sqrt{1-x^2}} \tag{5.16}$$

This integral has 4 poles at $x = \pm 1$ and at $x = \pm\frac{\sqrt{4\rho_e+k^2}}{2V_p}$. Defining $x_0 = \frac{\sqrt{4\rho_e+k^2}}{2V_p}$ and noticing that

$$\int_{-R}^{-1}\frac{k^2xe^{-k^2a^2}dx}{4V_p^2(x-x_0)(x+x_o)i\sqrt{x^2-1}} + \int_1^R\frac{k^2xe^{-k^2a^2}dx}{4V_p^2(x-x_0)(x+x_o)i\sqrt{x^2-1}} = 0, \tag{5.17}$$

because of symmetry. We can rewrite the integral as

$$F_\parallel^{(1)} = \frac{2g_p^2}{\pi^2}\lim_{R\to\infty}\int_0^{k_{max}}\int_{-R}^{R}\frac{ik^2xe^{-k^2a^2}dxdk}{4V_p^2(x-x_0)(x+x_0)\sqrt{1-x^2}}. \tag{5.18}$$

The integral over x can now be preformed by finding the Principal values. We have by Cauchy's residue theorem that [50]

$$\mathrm{PV}\int_{-\infty}^{\infty}f(x)dx = \pi i\sum\mathrm{Res}f(z). \tag{5.19}$$

And the force takes the form

$$F_{\parallel}^{(1)} = \frac{-g_p^2}{V_p \pi} \int_0^{k_{max}} \frac{k^2 e^{-k^2 a^2} dk}{\sqrt{k_{max}^2 - k^2}}. \tag{5.20}$$

This last integral can be solved by using mathematica. The parallel component of the force for $V_p > 1$ becomes at last

$$F_{\parallel}^{(1)} = -\frac{g_p^2}{4V_p} k_{max}^2 e^{-a^2 k_{max}^2/2} \left[I_0\left(\frac{a^2 k_{max}^2}{2}\right) - I_1\left(\frac{a^2 k_{max}^2}{2}\right)\right]. \tag{5.21}$$

Where I_n is the modified Bessel function of the first kind. Note that this expression doesn't work in the presence of vortices. This is because the vortex state is not a steady state, and the density perturbations $\delta\psi_1$ is not small when the impurity nucleates vortices. The expression works well for small impurities, since they have a low probability of nucleating vortices [25].

5.2 Heating

When doing experiments on the superfluidity in BECs one typical approach is to measure the heating of the condensate due to a moving laser [25, 51]. The laser can be modeled in the same way as the impurity we considered above. Dependent on the wavelength of the laser the potential can be either repulsive or attractive [51]. From eq. (2.18) we have that the heating of the condensate due to a time dependent potential is

$$\partial_t \mathcal{H} = \int |\psi|^2 \partial_t \mathcal{U}_p d^2\mathbf{r}. \tag{5.22}$$

We now use that $\mathcal{U}_p(\mathbf{r}, t) = \mathcal{U}_p(\mathbf{r} - \mathbf{r}_p(t))$. Applying the chain rule we get

$$\partial_t \mathcal{U}_p = \frac{\partial \mathcal{U}}{\partial z_i} \partial_t z_i. \tag{5.23}$$

Where $\mathbf{z} = \mathbf{r} - \mathbf{r}_p(t)$ and $\partial_t z_i = -\dot{r}_{p,i}(t)$ for a laser that is moving in the condensate. Inserting this into eq. (5.22) we get

$$\partial_t \mathcal{H} = -\mathbf{V}_p \cdot \int |\psi|^2 \nabla \mathcal{U}_p d^2\mathbf{r}. \tag{5.24}$$

Notice that the integral is the force we calculated in the last section. The negative of this force is the force that the laser is exerting on the condensate. The heating due to a laser that is moving linearly in an otherwise uniform BEC is then given by

$$\partial_t \mathcal{H} = -\mathbf{V}_p \cdot \mathbf{F}^{(1)}, \tag{5.25}$$

in the steady-state [25]. Which we also could have guessed without doing the calculation. The force and the velocity are pointing in the opposite direction such that the effect of

stirring the condensate is to increase its energy. Inserting the expression of the force from eq. (5.21) we get

$$\partial_t \mathcal{H} = \frac{g_p^2}{4} k_{max}^2 e^{-a^2 k_{max}^2/2} \left[I_0\left(\frac{a^2 k_{max}^2}{2}\right) - I_1\left(\frac{a^2 k_{max}^2}{2}\right)\right]. \tag{5.26}$$

This is the same expression as was found in [51] by another method. They also simulated

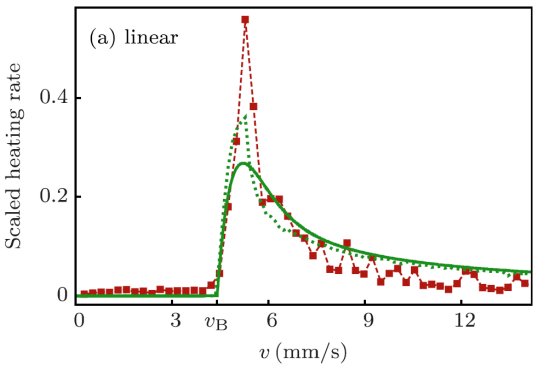

Figure 5.1: The figure shows the heating in a BEC. The green continuous line is the analytical expression similar to eq. (5.26), while the red squares conected by doted line are the values mesured in a simulation. The green doted line is the heating for a lattice system. Figure from [51].

the heating in a BEC and compared it to the analytical formula. The result of this is shown in figure 5.1. We see that eq. (5.26) captures the main behavior of the force well, except right above the critical velocity.

5.3 The Bogoliubov-Čerenkov Wake

We are now going to have a qualitative discussion on the shape of the exitations in the superfluid. We will show that the emitted waves in the long wavelength limit creates a conical wake similar to the wave cone associated with Čerenkov emission which is observed when charged particles are moving at relativistic velocities in a dielectricum. After that we will show that the short wavelengths are associated with parabolic wavefronts in front of the impurity. We are following the discussion in [52].

We start by considering the long wavelength exitations. In the comoving frame we can write the Fourier modes of the perturbed density as

$$\delta\tilde{\rho}_1(\mathbf{k}) = \frac{k^2 e^{-k^2 a^2/2}}{(\mathbf{V}_p \cdot \mathbf{k})^2 - \omega^2}. \tag{5.27}$$

Where ω is the dispersion relation for $\gamma = 0$. From this we see that the dominant modes are those with wavenumber satisfying the equation

$$\omega^2 = (\mathbf{V}_p \cdot \mathbf{k})^2. \tag{5.28}$$

For small wavenumbers the dispersion relation is linear and the dominant exitations satisfy

$$k_y^2 = (V_p^2 - 1)k_x^2. \tag{5.29}$$

We have here assumed that the impurity is moving with constant velocity $\mathbf{V}_p$ in the x direction. This equation have real solutions only when $V_p > 1$. In this case the solutions makes the two lines

$$k_y = \pm\sqrt{V_p^2 - 1}k_x. \tag{5.30}$$

Which is plotted on the top of figure 5.2. One can show that the angle between the

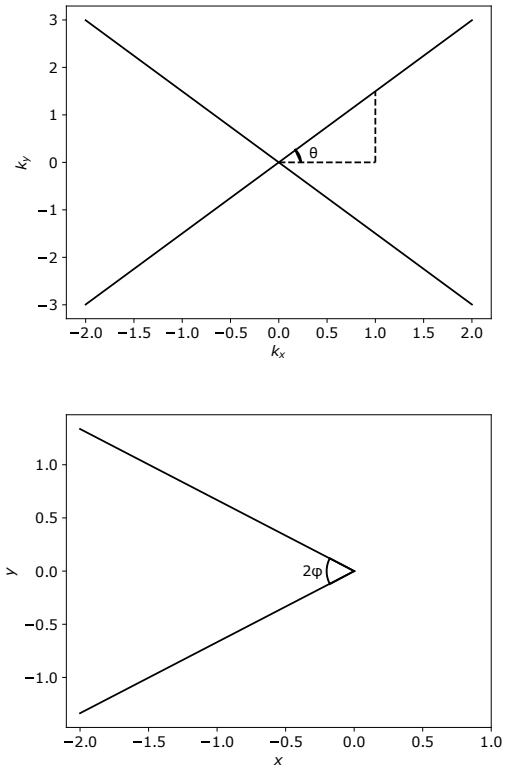

Figure 5.2: The top figure shows the wavevectors that dominates the integral in eq. (5.27). The bottom plots shows the mach cone that the long wavelength waves create in the condensate. The condensate is unperturbed everywhere except on the surface of the cone.

k_x-axis and the line satisfies $\cos\theta = 1/V_p$, by using simple trigonometric relations on the triangle that is shown in the figure. This is the **k**-space Čerenkov cone. The waves with wavevector lying on the surface of this cone have a constant group velocity given by $\mathbf{v}_r = \nabla_{\mathbf{k}}(\omega - \mathbf{k}\cdot\mathbf{V}_p) = \frac{1}{V_p}\left[(1 - V_p^2)\hat{z}_x \pm \sqrt{V_p^2 - 1}\hat{z}_y\right]$ in the comoving frame. The different modes are therefore propagating in the same two directions as seen from the

particle. The group velocities defines a conical surface given by

$$z_y^2 = \frac{z_x^2}{V_p^2 - 1}, \tag{5.31}$$

with $|z_x| < 0$. This lines are plotted in the bottom of figure 5.2. The waves that are propagating from the particle have a continuous range of wavevectors satisfying eq. (5.29). They are therefore interfering destructively everywhere except on the surface of the cone. This cone is referred to as the mach cone in analogy to the cone that is generated by supersonic particles in a classical fluid. The angle of the surfaces satisfies the relation $\sin\phi = 1/V_p$, and it is clear that it narrows when the speed of the impurity increases.

The dispersion relation for the condensate is only linear in the small k limit. The waves with larger k values will also contribute to the shape of the emitted waves. If we now consider the limit with small wavelengths the dispersion relation becomes approximately $\omega = \frac{k^2}{2}$. We can find the approximate shape of the waves by assuming that we have a point like defect, i.e taking the limit $a \to 0$ where the potential is a delta function. The perturbed wavefunction is then

$$\delta\psi_1(\mathbf{z}) = -\int \frac{d^2\mathbf{k}}{(2\pi)^2} \frac{(2k^2 + 4\mathbf{V}_p \cdot \mathbf{k})e^{i\mathbf{k}\cdot\mathbf{z}}}{k^4 - 4(\mathbf{k}\cdot\mathbf{V}_p)^2}. \tag{5.32}$$

This can be rewriten to

$$\delta\psi_1(\mathbf{z}) = -\int \frac{d^2\mathbf{k}}{(2\pi)^2} \frac{e^{i\mathbf{k}\cdot\mathbf{z}}}{\frac{k^2}{2} - \mathbf{k}\cdot\mathbf{V}_p} = -\int \frac{d^2\mathbf{k}}{(2\pi)^2} \frac{e^{i\mathbf{k}\cdot\mathbf{z}} e^{i\mathbf{V}_p\cdot\mathbf{z}}}{\frac{k^2}{2} - \frac{V_p^2}{2}}. \tag{5.33}$$

Where we in the last integral have taken the coordinate transform $\mathbf{k} \to \mathbf{k} + \mathbf{V}_p$. This integral is solved in [52] by noticing that it is the Greens function for the two-dimensional Helmholtz equation [53]. The Greens function is proportional to the Hankel function $H_0^{(1)}(V_p z)$ and the wavefunction becomes

$$\delta\psi_1(\mathbf{z}) = -\frac{2\pi i C_2}{\sqrt{z}} e^{iV_p z} e^{iV_p z_x}, \tag{5.34}$$

in the limit $z >> 1$ [54]. Here C_2 is a constant that is proportional to $1/\sqrt{V_p}$. The perturbed density is then

$$\delta\rho_1 = \frac{4\pi C_2}{\sqrt{z}} \sin\left(V_p(z + z_x)\right). \tag{5.35}$$

A plot of this density is shown in figure 5.3 for $V_p = 1.6$. The wavefronts that is defined by this density makes parabolic surfaces in the condensate. We can show this by considering the wave tops. These are defined as the surfaces where the argument of the sine is $\pi/2$ plus an integer multiple of 2π. They therefore satisfy

$$V_p\sqrt{z_x^2 + z_y^2} + V_p z_x = 2\pi N + \frac{\pi}{2}, \tag{5.36}$$

where N is an integer. By squaring this equation we see that the fronts are the parabolas

$$V_p^2 z_y^2 = \pi^2(2N + \frac{1}{2})^2 - 2\pi(2N + \frac{1}{2})V_p z_x. \tag{5.37}$$

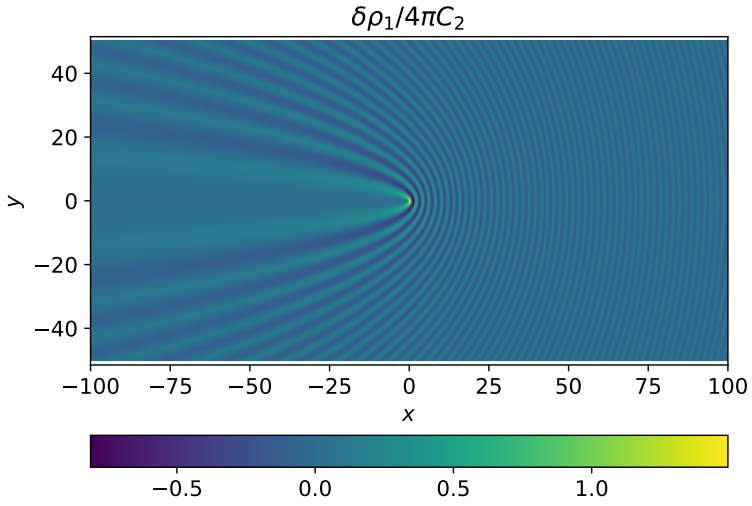

Figure 5.3: Figure of the density perturbation for a condensate with a quadratic dispersion relation. The impurity's velocity is $V_p = 1.6$ in the x-direction. We can see that the wavefronts makes parabolic surfaces. This surfaces are given by eq. (5.37).

We have now seen how the exitations behaves in the short and long wavelength limit. In the long wavelength limit the exitations makes a wake of angle $\sin\phi = 1/V_p$ behind the impurity, while the short wavelength exitations makes parabolic waves in front of it. In the intermediate range we expect the behavior to go gradually between the regimes when the wavelength is changed.

Chapter 6

Numerical Methods

In this chapter we discuss the numerical methods that were used in this project. We start by discussing the exponential time differencing method that we use to solve the damped Gross-Pitaevskii equation. Then we discuss the numerical setup in detail.

6.1 Time Exponentiation

When considering a non-linear partial differential equation(PDE) with periodic boundary conditions on an uniform lattice it is convenient to transform it to Fourier space where one get one ordinary differential equation(ODE) for each Fourier mode [55]. The ODEs one gets are in general stiff, so they require some care to get accurate solution in an efficient way. The stiffness is often due to the linear part of the equation. We are therefore going to use the method of time exponentiation, where we solve the linear part exactly and find an approximation for the integral over the non-linear terms.

Consider a general non-linear PDE that can be written on the form [41, 55]

$$\partial_t \psi(\mathbf{r}, t) = \omega(\nabla)\psi(\mathbf{r}, t) + N(\psi, t). \tag{6.1}$$

Here $\omega(\nabla)$ is a linear differential operator and $N(\mathbf{r}, t)$ is a general function representing the non-linear part. To ease the notation we have assumed that all spacial dependence of N is through ψ. The derivation is still valid if this is not the case. Evaluating this in Fourier space we get

$$\partial_t \tilde{\psi}(\mathbf{k}, t) = \tilde{\omega}(\mathbf{k})\tilde{\psi}(\mathbf{k}, t) + \tilde{N}(\psi, t). \tag{6.2}$$

Multiplying with an integrating factor $e^{-\tilde{\omega}t}$ and moving the linear operator to the left hand side the equation becomes

$$\partial_t (e^{-\tilde{\omega}t}\tilde{\psi}) = e^{-\tilde{\omega}t}\tilde{N}. \tag{6.3}$$

Integrating this from t to $t + \Delta t$ we find the solution

$$\tilde{\psi}(k, t + \Delta t)e^{-\tilde{\omega}(k)(t+\Delta t)} = \tilde{\psi}(k, t)e^{-\tilde{\omega}(k)t} + \int_t^{t+\Delta t} \tilde{N}(\psi, t')e^{-\tilde{\omega}t'}\, dt'. \tag{6.4}$$

Dividing by $e^{-\tilde{\omega}(k)(t+\Delta t)}$, and substituting $\tau = t' - t$ we get

$$\tilde{\psi}(k, t+\Delta t) = \tilde{\psi}(k,t)e^{\tilde{\omega}(k)\Delta t} + e^{\tilde{\omega}\Delta t}\int_0^{\Delta t} \tilde{N}(\psi, t+\tau)e^{-\tilde{\omega}\tau}d\tau. \tag{6.5}$$

In order to compute the integral we approximate $\tilde{N}(\psi, t+\tau) = \tilde{N}_0$ to be constant on the interval $\tau \in (0, \Delta t)$ [41, 55]. Inserting this into the above expression gives

$$\tilde{\psi}(k, t+\Delta t) = \tilde{\psi}(k,t)e^{\tilde{\omega}(k)\Delta t} + e^{\tilde{\omega}\Delta t}\int_0^{\Delta t} \tilde{N}_0 e^{-\tilde{\omega}\tau}d\tau \tag{6.6}$$

After preforming the integral we get the following expression for $\tilde{\psi}$

$$\tilde{\psi}(\mathbf{k}, t+\Delta t) = \tilde{\psi}(\mathbf{k},t)e^{\tilde{\omega}(\mathbf{k})\Delta t} + \frac{\tilde{N}_0}{\tilde{\omega}(\mathbf{k})}(e^{\tilde{\omega}(k)\Delta t} - 1) \tag{6.7}$$

This is a first order scheme for ψ analog to the Euler method. We can improve it by using the newly obtained value for ψ to find an estimate for $N(\psi, t+\Delta t)$. In other words we approximate the non-linear part as $N\left(\psi(t+\tau), t+\tau\right) = N_0 + \left[N\left(\psi_0(t+\Delta t), t+\Delta t\right) - N_0\right]\tau/\Delta t$. Where ψ_0 is the wavefunction calculated above. Inserting this approximation into the integral in eq. (6.5) we obtain the following scheme

$$\begin{aligned}
\tilde{\psi}_0 &= \tilde{\psi}(\mathbf{k},t)e^{\tilde{\omega}(\mathbf{k})\Delta t} + \frac{\tilde{N}_0}{\tilde{\omega}(\mathbf{k})}(e^{\tilde{\omega}(k)\Delta t} - 1), \\
\tilde{\psi}(\mathbf{k}, t+\Delta t) &= \tilde{\psi}_0 + \left(\tilde{N}(\psi_0, t+\Delta t) - N_0\right)\frac{1}{\tilde{\omega}}\left((e^{\tilde{\omega}\Delta t} - 1)\frac{1}{\tilde{\omega}\Delta t} - 1\right).
\end{aligned} \tag{6.8}$$

This is a second order scheme analog to the improved Euler method [55].

6.2 Numerical Setup

To test the analytical predictions that will be presented in chapter 7 we consider a system of size 256×128 in units of ξ. The distance between grid points on the lattice is $dx = 0.25\xi$ and time is discretized in units of $dt = 0.01\tau$. The impurity is situated in the middle of the domain at position $(128\xi, 64\xi)$, and the simulations are done in the comoving frame of the particle. We use the fringe method from [56] to avoid that density perturbations created by the impurity are recycled by the periodic boundary conditions. This is done by adding buffer(fringe) regions around the computation domain with a large value of γ as illustrated in figure 6.1. The buffer regions are damping out the perturbations and making the incoming flow steady. γ then becomes spatially dependent and is given by $\gamma(\mathbf{r}) = \max\left[\gamma(x), \gamma(y)\right]$ with

$$\gamma(x) = \frac{1}{2}\big(2 + \tanh\left[(x - x_p - w_x)/d\right] - \tanh\left[(x - x_p + w_x)/d\right]\big) + \gamma_0, \tag{6.9}$$

and similarly for $\gamma(y)$. Here (x_p, y_p) is the position of the particle, and γ_0 is the

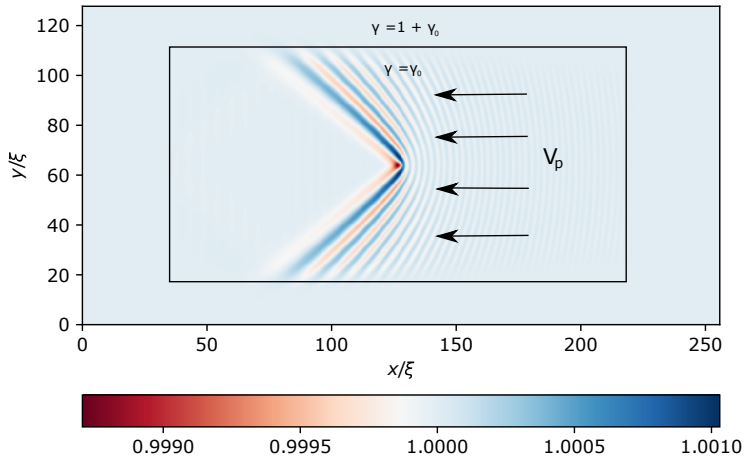

Figure 6.1: The figure shows the buffer regions far away from the impurity, where the thermal drag is large in order to remove any disturbances in the recycled flow. The picture is showing the density in the steady state in the comoving frame for $V_p = 1.6$ and $\gamma = 0$. The direction of the flow is indicated with the arrows.

thermal drag inside the bulk region. The parameters w_x and w_y sets the extent of the bulk region. On the x-axis it goes from $x = x_p - w_x$ to $x = x_p + w_x$, and equivalent for the y-axis. The parameter d is controlling how fast the value of γ is changing on the border of the buffer region. It is important that this parameter is not to small, since that would cause the exitations to be reflected by the fringe. The values we are using for these parameters are $w_x = 100\xi$, $w_y = 50\xi$ and $d = 7\xi$. As mentioned we are simulating the system in the frame comoving with the particle. In this frame the dGPE takes the form

$$\partial_t \psi - \mathbf{V}_p \cdot \nabla \psi = (i + \gamma) \left[\frac{1}{2} \nabla^2 \psi + \left(1 - \mathcal{U}_p - |\psi|^2 \right) \psi \right]. \tag{6.10}$$

To model the impurity we use the Gaussian potensial in eq. (5.4) with $a = 1$ and $g_p = 0.01$. As an initial condition we start with the Thomas-Fermi ground state and evolve it in imaginary time with $V_p = 0$ and $\gamma = 0$ to find the ground state of the condensate with the particle at rest. At $t = 0$ we solve eq. (6.10) with the numerical scheme given by eq. (6.8). For the imaginary time evolution the ω and N in eq. (6.8) are $\omega = (1 + \frac{1}{2}\nabla^2)$ and $N(\mathbf{r}, t) = -(\mathcal{U}_p + |\psi|^2)\psi$. When we solve the dGPE in the comoving frame they are $\omega = i(1 + \frac{1}{2}\nabla^2) + \mathbf{V}_p \cdot \nabla$ and $N(\mathbf{r}, t) = -(i+\gamma)(\mathcal{U}_p + |\psi|^2)\psi + \gamma\psi + \frac{1}{2}\gamma\nabla^2\psi$. It is important to remember that γ is a function of space when preforming the Fourier transform.

This setup is ideal for studying the steady-state and transient behaviour of an impurity traveling linearly in an infinite system, since the buffer regions prevent the particle form interacting with itself. Another way of modeling this could have been to consider the system in the lab frame, i.e the frame with the condensate at rest, and stop the simulation before the perturbations comes back to the particle. The drawback of this is that one needs a larger system in order to reach the steady-state. Especially when the velocity of the impurity gets close to the critical velocity. Another weakness of this is that the restriction to short time intervals is making the calculated averages less certain.

The fringe method don't have this shortcomings, since we don't have to worry about the perturbations coming back. This setup is also ideal for studying the vortex shedding from the impurity, and this is what it is used for in [56]. Here they classify the different vortex regimes that one can observe in the stirred condensate. They observe three regimes the dipole regime, the charge 2 Von Kármán regime and the turbulent regime. In figure 6.2 one can see how this buffer regions work in two of these vortex regimes. In order to create vortices one have to consider an impurity that is strongly coupled, and not to small.

In figure 6.2 we have used an impurity with potential $\mathcal{U}_p = 0.8e^{(\mathbf{r}-\mathbf{r}_p)^2/2\cdot 4^2}$. The thermal drag is zero in the bulk and the velocity of the impurity is 0.6 on the top and 0.8 on the bottom. The top picture in the figure is from the dipole regime. This system have reached an ordered state where the impurity nucleates vortices in dipoles at a constant rate. One can find the nucleation frequency by Fourier transforming the force that is acting on the particle. When the dipoles reaches the buffer region the distance between the vortex and antivortex decreases and they annihilate each other. This is because the large thermal drag is making the counter rotating vortices approach each other until they collide. When they collide they make waves that are damped inside the region. It is important that the fringe is large enough that the vortices have time to collide. In the bottom picture we are in the turbulent regime, and we don't observe the ordered state that we see at the top. Here the vortices are shed seemingly at random and not only dipoles, but also free vortices and clusters are shed. We observes two problems in this regime. The first is that some of the vortices that are shed in dipoles are so far away from each other that they don't have the time to collide when they are in the buffer. Another problem is that the vortics can't gradualy decay, as discussed in section 2.9, so the free vortices and clusters are not removed by the buffer and comes around in the incoming flow. This is also a problem in the Von Kármán regime where the vortices are shed in clousters of corotating vortices. When these vortices are coming around they will interact with the particle and other vortices. This recycling is something we want to avoid, since we want to model an impurity moving linearly in an otherwise uniform condensate. We can prevent that the dipoles comes around by enlarging the buffer region, but this is only a temporary fix and we will still have problems with the free vortices and the clusters.

In [56] they deal with this problem by phase imprinting a vortex-antivortex pair on top of the vortices inside the buffer region. This annihilates the dipoles and moves the vortices without a counter rotating partner back to the start of the region so that it is not recycled into the bulk. Since there are vortices continuously moving into the

buffer they will eventually be annihilated. The energy that is added when imprinting the dipole is removed by the high dissipation in the buffer. We have not added this phase imprinting of vortex-antivortex pairs, since we are considering impurities that are too weak to produce vortices. This is because the expressions that we are testing are found by assuming that the coupling between the condensate and the impurity is weak, and we have assumed that there are only small perturbations in the condensate. In order to create vortices the impurity can't be too small, and nucleation of vortices are associated with large perturbations near the impurity.

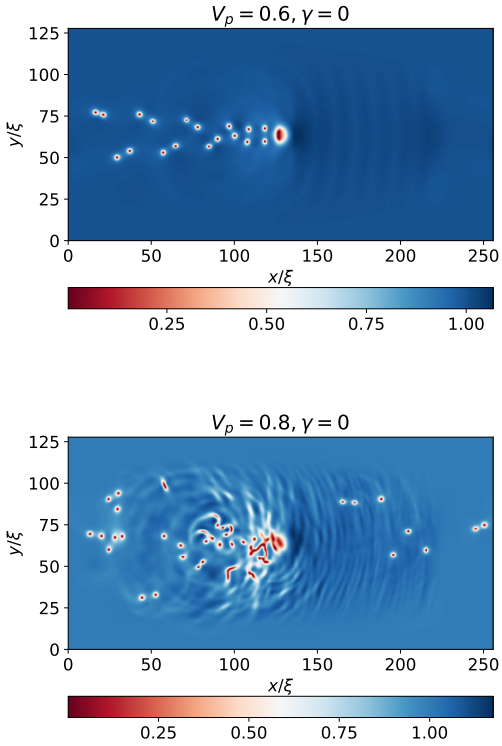

Figure 6.2: Snapshot of condensate that is stirred by a large impurity. Here the impurity is large enough to produce vortices, and we can see two different vortex regimes. The top snapshot shows the dipole regime. In this regime the buffer region have no trouble annihilating the vortex-antivortex pairs. The bottom picture is in the turbulent regime. Here we see the appearance of free vortices. On the right we see the vortices that are recycled into the incoming flow. Both pictures are taken at the time $t = 1800$.

Chapter 7

Analogy to Classical Forces

In this chapter we discus the force acting on an impurity submerged in the BEC at finite temperatures, and compare with the classical analog eq. (4.25). In section 7.1 we obtain theoretical expresions for the force. In section 7.2 we use the numerical scheme discused in chapter 6 to compare the analytical obtained expressions with eq. (5.3). The content in this chapter was submited in ref. [32]. Note that the derivation and content in section 7.1.2 deviates a bit from the discussion in the manuscript. We have here included an expression for the Fourier modes of the disturbed density for an arbitrary moving impurity.

In this chapter we have only considered the interactions between the impurity and the condensate. In addition the impurity will interact with the thermal cloud. The additional forces that comes from these interactions are beyond the scope of this project. However at sufficiently low temperatures the thermal cloud is sparsely populated, so that the scattering rate between the impurity and the exited states is low. The drag from the thermal cloud is therefore small as long as we are considering low temperatures.

7.1 Perturbation Theory

We will now consider an impurity in the condensate at finite temperature. This corresponds to having $\gamma > 0$ in eq. (2.31). As in chapter 5 we are modeling the impurity with the potential

$$\mathcal{U}_p(\mathbf{r} - \mathbf{r}_p(t)) = \frac{g_p}{2\pi a^2} e^{-(\mathbf{r}-\mathbf{r}_p(t))^2/2a^2}, \tag{7.1}$$

and considers a weakly coupled impurity with $g_p << 1$. As in section 5.1 we decompose the wavefunction into the wavefunction that is undisturbed by the impurity ψ_0 and the perturbations due to the interaction with the impurity $\delta\psi_1$. The unpdisturbed part can again be decomposed into $\psi_0 = 1 + \delta\psi_0$, allowing for small perturbations away from the uniform equilibrium state. These small perturbations can be due to an external stirring potential or from non-equilibrium initial conditions. We will assume that any stirring potential is far away so that the only potential we need to worry about is the impurity. Using this decomposition we get the following first order expansions for the

wavefunction, density and velocity

$$\psi = 1 + \delta\psi_0 + g_p\delta\psi_1, \tag{7.2}$$
$$\rho = 1 + \delta\rho_0 + g_p\delta\rho_1, \tag{7.3}$$
$$\mathbf{v} = \delta\mathbf{v}^{(0)} + g_p\delta\mathbf{v}^{(1)}. \tag{7.4}$$

Where the density and the velocity perturbations are given by

$$\delta\rho_i = \delta\psi_i + \delta\psi_i^*, \tag{7.5}$$
$$\delta\mathbf{v}^{(i)} = \frac{1}{2i}\nabla(\delta\psi_i - \delta\psi_i^*). \tag{7.6}$$

The densities can now be inserted into eq. (5.3) to find the force. Like in the classical analog in section 4.2 the force can be decomposed as $\mathbf{F} = \mathbf{F}^{(0)} + \mathbf{F}^{(1)}$ where

$$\mathbf{F}^{(0)} = -\frac{g_p}{2\pi a^2}\int d^2\mathbf{r} e^{-(\mathbf{r}-\mathbf{r}_p(t))^2/2a^2}\nabla\delta\rho_0(\mathbf{r},t), \tag{7.7}$$
$$\mathbf{F}^{(1)} = -\frac{g_p^2}{2\pi a^2}\int d^2\mathbf{r} e^{-(\mathbf{r}-\mathbf{r}_p(t))^2/2a^2}\nabla\delta\rho_1(\mathbf{r},t). \tag{7.8}$$

Here $\mathbf{F}^{(0)}$ is the force caused by the density variations in the fluid in the absence of the impurity. The classical analog are the inertial force eq. (4.17) and we will therefore refer to $\mathbf{F}^{(0)}$ as the inertial force. The $\mathbf{F}^{(1)}$ component is the force that is caused by the flow perturbations that the particle are inducing in the fluid. We therefore refer to it as the self-induced force. We wish to find an equation of motion for the impurity that is analog to the classical expressions. To do this we need to express the two force components in terms of the particle velocity $\mathbf{V}_p$ and the unperturbed velocity field $\delta\mathbf{v}_0$. For $\mathbf{F}^{(0)}$ we are able to do this for an arbitrary moving impurity. While for $\mathbf{F}^{(1)}$ we are able to find an expression for arbitrary moving impurities, but it does not depend on the undisturbed flow. However in the steady-state we manage to reduce this expression to a force analog to the Stokes' drag in the classical fluid.

To find the forces $\mathbf{F}^{(0)}$ and $\mathbf{F}^{(1)}$ we need to find the density perturbations. We find these from the wavefunction. Inserting the perturbed wavefunctions eq. (7.2) into the dimentionles dGPE eq. (2.31) gives the two linearized equations

$$\partial_t\delta\psi_0 = (i+\gamma)(\frac{1}{2}\nabla^2 - 1)\delta\psi_0 - (i+\gamma)\delta\psi_0^*, \tag{7.9}$$
$$\partial_t\delta\psi_1 = (i+\gamma)(\frac{1}{2}\nabla^2 - 1)\delta\psi_1 - (i+\gamma)\delta\psi_1^* - (i+\gamma)\frac{1}{2\pi a^2}e^{-(\mathbf{r}-\mathbf{r}_p)^2/2a^2}. \tag{7.10}$$

The problem is now to solve these linearized equations to find how the density fields depend on the undisturbed velocity field.

7.1.1 The Inertial Force

First we consider the Inertial force given by eq. (7.7). We start by considering eq. (7.9) to find an expression for the perturbed density variations $\delta\rho_0$ as a function of the

unperturbed velocity $\delta\mathbf{v}_0$. If we subtract the equation by its complex conjugate it gives

$$\partial_t(\delta\psi_0 - \delta\psi_0^*) = i(\frac{1}{2}\nabla^2 - 2)(\delta\psi_0 + \delta\psi_0^*) + \gamma\frac{1}{2}\nabla^2(\delta\psi_0 - \delta\psi_0^*). \tag{7.11}$$

Taking the gradient of this equation it becomes

$$(\partial_t - \frac{\gamma}{2}\nabla^2)\nabla(\delta\psi_0 - \delta\psi_0) = i(\frac{1}{2}\nabla^2 - 2)\nabla(\delta\psi_0 + \delta\psi_0^*). \tag{7.12}$$

Using the expression for the perturbed densities and velocities eq. (7.5) and (7.6) this expression becomes

$$(\nabla^2 - 4)\nabla\delta\rho_0 = 4(\partial_t - \frac{\gamma}{2}\nabla^2)\delta\mathbf{v}_0. \tag{7.13}$$

Since the equation for the force eq. (7.7) is integrating the density around the impurity it is convenient to work in a coordinate system that has it as it center. We therefore change our coordinates to $\mathbf{z} = \mathbf{r} - \mathbf{r}_p(t)$. The velocity field in the new coordinate system is given by $\delta\mathbf{w}_0 = \delta\mathbf{v}_0 - \mathbf{V}_p$, where $\mathbf{V}_p = \dot{\mathbf{r}}_p$. Equation 7.13 in the comoving frame is

$$(\nabla_\mathbf{z}^2 - 4)\nabla_\mathbf{z}\delta\rho_0 = 4(\partial_t - \mathbf{V}_p\cdot\nabla_\mathbf{z} - \frac{\gamma}{2}\nabla_\mathbf{z}^2)\delta\mathbf{w}^{(0)} + 4\dot{\mathbf{V}}_p. \tag{7.14}$$

We solve this equation by finding the Greens function for the operator $(\nabla_\mathbf{z}^2 - 4)$. The equation for the Greens function is

$$(\nabla_\mathbf{z}^2 - 4)G(\mathbf{z}) = \delta(\mathbf{z}). \tag{7.15}$$

With the boundary condition $G(|\mathbf{z}| \to \infty) \to 0$, since we expect $\nabla_\mathbf{z}\delta\rho_0$ to vanish at infinity. The solution to this equation is $G(\mathbf{z}) = -K_0(2|\mathbf{z}|)/(2\pi)$, where K_0 is the modified Bessel function of the second kind of order zero. One finds this by using the Greens function for the Helmholtz equation and the expression $K_0(x) = \pi i H_0^{(1)}(ix)/2$, where $H_0^{(1)}(x)$ is the Hankel function [50, 53, 54]. The gradient of the perturbed density is then given by the Greens function as

$$\nabla_z\delta\rho_0(\mathbf{z},t) = -\frac{2}{\pi}\int d^2\mathbf{z}' K_0(2|\mathbf{z}-\mathbf{z}'|)\big[(\partial_t - \mathbf{V}_p\cdot\nabla_{\mathbf{z}'} - \frac{\gamma}{2}\nabla_{\mathbf{z}'}^2)\delta\mathbf{w}^{(0)} + \dot{\mathbf{V}}_p\big]. \tag{7.16}$$

Inserting this into eq. (7.7) we get that the force is given by

$$\mathbf{F}^{(0)}(t) = -\frac{g_p}{\pi^2 a^2}\int d^2\mathbf{z} e^{-z^2/2a^2}\int d^2\mathbf{z}' K_0(2|\mathbf{z}-\mathbf{z}'|)\big[(\partial_t - \mathbf{V}_p\cdot\nabla_{\mathbf{z}'} - \frac{\gamma}{2}\nabla_{\mathbf{z}'}^2)\delta\mathbf{w}^{(0)} + \dot{\mathbf{V}}_p\big]. \tag{7.17}$$

This expression is the weighted average of properties of the fluids velocity in a neighborhood around the impurity. We can compare it with the classical analog eq. (4.13). In the classical expression the volume integral is over the volume of the sphere, while in the condensate the integrals are over all space weighted by the Bessel function and the Gaussian. The Gaussian and the Bessel function are restricting the size of the neighborhood that is affecting the particle. The size of this neighborhood is given by the range

of the Gaussian and the size of the Bessel functions kernel. The range of the Gaussian, a, corresponds to the radius of the sphere in the classical case. The size of the Bessel functions kernel is in dimensional units in the order of the correlation length ξ. This have no analog in the classical case, and is due to quantum effects. If the condensates velocity field is slowly varying on scales below a and ξ we can approximate it with a Taylor expansion as we did in the classical case. First we consider an expansion around z as

$$\delta w_i^{(0)}(\mathbf{z}',t) = \delta w_i^{(0)}(\mathbf{z},t) + e_{ij}(\mathbf{z},t)(z_j' - z_j) + e_{ijk}(\mathbf{z},t)(z_j' - z_j)(z_k' - z_k) + ... \quad (7.18)$$

Where repeated indices are summed over. Here $e_{ij}(\mathbf{z},t) = \partial_j \delta w_i^{(0)}(\mathbf{z},t)$ and $e_{ijk}(\mathbf{z},t) = \partial_j\partial_k \delta w_i^{(0)}(\mathbf{z},t)$. Inserting the above expansion into eq. (7.17) and using that terms linear in $\mathbf{z}'$ vanish upon integration, the integral over the Bessel function reads

$$\int d^2\mathbf{z}' K_0(2|\mathbf{z}-\mathbf{z}'|)\Big[\partial_t \delta w_i^{(0)}(\mathbf{z},t) - V_p\cdot\nabla_z \delta w_i^{(0)} - \frac{\gamma}{2}\nabla_z^2 \delta w_i^{(0)} + \frac{1}{2}\partial_t e_{ijk}(\mathbf{z},t)(z_j'-z_j)(z_k'-z_k) + \dot{V}_{p,i}\Big]. \quad (7.19)$$

Using that $\int d^2\mathbf{z} K_0(2|\mathbf{z}|) = 2\pi\int_0^\infty dz z K_0(2z) = \pi/2$ and
$\int d^2\mathbf{z} K_0(2|\mathbf{z}|) z_i z_j = \delta_{ij}/2\int_0^\infty dz 2\pi z^3 K_0(2|z|) = \pi\delta_{ij}/4$, the expresion above becomes

$$\frac{\pi}{2}\left(\partial_t \delta w_i^{(0)} - \mathbf{V}_p\cdot\nabla_z \delta w_i^{(0)} - \frac{\gamma}{2}\nabla^2\delta w_i^{(0)} + \dot{V}_{p,i} + \frac{1}{4}\partial_t\nabla^2\delta w_i^{(0)}\right). \quad (7.20)$$

We insert this into eq. (7.17) and arrive at

$$\mathbf{F}^{(0)} = \frac{g_p}{2\pi a^2}\int d^2\mathbf{z} e^{-\frac{z^2}{2a^2}}\left(\left[\partial_t - \mathbf{V}_p\cdot\nabla_z - \frac{\gamma}{2}\nabla^2 + \frac{1}{4}\partial_t\nabla^2\right]\delta w_i^{(0)} + \dot{\mathbf{V}}_p\right). \quad (7.21)$$

We now repeat the procedure to get rid of the Gaussian. The expansion of the velocity around $\mathbf{z} = 0$ is

$$\delta w_i^{(0)}(\mathbf{z},t) = \delta w_i^{(0)}(0,t) + e_{ij}(0,t)z_j + e_{ijk}(0,t)z_j z_k + ... \quad (7.22)$$

Inserting this expansion into eq. (7.21) and removing terms proportional to $\mathbf{z}$ since they vanish upon integration we get

$$\mathbf{F}^{(0)} = \frac{g_p}{2\pi a^2}\int d^2\mathbf{z} e^{-\frac{z^2}{2a^2}}\left[\partial_t \delta w_i^{(0)}(t) + \frac{1}{2}\partial_t e_{ijk}(t) z_k z_j - V_{p,j}e_{ij}(t) - \frac{\gamma}{2}e_{ijj}(t) + \frac{1}{4}\partial_t e_{ijj}(t)\right]. \quad (7.23)$$

Using that $\int d^2\mathbf{z} e^{-z^2/2a^2} = 2\pi a^2$ and $\int d^2\mathbf{z} z_j z_k e^{-z^2/2a^2} = 2\pi a^4\delta_{jk}$ the inertial force becomes at last

$$\mathbf{F}^{(0)} = g_p\dot{\mathbf{V}}_p(t) + g_p\left[\partial_t - \mathbf{V}_p(t)\cdot\nabla_z + \frac{a^2}{2}\partial_t\nabla_z^2 - \frac{\gamma}{2}\nabla_z^2 + \frac{1}{4}\partial_t\nabla_z^2\right]\delta\mathbf{w}^{(0)}(\mathbf{z},t)|_{\mathbf{z}=\mathbf{0}}. \quad (7.24)$$

The terms containing the Laplacian are analog to the Faxén corrections in the classical equations of motion eq. (4.25). In the classical case the Faxén corrections appears because of the finite size of the particle. Here they comes both from the effective size of the impurity a, the coherent length ξ and the interactions between the condensate and the thermal cloud γ. The last two effect remains even for a point particle in the limit $a \to 0$.

If the flow inhomogenities are small on the scale of a and ξ we can neglect the Faxén corrections. Going back to the variables $(\mathbf{r}, t)$ the equation for the force reads

$$\mathbf{F}^{(0)} = g_p \partial_t \delta\mathbf{v}^{(0)}(\mathbf{r}, t)|_{\mathbf{r}=\mathbf{r}_p}. \tag{7.25}$$

As for the classical case [43, 44] the difference of the partial derivative ∂_t and the material derivative D/Dt vanish here to leading order. Also in this case we think using D/Dt is more correct on physical grounds. If we consider a point like particle $a \to 0$ the interaction potential between the condensate and the impurity becomes a delta function. Since the interactions between the condensate particles are also a delta function(see section 2.3), one will expect that the acceleration of the impurity and a condensate particle is proportional. The force is then

$$\mathbf{F}^{(0)} = g_p \frac{D}{Dt} \delta\mathbf{v}^{(0)}(\mathbf{r}, t)|_{\mathbf{r}=\mathbf{r}_p}. \tag{7.26}$$

This corresponds to the classical inertial force eq. (4.17). In dimensional units this force is

$$\mathbf{F}^{(0)} = \frac{g_p}{g} m \frac{D}{Dt} \delta\mathbf{v}^{(0)}(\mathbf{r}, t)|_{\mathbf{r}=\mathbf{r}_p}. \tag{7.27}$$

Here $g_p m/g$ corresponds to the displaced mass in the classical expression. Where g_p/g have the same roll as the volume of fluid displaced by the sphere in the classical case.

7.1.2 Self-Induced Force.

We now turn our attention to the self induced force $\mathbf{F}^{(1)}$. As in the classical case our goal is to express this as a function of the impurities velocity $\mathbf{V}_p$ and the undisturbed condensate velocity $\mathbf{v}^{(0)}$. In this case we have only managed to find an expression for the density in Fourier space. We use this general expression to find the force on an impurity that is moving with a constant linear velocity in the steady-state. This expression is in the low velocity limit analogous to the Stoke drag, second term in eq. (4.25), in classical fluids.

As above we start by finding an equation for the density perturbation. We do this by considering eq. (7.10) and its complex conjugate

$$\partial_t \psi_1 = (i+\gamma)(\frac{\nabla^2}{2} - 1)\psi_1 - (i+\gamma)u_p(\mathbf{r} - \mathbf{r}_p) - (i+\gamma)\psi_1^*, \tag{7.28}$$

$$\partial_t \psi_1^* = (\gamma - i)(\frac{\nabla^2}{2} - 1)\psi_1^* - (\gamma - i)u_p(\mathbf{r} - \mathbf{r}_p) - (\gamma - i)\psi_1. \tag{7.29}$$

Where we have here written the potential on the form $\mathcal{U}_p(\mathbf{r}-\mathbf{r}_p) = g_p u_p(\mathbf{r}-\mathbf{r}_p)$. By adding and subtracting these two equations they can be rewritten to

$$\left[\partial_t - \gamma(\frac{1}{2}\nabla^2 - 2)\right](\delta\psi_1 + \delta\psi_1^*) = \frac{i}{2}\nabla^2(\delta\psi_1 - \delta\psi_1^*) - 2\gamma u_p, \tag{7.30}$$

$$(\partial_t - \frac{1}{2}\gamma\nabla^2)(\delta\psi_1 - \delta\psi_1^*) = i(\frac{1}{2}\nabla^2 - 2)(\delta\psi_1 + \delta\psi_1^*) - 2iu_p. \tag{7.31}$$

We could use this to find an expression for $\delta\rho_1$ as a function of $\delta\mathbf{v}^{(1)}$, but as stated before we want an expression that are only dependent on the velocity of the undisturbed flow $\delta\mathbf{v}^{(0)}$. We therefore remove the dependence on $\delta\mathbf{v}^{(1)}$ by acting with the operator $(\partial_t - \frac{1}{2}\gamma\nabla^2)$ on eq. (7.30) and using eq. (7.31). Using that $\delta\rho_1 = \delta\psi_1 + \delta\psi_1^*$ we get the folowing expression for the perturbed density

$$\left[\partial_t^2 + \gamma\partial_t(2-\nabla^2) - (1+\gamma^2)\nabla^2\big(1 - \frac{1}{4}\nabla^2\big)\right]\delta\rho_1 = \left[(1+\gamma^2)\nabla^2 - 2\gamma\partial_t\right]u_p. \tag{7.32}$$

This equation is a damped wave equation with $\left[(1+\gamma^2)\nabla^2 - 2\gamma\partial_t\right]u_p$ as a source term. Notice that the square bracket on the left and the quadratic equation for the dispersion relation eq. (3.9) are the same. This is expected since waves that are far away from the impurity should follow the dispersion relation. We can solve this equation by first taking the Fourier transform and then the Laplace transform. The solution reads

$$\delta\tilde{\rho}(k,s) = e^{-k^2a^2/2}\frac{2\gamma e^{-i\mathbf{k}\cdot\mathbf{r}_p(0)} - \left[(1+\gamma^2)k^2 + 2\gamma s\right]L(k,s)}{s^2 + \gamma s(2+k^2) + (1+\gamma^2)k^2(1+\frac{1}{4}k^2)}. \tag{7.33}$$

Here $L(k,s) = \int_0^\infty e^{-i\mathbf{k}\cdot\mathbf{r}_p(t)}e^{-st}dt$. We have assumed the initial conditions $\delta\rho_1 = \partial_t\delta\rho_1 = 0$, i.e the impurity is put into the condensate at $t = 0^+$. Taking the inverse Laplacian transform of this one get

$$\delta\tilde{\rho}(k,t) = e^{-k^2a^2/2}\Bigg[\frac{2\gamma e^{-\alpha t}\sin\Omega t}{\Omega}e^{-i\mathbf{k}\cdot\mathbf{r}_p(0)} - \int_0^t d\tau e^{-i\mathbf{k}\cdot\mathbf{r}_p(\tau)}e^{-\alpha(t-\tau)}\left(\frac{(1-\gamma^2)k^2 - 2\gamma\alpha}{\Omega}\sin\Omega(t-\tau) + 2\gamma\cos\Omega(t-\tau)\right)\Bigg]. \tag{7.34}$$

We have introduced the constants $\Omega^2 = (1+\gamma^2)k^2(1+\frac{k^2}{4}) - \alpha^2$ and $\alpha = \gamma(1+\frac{k^2}{2})$. Note that α and Ω are the imaginary and real part of the dispersion relation eq. (3.13). We see that α have taken the roll of a damping factor, while Ω is the frequency of the oscillations.

Equation (7.33) and (7.34) are the expressions for the density perturbations induced by an arbitrary moving impurity. In the general case it have been hard to transform the force obtained back to real space to compare it to the classical force. We have however managed to do this in the special case where the impurity is moving with constant low

velocity in the steady-state. Considering a constant velocity after $t = 0$ the solution of the integral in eq. (7.34) is

$$\begin{aligned}\delta\tilde{\rho} = e^{-k^2a^2/2}\Bigg[&\frac{2\gamma e^{-\alpha t}\sin\Omega t}{\Omega} \\ &- \Big((1-\gamma^2)k^2 - 2\gamma\alpha\Big)e^{-\alpha t}\frac{\Omega e^{(\alpha - i\mathbf{k}\cdot\mathbf{V}_p)t} - (\alpha - i\mathbf{k}\cdot\mathbf{V}_p)\sin\Omega t - \Omega\cos\Omega t}{\Omega[(\alpha - i\mathbf{k}\cdot\mathbf{V}_p)^2 + \Omega^2]} \\ &- 2\gamma e^{-\alpha t}\frac{(\alpha - i\mathbf{k}\cdot\mathbf{V}_p)e^{(\alpha - i\mathbf{k}\cdot\mathbf{V}_p)t} - (\alpha - i\mathbf{k}\cdot\mathbf{V}_p)\cos\Omega t + \Omega\sin\Omega t}{(\alpha - i\mathbf{k}\cdot\mathbf{V}_p)^2 + \Omega^2}\Bigg]. \quad (7.35)\end{aligned}$$

Where we have assumed that $\mathbf{r}_p(t = 0) = 0$. Assuming that the system have evolved to the steady-state we remove the terms that are decaying. We then get

$$\delta\tilde{\rho}_1 = -e^{k^2a^2/2}e^{-i\mathbf{k}\cdot\mathbf{V}_p t}\frac{(1+\gamma^2)k^2 - 2\gamma\alpha + 2\gamma(\alpha - i\mathbf{k}\cdot\mathbf{V}_p)}{(\alpha - i\mathbf{k}\cdot\mathbf{V}_p)^2 + \Omega^2}. \quad (7.36)$$

The factor $e^{-i\mathbf{k}\cdot\mathbf{V}_p t}$ is removed when transforming to the comoving frame. After some cleaning we see that the density perturbations induced by the particle is

$$\delta\tilde{\rho}_1 = e^{-k^2a^2/2}\frac{4(1+\gamma^2)k^2 - 8\gamma i\mathbf{k}\cdot\mathbf{V}_p}{4(\mathbf{k}\cdot\mathbf{V}_p)(\mathbf{k}\cdot\mathbf{V}_p + 2i\gamma + i\gamma k^2) - (1+\gamma^2)k^2(4+k^2)}. \quad (7.37)$$

We now insert the obtained expression for the density perturbations into eq. (7.8) and use the convolution theorem. The force is

$$\mathbf{F}^{(1)} = -\frac{g_p^2}{(2\pi)2}\int d^2\mathbf{k} i\mathbf{k}\delta\tilde{\rho}_1 e^{-k^2a^2/2}. \quad (7.38)$$

As in section 5.1 we decompose it into the component parallel with the velocity $\mathbf{V}_p$ and the component perpendicular to it. The component perpendicular to the velocity is zero because of symmetry. Inserting the expression for the Fourier modes of the density perturbations the parallel component of the force becomes

$$F_\parallel^{(1)} = -i\frac{g_p^2}{(2\pi)^2}\int\frac{k\cos\theta[4k^2(1+\gamma^2) - 8i\gamma kV_p\cos\theta]e^{-k^2a^2}kdkd\theta}{4kV_p\cos\theta(V_pk\cos\theta + i\gamma k^2 + 2i\gamma) - k^2(4+k^2)(1+\gamma^2)}. \quad (7.39)$$

In the limit $\gamma \to 0$ this becomes eq. (5.14). As stated above we want to find an expression similar to the Stokes' drag for classical fluids. To do that we assume that $V_p << 1$ and Taylor expand the integrand to first order in V_p. The force is then

$$F_\parallel^{(1)} = -\frac{4g_p}{\pi^2}\frac{\gamma}{1+\gamma^2}V_p\int_0^\infty\int_0^{2\pi}\frac{k^3\cos^2\theta e^{-k^2a^2}}{k^2+4}d\theta dk. \quad (7.40)$$

After integrating out θ it looks like

$$F_\parallel^{(1)} = -\frac{2g_p}{\pi^2}\frac{\gamma}{1+\gamma^2}V_p\int_0^\infty\frac{k^3e^{-k^2a^2}}{k^2+4}dk. \quad (7.41)$$

We can solve the integral by change of variables to $u = a^2(k^2 + 4)$. We then get

$$F_{\parallel}^{(1)} = -V_p \frac{\gamma}{1+\gamma^2} g_p \frac{1}{\pi} \left[e^{4a^2} E_1(4a^2)(1 + 4a^2) - 1 \right]. \tag{7.42}$$

Here $E_1(x) = \int_x^\infty du e^{-u} u^{-1}$ is the positive exponential integral. The force in the low V_p limit is similar to the Stoke drag in the classical case (second term eq. (4.25)). This force is caused by condensate particles scattering on the impurity, and it is related to a local heating of the condensate. Since there is not produced any exitations in the condensate it is implied that condensate particles are exited into the thermal cloud. The force vanishes at $\gamma = 0$ as it should. For a small particle we can expand the positive exponential integral as

$$E_1(4a^2) = -\gamma_E - \ln 4a^2. \tag{7.43}$$

Where $\gamma_E = 0.577...$ is the Euler-Mascheroni constant. The expression for the force then becomes

$$F_{\parallel} = -V_p \frac{\gamma}{1+\gamma^2} g_p^2 \frac{1}{\pi} [-\gamma_E - 1 - \ln 4a^2] = -V_p \frac{\gamma}{1+\gamma^2} g_R^2 \frac{1}{\pi}. \tag{7.44}$$

Where $g_R^2 = g_p^2[-\gamma_E - 1 - \ln 4a^2]$ is the renormalized coupling constant. In the limit of a point like particle $a \to 0$ it diverges.

7.2 Comparison With Numerics

7.2.1 Density Variations and Self-Induced Drag

When we start the simulation as described in chapter 6 the impurity emits waves. This is because we start the simulation in the condensates ground state with the impurity at rest, and then start to move the impurity with velocity $\mathbf{V}_p$ at time $t = 0$. The ground state with the impurity at rest is not the ground state with the impurity moving at constant velocity V_p, which causes the system to emit exitations. The simulation is done in the comoving frame of the impurity. In this cordinate frame the impurity is stationary, and $\mathbf{V}_p$ is the far field velocity of the condensate. We refer to the velocity $\mathbf{V}_p$ as the impurity's velocity, since the condensate is stationary in the lab frame. The initial

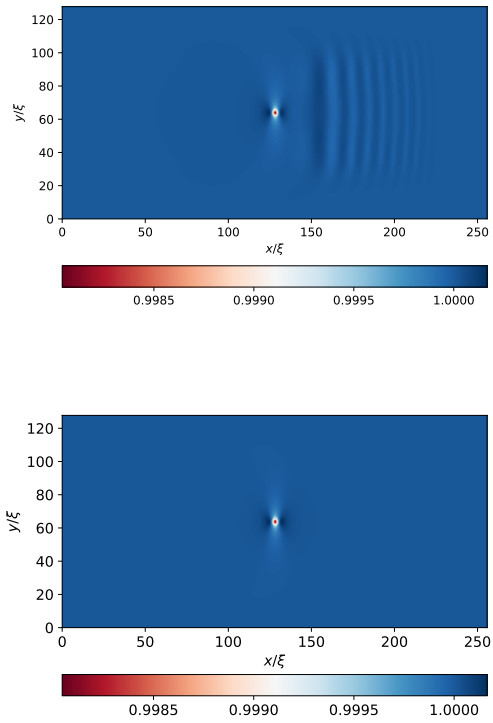

Figure 7.1: Snapshots of the density profile of the condensate for $V_p = 0.9$ and $\gamma = 0$. The top picture is taken at time $t = 200$ and shows the initial waves have detached from the impurity and are propagating away from it. The waves traveling down stream have already reached the buffer region. The botom picture is taken at time $t = 2000$. Here all the density perturbations have reached the buffer region and have dissipated out of the system. The condensate have become symmetric around the impurity.

waves created around the impurity will propagate away from the particle following the

dispersion relation in eq. (3.10). As we can see from eq. (3.11) the group velocity for waves in the long wavelength limit is for $\gamma = 0$ the Landau critical velocity $v_c = 1$ in dimensionless units. The waves with short wavelength travels faster. The behaviour of the system is depending on whether the impurity is moving slower or faster than the critical velocity.

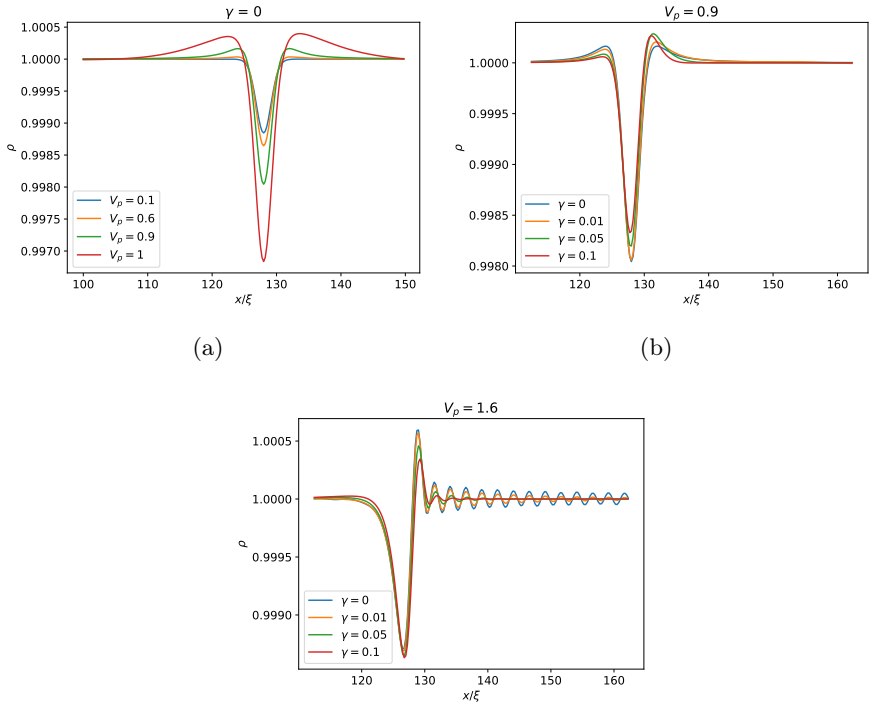

(a) (b)

(c)

Figure 7.2: One dimensional density profile of the condensate. In (a) $\gamma = 0$ and we can see that up to $V_p = 1$ the density is symmetric around the impurity. If one look close one can see that the $V_p = 1$ curve is slightly asymmetrical. In figure (b) and (c) the velocity is fixed as 0.9 and 1.6 respectively so that we can see the effect of γ. In (b) we see the asymmetries that are caused by the finite γ, while in (c) we see that γ is damping out the oscillations in front of the impurity. From eq. (5.3) we see that an asymmetric density is related to a non-zero force on the impurity.

If the impurity is moving with velocity $V_p < 1$ the waves moves faster than the particle, and they will eventually reach the buffer region with large γ and be dissipated. This is illustrated in figure 7.1. Which shows the condensate for $V_p = 0.9$ and $\gamma = 0$ in the transient regime and the steady-state. We can see that the waves have detached from the impurity and eventually dissipates out of the system. The time it takes for the waves to reach the buffer region increases with the impurity velocity, since the relative velocity between the waves and the impurity becomes smaller. When the initial waves have left the system it reaches a steady-state. For $\gamma = 0$ the density in the steady-

state is symmetric. This is shown in figure 7.2 (a) for different velocities up to $V_p = 1$. In the $V_p = 1$ case the density goes towards the symmetric state asymptotically, but we never see it reach a symmetric state. For $\gamma > 0$ the system also reaches a steady-state. However in this case the density does not become symmetric around the impurity. This is illustrated in figure 7.2 (b). Where we see the one dimensional profile of the condensate density for $V_p = 0.9$ and different values for γ. Here one can see that the density becomes asymmetric for non-zero γ. From the expression of the force eq. (5.3) we see that an asymmetric density means that there is a non-zero force acting on the impurity. This is consistent with the self-induced drag force in the steady-state eq. (7.39), which for subsonic velocities only gives a non-zero force for $\gamma > 0$.

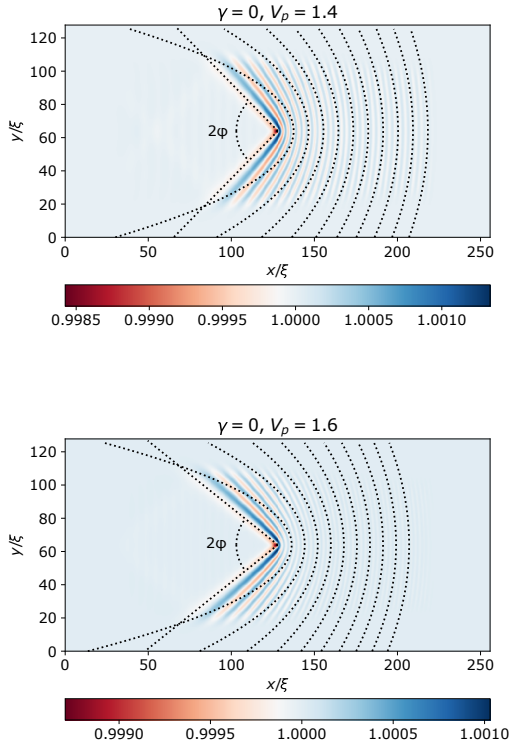

Figure 7.3: Snapshot of density profile of the condensate for large velocities in the steady-state for $\gamma = 0$. The top picture is at $V_p = 1.4$ and the bottom is $V_p = 1.6$. One can see that there are formed fringes in front of the impurity and a wake behind. The angle of the wake ϕ is marked with the doted lines. This angle decreases when the velocity increases. The parabolas given by eq. (5.37) are also plotted as doted lines. It looks like the parabolas describes the wave tops fare from the particle better than the one that are close. The waves that are fare from the particle is a bit hard to see.

If the impurity moves with velocity $V_p > 1$ it starts to emit exitations other than

the initial waves. In this case there are formed fringes in front of the impurity and a wake behind it as we have discussed in section 5.3. This is shown in figure 7.3, which shows a snapshot of the density of the condensate for $\gamma = 0$ and $V_p = 1.4$ and 1.6. We have also plotted the lines given by eq. (5.31) and the parabolas given by eq. (5.37) with $N = 4, 8, ..., 40$. There is preformed a coordinate change since we don't have the particle at the origin. We can see that the waves that are attached to the particle are described by the conical surface with an angle obeying $\sin\phi = 1/V_p$, while far away the waves become parabolic. The parabolas in eq. (5.37) describes the waves poorly close to the particle, but further away it looks like the fit is getting better. The parabolas does however not describe the tops perfectly and predict that the tops should be closer than they are. This poor fit of the parabolas are caused by the waves with intermediate wavelengths that are not described by neither the linear nor the quadratic dispersion relation, but has to be described by the full relation.

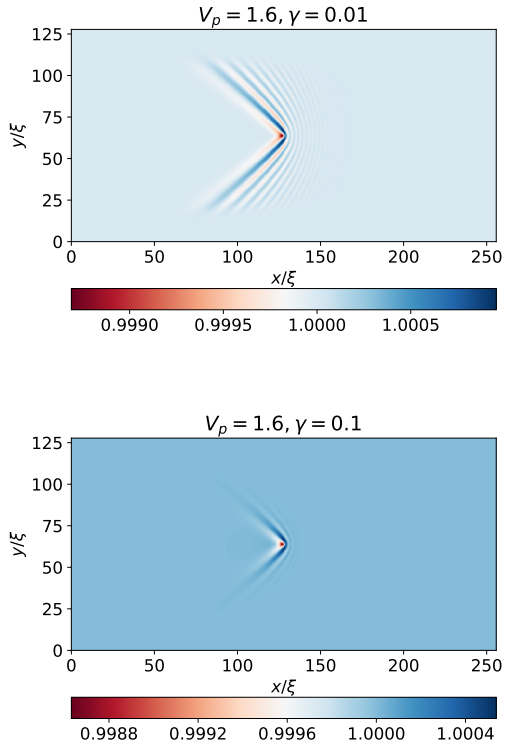

Figure 7.4: Snapshot of the condensate in the steady-state for an impurity traveling at $V_p = 1.6$ for different values of the thermal drag γ. On the top $\gamma = 0.01$ while on the bottom $\gamma = 0.1$. It is clear that a higher value of γ is damping the waves in the condensate.

For non-zero γ the fringes becomes damped. The damping effect of γ is shown in figure 7.4 and 7.2 (c). In the former we see the one dimensional density profile of the

condensate at $V_p = 1.6$ for different values of γ. In figure 7.4 we see the snapshots of the condensate for $V_p = 1.6$ for two different values of γ. We can here see that a higher value is related to a stronger damping of the waves, in agreement with the imaginary part of the dispersion relation eq. (3.10).

The numerically obtained force on the impurity in the steady-state as a function of velocity is shown in figure 7.5, together with the analytical predictions from eq. (7.39) and (7.42). We can see that the force is split in two regimes. The first regime is for $V_p < 1$. Here the impurity doesn't produce any exitations after the emission of the initial waves. For $\gamma > 0$ there is a non-zero drag force acting on the particle in this regime. This force in the steady-state is associated with a local heating, which is implying that condensate particles are escaping into the thermal cloud. We see that it increases with γ as long as $\gamma << 1$. In the insertion of the figure we see the low velocity limit. In this limit the drag force is linearly dependent on the velocity, and eq. (7.42) captures the behavior well. From the proportionality constant we can see that this Stokes like drag force is caused by the thermal drag. For $V_p > 1$ the impurity starts to emit waves. The emission of waves is related to a non-zero force even in the $\gamma = 0$ case. We can see that the size of the force is decreasing when γ increases. This is because the damping factor in the dispersion relation is proportional to γ and therefore the state becomes less asymmetric with increasing γ. If we look at the values for $\gamma = 0$ we can see a clear transition from a superfluid flow at $V_p = 1$. Looking close at the numerically obtained value at $V_p = 1$ one notice that it is slightly larger than zero. This is because we did not evolve the system long enough for the density to become symmetric. The curves for $\gamma > 0$ does also have a transition with an abrupt change in the behaviour of the force close to $V_p = 1$. This transition is more visible for small γ.

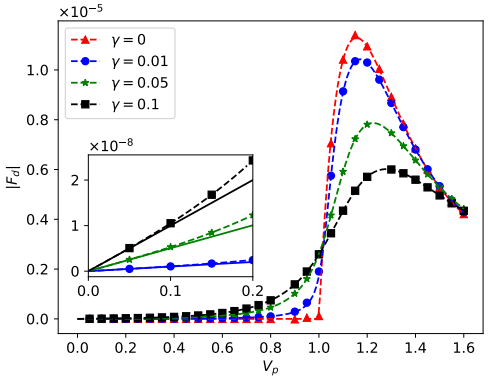

Figure 7.5: The figure shows the self-induced drag force on the impurity in the steady-state as a function of the velocity. The symbols are the average values of the force from eq. (5.3) in the steady-state based on simulations of the dGPE in the comoving frame as discussed in chapter 6. The dashed lines are the analytical predictions eq. (5.21) for $\gamma = 0$ and eq. (7.39) for $\gamma > 0$. The insertion shows the small V_p behavior for $\gamma > 0$. The solid lines are the linear approximation given by eq. (7.42).

7.2.2 Inertial Force

To measure the inertial force we consider test particles moving with the impurity. The test particles have a potential similar to the impurity eq. (7.1), with coupling strength g' and size a'. These potentials are not coupled to the condensate, such that the test particles are not altering the flow. The force on the particles are therefore only caused by the density perturbations induced by the impurity, and can be described by eq. (7.7). We can therefore approximate this force to leading order as eq. (7.25). We don't use eq. (7.26) since the difference between the expressions are small for the systems we are testing. A comparison between the potential force eq. (5.3) and the leading order approximation on a test particle located at position $(10, 20)$ relative to the impurity is shown in figure 7.6. The figure shows the x component of the force for different particle sizes and stirring velocities.

For small particles the approximation follows the main behavior of the potential force well, but it predicts a bit larger amplitudes. When we increase the size of the particle the approximation overshoots more and shows oscillations that is not present in the potential force. If one look at the second order corrections eq. (7.24) one should expect that a larger size of the test particle will cause larger deviation from the first order approximations. For $a' = 1$ the corrections due to the size of the particle should be twice the corrections due to the coherence length. At this impurity size we are at the limit of where we expect the Taylor expansion that were used to integrated out the Gaussian when deriving eq. (7.24) to be valid. The expansion is valid as long as the range of the Gaussian is small compared to variations in the condensate, but when $a = 1$ the particle size is the healing length ξ which sets the scales of variations. When $a > 1/2$ the Gaussian is falling off slower than the Bessel Function.

When we increase the velocity the overshoot of the amplitudes gets a bit larger, but the leading order approximation is still giving a good estimate for the small test particles for velocities up to the critical velocity $V_p = 1$. If we put the test particles at different positions in the condensate the forces would be similar, but the time the initial waves uses to pas the particles varies making the extent of the force different.

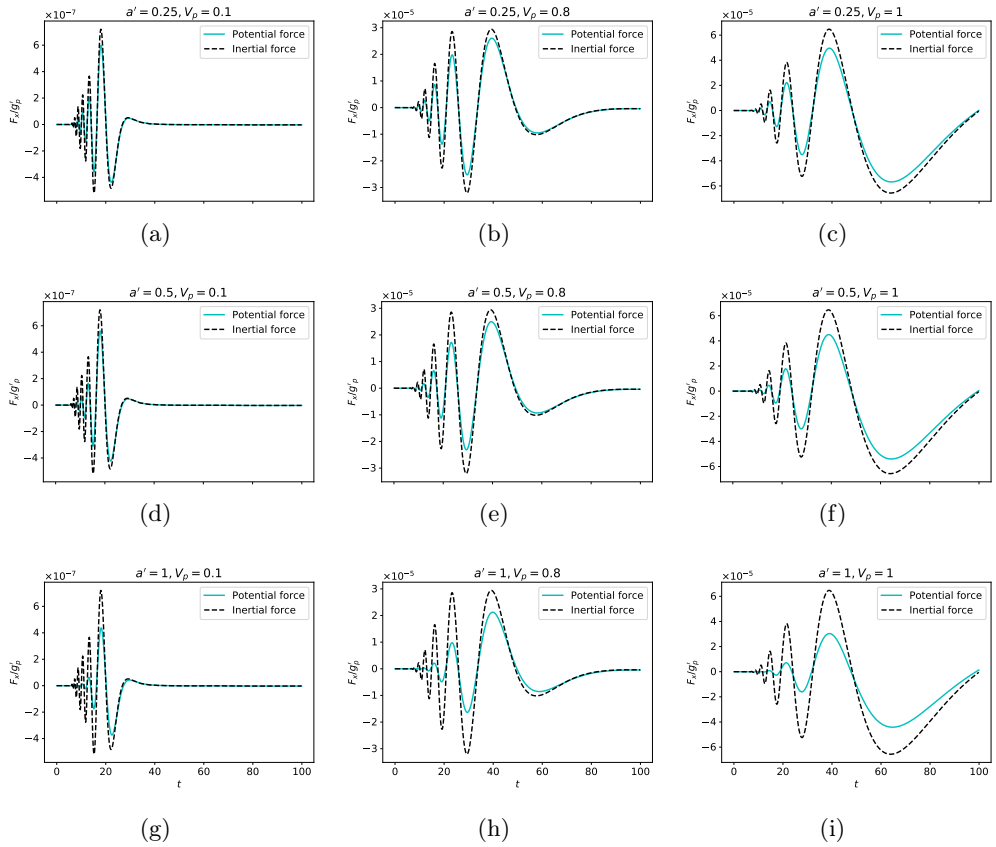

Figure 7.6: Plot of the x component of the inertial force F_x/g'_p on a test particle at relative position $(10, 20)$ with respect to the impurity that are creating the perturbations in the flow, for $\gamma = 0.01$ and $a' = 0.25, 0.5$ and 1. The cyan line is the force calculated from eq. (5.3), while the doted black line is the approximation given by eq. (7.25) in the comoving frame. The velocity V_p is the same for the impurity and the test particle. The size a' refers only to the size of the test particle. The size of the impurity is fixed as $a = 1$.

Chapter 8

Conclusion and Outlook

In this thesis we have studied the coupled dynamics between a two dimensional Bose-Einstein condensate and an impurity at finite temperatures. By theoretical analysis of the damped Gross-Pitaevskii equation we found the hydrodynamic forces acting on a small impurity placed in the condensate. The force on the impurity was treated analytical in the regime of a small impurity-condensate coupling g_p and thermal drag γ. We decomposed it into the self-induced force that was due to the perturbations caused by the particle and the inertial force that was caused by the undisturbed flow. We showed that the later was proportional to the local condensate acceleration in the limit where the condensate was slowly varying on the scales of the particle size and the healing length. This is in analogy to the inertial term in the Maxey-Riley equation for an inertial particle in a classical incompresible fluid. The corrections due to the finite size of the particle, the thermal drag and the healing length takes the same form as the Faxén corrections that are caused by the finite size of the sphere submerged into the classical fluid. The self-induced force was then found for a system in the steady-state in the impurity's reference frame, and we showed that in the low velocity limit this is proportional to the relative velocity between the impurity and the condensate. This is equivalent to the classical Stokes' drag. The proportionality constant is dependent on the thermal drag γ and the particle size a. In the limit where $\gamma = 0$ the drag force vanishes, allowing for a dissipationless flow. The full expression we found reduces to the known equation for the force in the $\gamma = 0$ limit. The obtained expressions was then tested numerically by integrating the damped Gross-Pitaevskii equation for a condensate that is stirred by an impurity moving with a constant velocity. We compared the forces with the force given by the Erhenfest theorem. The tests show that the inertial force agrees well with the analytical expression as long as the particle is small. The self-induced force shows good agreement in the steady-state for the parameters considered. During the testing we also observed several well known properties of the condensate like superfluid flow and the Bogoliubov-Čerenkov wake.

When working with the thesis there have come up some questions that can set the direction for further studies. One thing to notice is that the expression we found for the self-induced force is only valid in the steady-state, so we have not found a general

hydrodynamic equation for the motion of the impurity. We do expect that such an equation will include terms analog with the classical Basset-history integral and the added mass force. Also the forces we have gotten are not valid close to vortices, or for strongly coupled or large impurities. It would therefore be interesting to extend our discussion to the regions where the impurity is close to or nucleates vortices, and study the vortex-impurity interactions. Also it would be interesting to see which effect the noise terms that are neglected in the dGPE have on the interaction between the condensate and the impurity.

Another thing that would be interesting to look more into is how the impurity potential are changing the Landau critical velocity. In the discussion in section 3.2 we found an expression for the critical velocity in a condensate that was unaffected by any potential. It would be interesting to investigate numerically and analytically how a non-zero potential will affect the critical velocity. Also the wave pattern that is created by an impurity traveling at velocities larger than the critical velocity looks qualitatively the same regardless of the value of γ, but the waves becomes more damped. It would therefore be interesting to have a more detailed study of this, and see what the effects of γ is both analytically and numerically.

Appendix

Appendix A

Paper Submitted to the New Journal of Physics

Classical analogies for the force acting on an impurity in a Bose-Einstein condensate

Jonas Rønning[1], Audun Skaugen[2], Emilio Hernández-García[3], Cristóbal López[3], Luiza Angheluta[1]

[1]PoreLab, The Njord Centre, Department of Physics, University of Oslo, P. O. Box 1048, 0316 Oslo, Norway

[2]Computational Physics Laboratory, Tampere University, P.O. Box 692, FI-33014 Tampere, Finland

[3]IFISC (CSIC-UIB), Instituto de Fisica Interdisciplinar y Sistemas Complejos, 07122 Palma de Mallorca, Spain

Abstract.

We study the hydrodynamic forces acting on a small impurity moving in a two-dimensional Bose-Einstein condensate at non-zero temperature. The condensate is modelled by the damped-Gross Pitaevskii (dGPE) equation and the impurity by a Gaussian repulsive potential coupled to the condensate. For weak coupling, we obtain analytical expressions for the forces acting on the impurity, and compare them with those computed through direct numerical simulations of the dGPE and with the corresponding expressions for classical forces. For non-steady flows, there is a time-dependent force dominated by inertial effects and which has a correspondence in the Maxey-Riley theory for particles in classical fluids. In the steady-state regime, the force is dominated by a self-induced drag. Unlike at zero temperature, where the drag force vanishes below a critical velocity, at low temperatures the impurity experiences a net drag even at small velocities, as a consequence of the energy dissipation through interactions of the condensate with the thermal cloud. This dissipative force due to thermal drag is similar to the classical Stokes' drag. There is still a critical velocity above which steady-state drag is dominated by acoustic excitations and behaves non-monotonically with impurity's speed.

1. Introduction

The motion of an impurity suspended in a quantum fluid depends on several key factors such as the superfluid nature and flow regime, as well as the size of the impurity and its interaction with the surrounding fluid [1, 2, 3, 4, 5]. Therefore, it is disputable whether the forces acting on an impurity in a quantum fluid should bear any resemblance to classical hydrodynamic forces. In the case of an impurity immersed in superfluid liquid helium, classical equations of motion and hydrodynamic forces are assumed a priori [6], since impurities are typically much larger than the coherence length and then quantum hydrodynamic effects like the quantum pressure can be neglected. For Bose-Einstein condensates (BEC) in dilute atomic gases, impurities can be neutral atoms [7], ion impurities [8, 9] or quasiparticles [10]. The size of an impurity in a BEC is typically of the same order of magnitude or smaller than the coherence length, and quantum hydrodynamic effects cannot be readily ignored.

There are several theoretical and computational studies of the interaction force between an impurity and a BEC at zero absolute temperature, using different approaches depending on the nature of the particle and its interaction with the condensate. A microscopic approach is used to analyse the interaction of a rigid particle with a BEC by solving the Gross-Pitaevskii equation (GPE) for the condensate macroscopic wavefunction and using boundary conditions such that the condensate density vanishes at the particle boundary [11]. This methodology allows to study complex phenomena such as vortex nucleation and flow instabilities, but it is more oriented to find the effects of an obstacle on the flow rather than the coupled particle-flow dynamics. In addition, the boundary condition introduces severe nonlinearities which can only be addressed numerically. At a more fundamental level of description, the impurity is treated as a quantum particle with its own wavefunction described by the Schrödinger equation and that is coupled with the GPE for the macroscopic wavefunction of the BEC [12]. A more versatile model for the interaction of impurities with the BEC has been explored in several papers [3, 4, 13, 14, 5, 15]. Here, an additional repulsive interaction (a Gaussian or delta-function potential) is added to model scattering of the condensate particles with the impurity. The force on the impurity is determined by this repulsion potential and the superfluid density through the Ehrenfest theorem. The strong-coupling limit of this repulsive potential would be equivalent to the rigid boundary-condition approach. Within this modelling approach, some works have studied the complex motion of particles interacting with vortices in the flow, and the indirect interactions between them arising from the presence of the fluid [4, 14]. Another line of research using this type of modelling focused mainly on the superfluidity criterion of an equilibrium BEC [3, 16, 17, 18, 19, 5] and non-equilibrium BEC at zero temperature [20]. Within the Bogoliubov perturbation analysis for a small impurity with weak coupling, analytical expressions can be derived for the steady-state force on the impurity. At zero temperature, this force vanishes below a critical velocity and corresponds to the dissipationless motion. Above this velocity identified through Landau criterion as the

speed of the long-wavelength sound waves, there is a net drag force and the motion of the impurity is damped by acoustic excitations. While this is a form of drag, in that the force opposes motion by dissipating energy, it is not the same as the classical Stokes' drag in viscous fluids. Recent experiments probing superfluidity in a BEC are able to indirectly estimate the drag force by measuring the local heating rate in the vicinity of the moving laser beam and show that there is still a critical velocity even at non-zero temperatures and that the critical velocity is lower for a repulsive potential than for an attractive one [21].

In this paper, we study the forces exerted on an impurity moving in a two-dimensional BEC at low temperature, using an approach similar to [3, 4, 13, 14, 5], in which a repulsive Gaussian potential is used to describe the interaction of the particle with the BEC, but using a dissipative version of the GPE. Our aim is to bridge this microscopic approach with the phenomenological descriptions [6] that assume that the forces from the superfluid are the same as those from a classical fluid in the inviscid and irrotational case. As in the classical-fluid case, we find that the force is made of two contributions: One of them, dominant for very weak fluid-particle interaction, bears a rather complete analogy with the corresponding force in classical fluids (inertial or pressure-gradient force), which depends on local fluid acceleration and includes the so-called Faxén corrections arising from velocity inhomogeneities close to the particle position [22]. The difference is that, in a classical fluid, these corrections arise from the finite size of the particle and vanish when the particle size becomes zero. In the BEC, Faxén-type corrections arise both from the particle size (modeled by the range of the particle repulsion potential) and from the BEC coherence length. As fluid-particle interaction becomes more important, a second contribution to the force becomes noticeable, which takes into account the drag on the particle arising from the perturbation of the flow produced by the presence of the particle. This is also called the particle *self-induced* force. We are able to obtain explicit formulae for the steady-state motion of the particle in an otherwise homogeneous and steady BEC. This drag is a dissipative (damping) force due to thermal drag of the BEC with the thermal cloud. It occurs in addition to the drag due to acoustic excitations in the condensate that occurs only above a critical velocity. It can be compared with the corresponding force in classical fluids, namely the viscous Stokes drag. We find an analytical expression for this self-induced drag at arbitrary speeds and show that in the low speed limit, it reduces to a linear dependence on speed akin to the classical Stokes drag.

The rest of the paper is structured as follows. In Sect. 2, we discuss the general modelling setup and in Sect. 3 a perturbation analysis is used to derive the linearised equations for the perturbations in the wavefunction related to non-steady condensate flow and the particle repulsive potential. Subsections 3.1 and 3.2 derive analytical expressions within perturbation theory for the two contributions to the force experienced by the particle. In Section 4, we compare our theoretical predictions with numerical simulations of the dissipative GPE coupled to the impurity, and the final section summarises our conclusions.

2. Modelling approach

We model the interaction between the impurity and a two-dimensional (2D) BEC through a Gaussian repulsive potential which can be reduced to a delta-function limit similar to previous studies [3, 5]. The BEC at low temperatures is well-described by the damped Gross Pitaevskii equation (dGPE) for the condensate wavefunction $\psi(\boldsymbol{r}, t)$ [23, 24, 25, 26, 27, 28, 29]:

$$i\hbar\partial_t\psi = (1 - i\gamma)\left(-\frac{\hbar^2}{2m}\nabla^2 + g|\psi|^2 - \mu + V_{ext} + g_p\mathcal{U}_p\right)\psi, \tag{1}$$

where g is an effective scattering parameter between condensate atoms. V_{ext} is any external potential used to confine or stir the condensate. The damping coefficient $\gamma > 0$ also called the thermal drag is related to the net exchange of atoms through collisions between thermal atoms with each other or with the condensate at fixed chemical potential μ. In the low-temperature limit, this damping γ is very small and can be expressed as a function of temperature T [30, 25]. The dGPE is a phenomenological model that can also be derived from the stochastic GPE in the low temperature limit where noise is negligible [23, 24]. The dGPE has been used extensively to study different vortex regimes from vortex lattices [25] to quantum turbulence [28, 31, 27, 26, 32] and was shown to capture well, at least qualitatively, experimental observations [32].

A hydrodynamic description of the BEC uses the Madelung transformation of the wavefunction $\psi = |\psi|e^{i\phi}$ to define the condensate density as $\rho(\boldsymbol{r}, t) = |\psi(\boldsymbol{r}, t)|^2$ and the condensate velocity as $\boldsymbol{v}(\boldsymbol{r}, t) = (\hbar/m)\nabla\phi(\boldsymbol{r}, t)$. This velocity can also be obtained from the superfluid current $\boldsymbol{J}(\boldsymbol{r}, t)$ as

$$\boldsymbol{J} = \frac{\hbar}{2mi}\left(\psi^*\nabla\psi - \psi\nabla\psi^*\right) = \rho\boldsymbol{v}, \tag{2}$$

where ψ^* denotes the complex conjugate of ψ. In addition to damping the BEC velocity, the presence of $\gamma \neq 0$ in the dGPE also singles out the value $\rho_h = |\psi|^2 = g/\mu$ as the steady homogeneous density value when the phase is constant and $V_{ext} = 0$.

The interaction potential $\mathcal{U}_p(\boldsymbol{r} - \boldsymbol{r}_p)$ between the condensate and the impurity is modelled by a Gaussian potential $\mathcal{U}_p(\boldsymbol{r} - \boldsymbol{r}_p) = \mu/(2\pi\sigma^2)e^{-(\boldsymbol{r}-\boldsymbol{r}_p)^2/(2\sigma^2)}$. The parameter $g_p > 0$ is the weak coupling constant for repulsive impurity-condensate interaction, $\boldsymbol{r}_p = \boldsymbol{r}_p(t)$ denotes the center-of-mass position of the impurity, and σ its effective size. Here we consider an impurity of size σ of the order the coherence length $\xi = \hbar/\sqrt{m\mu}$ of the condensate. The impurity is too small to nucleate vortices in its wake [33]. Instead, it will create acoustic excitations with Bogoliubov-Čerenkov wake. Similar wave fringes in the condensate density have been reported numerically in [2] for a different realisation of non-equilibrium Bose-Einstein condensates. In the limit of a point-like impurity, the Gaussian interaction potential converges to a two-body scattering potential $\mathcal{U}_p(\boldsymbol{r}-\boldsymbol{r}_p, t) = \mu\delta(\boldsymbol{r}-\boldsymbol{r}_p(t))$ that has been used in previous analytical studies [3, 4, 13, 14]. Note that we are modelling only the interaction of the particle with the BEC, so that the viscous-like drag we obtain arises from the indirect coupling to the thermal bath

via the BEC. Any direct interaction of the particle with the thermal cloud will lead to additional forces which could be important at high temperatures, and which are not included here.

In order to gain insight into the forces and their relationship with the classical case, we keep the set-up as simple as possible. We consider a 2D condensate and assume that the size of the condensate is large enough so that we can neglect inhomogeneities in the confining part of V_{ext}. Also, we consider a neutrally buoyant impurity so that effects of gravity can be neglected. This would imply $V_{ext} = 0$ except if an external forcing is introduced to stir the system, in which case we assume the support of this external force is sufficiently far from the impurity.

The impurity and the condensate will exert an interaction force on each other that is determined by the Ehrenfest theorem for the evolution of the center-of-mass momentum of the particle. The potential force $-g_p \nabla \mathcal{U}_p(\boldsymbol{r} - \boldsymbol{r}_p)$ is the force exerted by an impurity on a condensate particle at position $\boldsymbol{r}$. By space averaging over condensate density, we then determine the force exerted by the impurity on the condensate as $-g_p \int d\boldsymbol{r} |\psi(\boldsymbol{r}, t)|^2 \nabla \mathcal{U}_p(\boldsymbol{r} - \boldsymbol{r}_p)$ [14]. Hence, the force acting on the impurity has the opposite sign and is equal to

$$\boldsymbol{F}_p(t) = + g_p \int d^2\boldsymbol{r} |\psi(\boldsymbol{r}, t)|^2 \nabla \mathcal{U}_p(\boldsymbol{r} - \boldsymbol{r}_p) \tag{3}$$

which, through an integration by parts, is equivalent to

$$\boldsymbol{F}_p(t) = - g_p \int d^2\boldsymbol{r}\ \mathcal{U}_p(\boldsymbol{r} - \boldsymbol{r}_p, t) \nabla |\psi(\boldsymbol{r}, t)|^2. \tag{4}$$

Note that this last expression can also be used, reversing the sign, to give the force exserted on the BEC by a laser of beam profile given by $\mathcal{U}_p$.

At zero temperature, i.e. $\gamma = 0$, and if we neglect the effect of quantum fluctuations [17, 16, 18, 19], the impurity moves without any drag through a uniform condensate below a critical velocity, which is the low-wavelength speed of sound $c = \sqrt{\mu/m}$, as determined by the condensate linear excitation spectrum, in agreement with Landau's criterion of superfluidity [3]. Above the critical speed, the impurity will create excitations, and depending on the size of the impurity these excitations range from acoustic waves (Bogoliubov excitation spectrum) to vortex dipoles and to von-Karman street of vortex pairs [33]. Previous studies focused on the theoretical investigations of the self-induced drag force and energy dissipation rate in the presence of Bogoliubov excitations emitted by a pointwise [3, 16, 19] or finite-size [5] particle, or numerical investigations of the drag force due to vortex emissions [1, 13, 14]. The energy dissipation rate depends on whether the impurity is heavier, neutral or lighter with respect to the mass of the condensate particles [14]. The dependence on the velocity of the self-induced drag force above the critical velocity changes with the spatial dimensions [3]. This means that the energy dissipation rate is also dependent on the spatial dimensions. If instead of a single impurity one considers many of them there will be, besides direct inter-particle interactions, additional forces between the impurities mediated by the flow, leading to a much more complex many-body dynamics even in an otherwise uniform condensate,

as discussed in [4]. Here we neglect all these effects and consider a single impurity in a 2D BEC.

We rewrite the dGPE in dimensionless units by using the characteristic units of space and time in terms of the long-wavelength speed of sound $c = \sqrt{\mu/m}$ in the homogeneous condensate and the coherence length $\xi = \hbar/(mc) = \hbar/\sqrt{m\mu}$. Space is rescaled as $\boldsymbol{r} \to \tilde{\boldsymbol{r}}\xi$ and time as $t \to \tilde{t}\xi/c$. In addition, the wavefunction is also rescaled $\psi \to \tilde{\psi}\sqrt{\mu/g}$, where g/μ is the equilibrium particle-number density corresponding to the solution with constant phase if $V_{ext}, \mathcal{U}_p = 0$. The external potential, $V_{ext} = \mu\tilde{V}_{ext}$, and the interaction potential, $g_p\mathcal{U}_p = \mu\tilde{g}_p\tilde{\mathcal{U}}_p$, are measured in units of the chemical potential μ with $\tilde{\mathcal{U}}_p = 1/(2\pi a^2)e^{-(\tilde{r}-\tilde{r}_p)^2/(2a^2)}$, and $a = \sigma/\xi$, $\tilde{g}_p = g_p/(\xi^2\mu)$. Henceforth, the dimensionless form of the dGPE reads as

$$\tilde{\partial}_t\tilde{\psi} = (i+\gamma)\left(\frac{1}{2}\tilde{\nabla}^2 + 1 - \tilde{V}_{ext} - \tilde{g}_p\tilde{\mathcal{U}}_p - |\tilde{\psi}|^2\right)\tilde{\psi}. \tag{5}$$

In these dimensionless units, the force from Eq. (4) exerted on an impurity reads as $\boldsymbol{F}_p = (\mu^2\xi/g)\tilde{\boldsymbol{F}}_p$, where

$$\tilde{\boldsymbol{F}}_p(t) = -\tilde{g}_p\int d^2\tilde{\boldsymbol{r}}\tilde{\mathcal{U}}_p(\boldsymbol{r}-\boldsymbol{r}_p)\tilde{\nabla}|\tilde{\psi}(\tilde{\boldsymbol{r}},t)|^2. \tag{6}$$

For the rest of the paper, we will now omit the tildes over the dimensionless quantities.

In the limit of a point-like particle, $\mathcal{U}_p = \delta(\boldsymbol{r}-\boldsymbol{r}_p)$, the force from Eq. (6) becomes

$$\boldsymbol{F}_p(t) = -g_p\nabla|\psi(\boldsymbol{r},t)|^2|_{\boldsymbol{r}=\boldsymbol{r}_p(t)}. \tag{7}$$

3. Perturbation analysis

For a weakly-interacting impurity, the condensate wavefunction ψ can be decomposed into an unperturbed wavefunction $\psi_0(\boldsymbol{r})$ describing the motion and density of the fluid in the absence of the particle and the perturbation $\delta\psi_1(\boldsymbol{r})$ due to the impurity's repulsive interaction with the condensate, hence $\psi = \psi_0 + g_p\delta\psi_1$. Weak particle-condensate interaction condition is that $\max(g_p\mathcal{U}_p) \ll 1$, or $g_p \ll 2\pi a^2$, which means that the particle-condensate interaction of strength g_p and range σ is small compared with the energy scale given by the chemical potential $\mu = 1$ (dimensionless units).

The unperturbed wavefunction $\psi_0(\boldsymbol{r},t)$ can be spatially-dependent, if it is initialised in a nonequilibrium configuration, or if external forces characterised by V_{ext} are at play. Here, we consider deviations with respect to the steady and uniform equilibrium state ($\psi_h = 1$ in dimensionless units). As stated before, we do not consider large extended inhomogeneities produced by a trapping potential, and assume that any stirring force acting on the BEC is far from the particle. Thus, we treat inhomogeneities close to the particle as small perturbations to the uniform state $\psi_h = 1$: $\psi_0(\boldsymbol{r},t) = 1 + \delta\psi_0(\boldsymbol{r},t)$. Combining the two types of perturbations, and using the relationships of the wavefunction to the density, velocity and current (Eq. (2), which in dimensionless

units reads $\rho\boldsymbol{v} = (\psi^*\nabla\psi - \psi\nabla\psi^*)/(2i))$ we find

$$\psi = 1 + \delta\psi_0 + g_p\delta\psi_1 \tag{8}$$

$$\rho = 1 + \delta\rho_0 + g_p\delta\rho_1, \tag{9}$$

$$\boldsymbol{v} = \delta\boldsymbol{v}^{(0)} + g_p\delta\boldsymbol{v}^{(1)}, \tag{10}$$

where

$$\delta\rho_0 = \delta\psi_0 + \delta\psi_0^*, \quad \delta\rho_1 = \delta\psi_1 + \delta\psi_1^*, \tag{11}$$

$$\delta\boldsymbol{v}^{(0)} = \frac{1}{2i}\nabla\left(\delta\psi_0 - \delta\psi_0^*\right), \quad \delta\boldsymbol{v}^{(1)} = \frac{1}{2i}\nabla(\delta\psi_1 - \delta\psi_1^*). \tag{12}$$

Combining Eq. (6) with the expressions for the density perturbations, we have that the total force can be split into the contribution from the density variations in the BEC by causes external to the particle (initial preparation, stirring forces in V_{ext}, ...), and the density perturbations due to the presence of the particle $\boldsymbol{F}_p = \boldsymbol{F}^{(0)} + \boldsymbol{F}^{(1)}$:

$$\boldsymbol{F}^{(0)}(t) = -\frac{g_p}{2\pi a^2}\int d^2\boldsymbol{r}e^{-\frac{(\boldsymbol{r}-\boldsymbol{r}_p(t))^2}{2a^2}}\nabla\delta\rho_0(\boldsymbol{r},t), \tag{13}$$

$$\boldsymbol{F}^{(1)}(t) = -\frac{g_p^2}{2\pi a^2}\int d^2\boldsymbol{r}e^{-\frac{(\boldsymbol{r}-\boldsymbol{r}_p(t))^2}{2a^2}}\nabla\delta\rho_1(\boldsymbol{r},t). \tag{14}$$

The perturbative splitting of the force in these two contributions is completely analogous to the corresponding classical-fluid case in the incompressible [22] and in the compressible [34] situations. The $\boldsymbol{F}^{(0)}$ contribution is the equivalent to the classical inertial or pressure-gradient force on a test particle, which does not disturb the fluid, in a inhomogeneous and unsteady flow. We call this the *inertial* force. The $\boldsymbol{F}^{(1)}$ contribution takes into account perturbatively the modifications on the flow induced by the presence of the particle, and it is called the *self-induced drag* on the particle. To complete the comparison with the classical expressions [22, 34], we need to express Eqs. (13) and (14) in terms of the unperturbed velocity field $\boldsymbol{v}^{(0)}(\boldsymbol{r},t) = \delta\boldsymbol{v}^{(0)}(\boldsymbol{r},t)$ and of the particle speed $\boldsymbol{V}_p(t) = \dot{\boldsymbol{r}}_p(t)$. We are able to do so in a general situation for the inertial force $\boldsymbol{F}^{(0)}$. For $\boldsymbol{F}^{(1)}$, we obtain analytical expressions in the simple case where the impurity is moving with a constant velocity in an otherwise uniform BEC.

The desired relationships between $\nabla\delta\rho_0$ and $\nabla\delta\rho_1$ in Eqs. (13)-(14), and $\delta\boldsymbol{v}^{(0)}$ and $\boldsymbol{V}_p$ will be obtained from the linearization of the dGPE Eq. (5) around the uniform steady state $\psi_h = 1$:

$$\partial_t\delta\psi_0 = (i+\gamma)\left(\frac{1}{2}\nabla^2 - 1\right)\delta\psi_0 - (i+\gamma)\delta\psi_0^*, \tag{15}$$

$$\partial_t\delta\psi_1 = (i+\gamma)\left(\frac{1}{2}\nabla^2 - 1\right)\delta\psi_1 - (i+\gamma)\delta\psi_1^* - (i+\gamma)\mathcal{U}_p(\boldsymbol{r}-\boldsymbol{r}_p)\ . \tag{16}$$

Terms containing V_{ext} are not included in Eq. (15) because of our assumption of sufficient distance between possible stirring sources and the neighborhood of the particle position, the only region that–as we will see– will enter into the calculation of the forces.

In the next sections we solve these linearised equations to relate density perturbations to undisturbed velocity field and particle velocity.

3.1. Inertial force

To convert Eq. (13) for the inertial force into an expression suitable for comparison with the corresponding term in classical fluids, we need to express $\nabla\delta\rho_0$ in terms of the undisturbed velocity field $\boldsymbol{v}^{(0)}(\boldsymbol{r},t) = \delta\boldsymbol{v}^{(0)}(\boldsymbol{r},t)$. To this end, we substract Eq. (15) from its complex conjugate, obtaining:

$$\left(\nabla^2 - 4\right)\nabla\delta\rho_0 = 4\left(\partial_t - \frac{\gamma}{2}\nabla^2\right)\delta\boldsymbol{v}^{(0)}, \tag{17}$$

where we have used Eqs. (11) and (12). Since the force formulae require to obtain the condensate density in a neighbourhood of the particle position, it is convenient to move to frame co-moving with the particle. Thus we change variables from $(\boldsymbol{r},t)$ to $(\boldsymbol{z},t)$, with $\boldsymbol{z} = \boldsymbol{r} - \boldsymbol{r}_p(t)$, and the velocity field will be now referred to the particle velocity $\boldsymbol{V}_p(t) = \dot{\boldsymbol{r}}_p(t)$: $\delta\boldsymbol{w}^{(0)}(\boldsymbol{z},t) = \delta\boldsymbol{v}^{(0)}(\boldsymbol{r},t) - \boldsymbol{V}_p(t)$. Equation (17) becomes:

$$\begin{aligned}\left(\nabla_z^2 - 4\right)\ \nabla_z\delta\rho_0 = \\ 4\left(\partial_t - \boldsymbol{V}_p\cdot\nabla_z - \frac{\gamma}{2}\nabla_z^2\right)\delta\boldsymbol{w}^{(0)} + \dot{\boldsymbol{V}}_p(t),\end{aligned} \tag{18}$$

which has the corresponding equation for its Green's function given by

$$\left(\nabla_z^2 - 4\right)G(\boldsymbol{z}) = \delta(\boldsymbol{z}) \tag{19}$$

with the boundary condition $G(|\boldsymbol{z}|\to\infty)\to 0$ (corresponding to vanishing $\nabla_z\delta\rho_0(\boldsymbol{r})$ at $|\boldsymbol{r}| = \infty$). The solution is given by the zeroth order modified Bessel function $G(\boldsymbol{z}) = -K_0(2|\boldsymbol{z}|)/(2\pi)$. Hence, the gradient of the density perturbation can be written as the convolution with the Green's function:

$$\nabla_z\delta\rho_0(\boldsymbol{z},t) = -\frac{2}{\pi}\int d\boldsymbol{z}' K_0(2|\boldsymbol{z}-\boldsymbol{z}'|)\left[\left(\partial_t - \boldsymbol{V}_p\cdot\nabla_{\boldsymbol{z}'} - \frac{\gamma}{2}\nabla_{\boldsymbol{z}'}^2\right)\delta\boldsymbol{w}^{(0)}(\boldsymbol{z}',t) + \dot{\boldsymbol{V}}_p(t)\right], \tag{20}$$

and the expression for the force (13), using the comoving variables $(\boldsymbol{z},t)$, becomes:

$$\boldsymbol{F}^{(0)}(t) = -\frac{g_p}{\pi^2 a^2}\int d\boldsymbol{z} e^{-\frac{z^2}{2a^2}}\int d\boldsymbol{z}' K_0(2|\boldsymbol{z}-\boldsymbol{z}'|)\left[\left(\partial_t - \boldsymbol{V}_p\cdot\nabla_{\boldsymbol{z}'} - \frac{\gamma}{2}\nabla_{\boldsymbol{z}'}^2\right)\delta\boldsymbol{w}^{(0)}(\boldsymbol{z}',t) + \dot{\boldsymbol{V}}_p(t)\right]. \tag{21}$$

The above expression is a weighted average of contributions from properties of the fluid velocity in a neighborhood of the impurity center-of-mass position ($\boldsymbol{z} = 0$ in the comoving frame). The size of this neighborhood is given by the combination of the range of the Bessel function kernel, which in dimensional units would be the correlation length ξ, and the range of the Gaussian potential, a, giving an effective particle size. In classical fluids, the analogous force on a spherical particle involves the average of properties of the undisturbed velocity field within the sphere size [34], and there is no equivalent to the role of ξ.

As in the classical case [22, 34], if fluid velocity variations are weak at scales below a and ξ, we can approximate the condensate velocity by a Taylor expansion near the impurity, i.e.:

$$\delta w_i^{(0)}(\mathbf{z}',t) \approx \delta w_i^{(0)}(t) + \sum_j e_{ij}(t) z'_j + \frac{1}{2}\sum_{jk} e_{ijk}(t) z'_j z'_k + \ldots, \tag{22}$$

where the indices $i,j,k = x,y$ denote the coordinate components. $e_{ij}(t) = \partial_j \delta w_i^{(0)}(\mathbf{z},t)|_{\boldsymbol{z}=0}$ and $e_{ijk}(t) = \partial_j\partial_k \delta w_i^{(0)}(\mathbf{z},t)|_{\boldsymbol{z}=0}$ are gradients of the unperturbed condensate relative velocity. Inserting this expansion into Eq. (21), and performing the integrals of the Gaussian and of the Bessel function (using for example $\int K_0(2|\boldsymbol{z}|)d\boldsymbol{z} = \pi/2$ and $\int z_i z_j K_0(2|\boldsymbol{z}|)d\boldsymbol{z} = (\delta_{ij}/2)\int_0^\infty 2\pi z^3 K_0(2z)dz = \delta_{ij}\pi/4$), we obtain:

$$\boldsymbol{F}^{(0)}(t) \approx g_p \dot{\boldsymbol{V}}_p(t) + g_p \left[\partial_t - \boldsymbol{V}_p(t)\cdot\nabla_z + \frac{a^2}{2}\partial_t\nabla_z^2 - \frac{\gamma}{2}\nabla_z^2 + \frac{1}{4}\partial_t\nabla_z^2\right]\delta\boldsymbol{w}^{(0)}(\boldsymbol{z},t)|_{\boldsymbol{z}=\boldsymbol{0}}\ . \tag{23}$$

The terms containing Laplacians are analogous to the Faxén corrections in classical fluids [22] which arise for particles with finite size. Here, they arise from a combination of the finite effective size of the particle, a, and of the quantum coherence length, $\xi = 1$. This last effect remains even in the limit of vanishing particle size $a \to 0$. Interestingly, one of the two terms in these quantum corrections depend on γ hence indirectly on the presence of the thermal cloud.

As in the classical case, if flow inhomogeneities are unimportant below the scales a and ξ, we can neglect the Laplacian terms in Eq. (23). Returning to the variables $(\boldsymbol{r},t)$ in the lab frame of reference, the terms containing $\boldsymbol{V}_p$ cancel out, showing that the inertial force is mainly given by the local fluid acceleration:

$$\boldsymbol{F}^{(0)}(t) = g_p \partial_t \delta\boldsymbol{v}^{(0)}(\boldsymbol{r},t)\big|_{\boldsymbol{r}=\boldsymbol{r}_p(t)}. \tag{24}$$

We have assumed a small non-uniform unperturbed velocity field $\boldsymbol{v}^{(0)}(\boldsymbol{r},t) = \delta\boldsymbol{v}^{(0)}(\boldsymbol{r},t)$. To leading order in velocity, the partial derivative $\partial_t\delta\boldsymbol{v}^{(0)}$ and the material derivative $D\delta\boldsymbol{v}^{(0)}/Dt = \partial_t\delta\boldsymbol{v}^{(0)} + \delta\boldsymbol{v}^{(0)}\cdot\nabla\delta\boldsymbol{v}^{(0)}$ are identical. In classical fluids the same ambiguity occurs and it has been established, on physical grounds and by going beyond linearisation, that using the material derivative is more correct [22]. After all, using this material derivative in the equation of motion simply means that, under the above approximations and in places where stirring and other external forces are absent, the local acceleration on the impurity arises from the corresponding acceleration of the condensate. Since for $a \to 0$ the condensate-impurity interaction has a similar scattering potential (delta function) as that for the interaction between condensate particles, similar accelerations would be experienced by a condensate particle and by the impurity, just modulated by a different coupling constant. Thus, replacing ∂_t by D/Dt in (24) the approximate inertial force becomes:

$$\boldsymbol{F}^{(0)}(t) = g_p \left.\frac{D\boldsymbol{v}^{(0)}}{Dt}\right|_{\boldsymbol{r}=\boldsymbol{r}_p(t)}\ , \tag{25}$$

or, if we return back to dimensional variables:

$$\boldsymbol{F}^{(0)}(t) = \frac{g_p}{g} m \left. \frac{D\boldsymbol{v}^{(0)}}{Dt} \right|_{\boldsymbol{r}=\boldsymbol{r}_p(t)} . \tag{26}$$

This is equivalent to the equation for the inertial force in classical fluids [22] except that the coefficient of the material derivative in the classical case is the mass of the fluid fitting in the size of the impurity. In the comoving frame, replacement of the partial by the material derivative amounts to replace $(\partial_t - \boldsymbol{V}_p \cdot \nabla_{\boldsymbol{z}'})\delta\boldsymbol{w}^{(0)}$ in Eq. (21) by $D\delta\boldsymbol{w}^{(0)}/Dt$. Eq. (25) is expected to be valid for small values of g_p and in regions where fluid velocity and density inhomogeneities are both small and weakly varying. At this level of approximation neither compressibility nor dissipation effects appear explicitly in the inertial force, in analogy with classical compressible fluids [34]. But these effects are indirectly present by determining the structure of the field $\boldsymbol{v}^{(0)}(\boldsymbol{r}, t)$.

3.2. Self-induced drag force

The consideration of the self-induced force on a particle moving through a classical fluids leads to different terms, namely [22, 34] the viscous (Stokes) drag, the unsteady-inviscid term that in the incompressible case becomes the added-mass force, and the unsteady-viscous term that in the incompressible case becomes the Basset history force. They are expressed in terms of the undisturbed velocity flow $\boldsymbol{v}^{(0)}$ and the particle velocity $\boldsymbol{V}_p(t)$. Here, for the BEC case, we are able to obtain the self-induced force only for a particle moving at constant speed on the condensate. For the classical fluid case, in this situation the only non-vanishing force is the Stokes drag, so that this is the force we have to compare our result with. We note that the condensate itself in the absence of the particle perturbation can be in any state of (weak) motion since in our perturbative approach summarised in Eqs (15)-(16), the inhomogeneity $\delta\psi_0$ and the g_p-perturbation $\delta\psi_1$ are uncoupled.

It is convenient to transform the problem to the co-moving frame $(\boldsymbol{r}, t) \to (\boldsymbol{z}, t)$ with $\boldsymbol{z} = \boldsymbol{r} - \boldsymbol{r}_p(t)$, so that Eq. (16) becomes

$$\partial_t \delta\psi_1 - \boldsymbol{V}_p \cdot \nabla\delta\psi_1 = (i+\gamma)\left(\frac{1}{2}\nabla^2 - 1\right)\delta\psi_1 - (i+\gamma)\delta\psi_1^* - (i+\gamma)\mathcal{U}(\boldsymbol{r}) . \tag{27}$$

Note that such Galilean transformations of the GPE using a constant $\boldsymbol{V}_p$ are often accompanied by a multiplication of the transformed wavefunction by a phase factor $\exp(i\boldsymbol{V}_p \cdot \boldsymbol{z} + \frac{i}{2}V_p^2 t)$, in order to transform the condensate velocity (see below) to the new frame of reference, and account for the shift in kinetic energy. Indeed, such a combined transformation leaves the GPE unchanged at $\gamma = 0$ [35] (but not for $\gamma > 0$). The density perturbation $\delta\rho_1$ is already given correctly by $\delta\psi_1 + \delta\psi_1^*$, where $\delta\psi_1(\boldsymbol{z}, t)$ is the solution of (27), without the need of any additional phase factor. The velocity in the co-moving frame would need to be corrected as $\delta\omega^{(1)}(\boldsymbol{z}, t) = \delta\boldsymbol{v}^{(1)} - \boldsymbol{V}_p$, with $\delta v^{(1)}$ given by Eq. (12) in terms of the solution of Eq. (27).

Eq. (27) in the steady-state can be solved by using the Fourier transform $\delta\psi_1(\boldsymbol{z}) = 1/(2\pi)^2 \int d^2\boldsymbol{k} e^{i\boldsymbol{k}\cdot\boldsymbol{z}} \delta\hat{\psi}_1(\boldsymbol{k})$. It follows that the linear system of equations for $\delta\hat{\psi}_1(\boldsymbol{k})$ and $\delta\hat{\psi}_1^*(-\boldsymbol{k})$ is given by

$$\begin{aligned} \left[-2i\boldsymbol{k}\cdot\boldsymbol{V}_p + (i+\gamma)(k^2+2)\right] \quad \delta\hat{\psi}_1 + 2(i+\gamma)\delta\hat{\psi}_1^* &= -2(i+\gamma)e^{-\frac{a^2k^2}{2}}, \\ \left[-2i\boldsymbol{k}\cdot\boldsymbol{V}_p + (-i+\gamma)(k^2+2)\right] \delta\hat{\psi}_1^* + 2(-i+\gamma)\delta\hat{\psi}_1 &= -2(-i+\gamma)e^{-\frac{a^2k^2}{2}}. \end{aligned} \tag{28}$$

By solving these equations, we find $\delta\hat{\psi}_1(\boldsymbol{k})$ and $\delta\hat{\psi}_1^*(-\boldsymbol{k})$, and the Fourier transform of the density perturbation $\delta\rho_1 = \delta\psi_1^* + \delta\psi_1$ then follows as

$$\delta\hat{\rho}_1 = \frac{e^{-\frac{k^2a^2}{2}}(4k^2(1+\gamma^2) - 8i\gamma\boldsymbol{k}\cdot\boldsymbol{V}_p)}{4\boldsymbol{k}\cdot\boldsymbol{V}_p(\boldsymbol{V}_p\cdot\boldsymbol{k} + i\gamma k^2 + 2i\gamma) - k^2(4+k^2)(1+\gamma^2)}. \tag{29}$$

Using the convolution theorem, we can express the self-induced force (14) (in the co-moving frame, i.e. with $\mathbf{r}_p = 0$) in terms of $\delta\hat{\rho}_1$ as

$$\boldsymbol{F}^{(1)} = -\frac{g_p^2}{(2\pi)^2}\int d^2\boldsymbol{k} i\boldsymbol{k}\delta\hat{\rho}_1(\boldsymbol{k}) e^{-\frac{k^2a^2}{2}}. \tag{30}$$

This force can be decomposed into the normal and tangential components relative to the particle velocity $\boldsymbol{V}_p$: $\boldsymbol{F}^{(1)} = F_\parallel \boldsymbol{e}_\parallel + F_\perp \boldsymbol{e}_\perp$. Due to symmetry, the normal component vanishes upon polar integration, and we are left with the tangential, or drag, force

$$F_\parallel = -\frac{g_p^2}{(2\pi)^2}\int_0^\infty dk \int_0^{2\pi} d\theta e^{-k^2a^2} \frac{ik^2\cos(\theta)\left[4k^2(1+\gamma^2) - 8i\gamma k V_p\cos(\theta)\right]}{4kV_p\cos(\theta)(kV_p\cos(\theta) + i\gamma k^2 + 2i\gamma) - k^2(4+k^2)(1+\gamma^2)}. \tag{31}$$

V_p is the modulus of $\boldsymbol{V}_p$. At zero temperature, i.e. when $\gamma = 0$, the drag force reduces to the one that has also been calculated for a point particle in Refs. [3] and in [5] for a finite-a particle:

$$F_\parallel = -\frac{g_p^2}{\pi^2}\int_0^\infty dk \int_0^{2\pi} d\theta \frac{ik^2\cos\theta e^{-k^2a^2}}{4V_p^2\cos^2\theta - (4+k^2)}\ , \tag{32}$$

which is zero for particle speed smaller than the critical value given by the long-wavelength sound speed, $V_p < c = 1$. Above the critical speed, the integral has poles and acquires a non-zero value given by

$$F_\parallel = -\frac{g_p^2 k_{max}^2}{4V_p} e^{-\frac{a^2k_{max}^2}{2}} \left[I_0\left(\frac{a^2k_{max}^2}{2}\right) - I_1\left(\frac{a^2k_{max}^2}{2}\right)\right] \tag{33}$$

in terms of the modified Bessel functions of the first kind $I_n(x)$ and where $k_{max} = 2\sqrt{V_p^2 - 1}$. For vanishing a the dominant term is proportional to $(V_p^2 - 1)/V_p$ [3]. This drag is pertaining to energy dissipation by radiating sound waves in the condensate away from the impurity. We emphasise again that a is small enough such that emission of other excitations, such as vortex pairs, does not occur. It is important to note [3, 5]

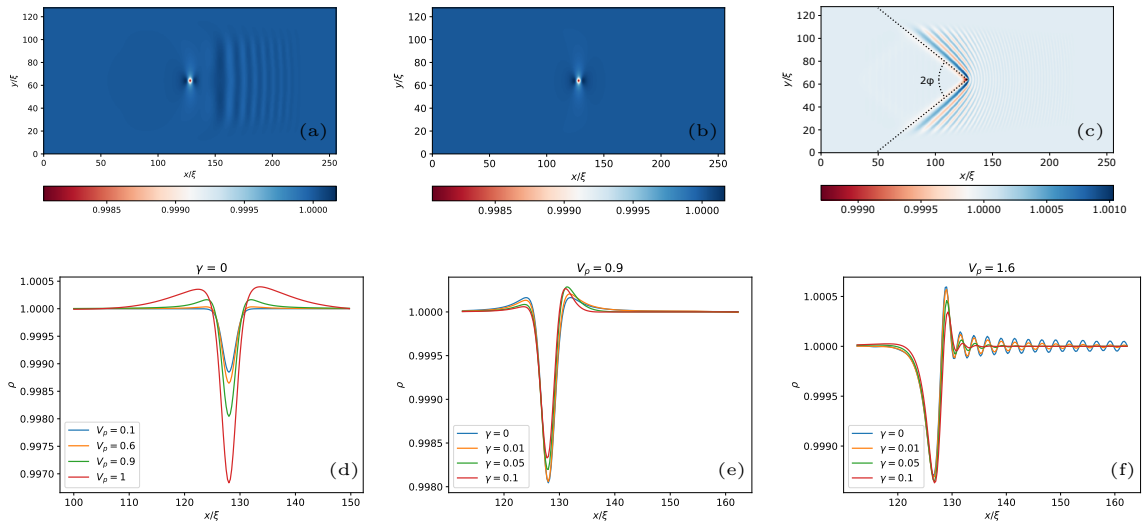

Figure 1. Panels (a)-(c) show 2D snapshots of the condensate density for $\gamma = 0$. The impurity is at $x/\xi = 128$ and $y/\xi = 64$. (a) is at $V_p = 0.9$ and at time $t = 200$, with transient waves still in the system. (b) is for the same $V_p = 0.9$ and at $t = 2000$, when the final steady state has been reached. Panel (c) is for $V_p = 1.6 > 1$, for which some waves remain attached to the impurity as front fringes and the Bogoliubov-Čerenkov wake with $\sin(\phi) = 1/V_p$. Panels (d-f) show cross-section profiles along the x direction of the steady-state condensate density around the impurity. Panel (d) shows the front-rear symmetry of the steady profiles when $V_p \leq 1$ and $\gamma = 0$. An asymmetry develops (panel (e)) for $\gamma > 0$, which relates to the net viscous-like drag. Panel (f) displays density profiles for $V_p = 1.6 > 1$ and different values of γ. The asymmetric density profile corresponds to waves trapped in front of the moving particle. With increasing γ, these waves are damped out.

that in order to obtain a real value for the force in Eq. (33) one has to consider that it has been obtained from the limit $\gamma \to 0^+$ in (31), which implies that an infinitesimal positive imaginary part needs to be considered in the denominator to properly deal with the poles in the integral.

In general, for a non-zero γ, Eq. (31) simplifies upon an expansion in powers of V_p to the leading order. For the linear term in V_p, we can perform the polar integration and arrive at

$$F_{\parallel} = -\frac{2}{\pi} V_p \frac{\gamma}{1+\gamma^2} g_p^2 \int \frac{k^3 e^{-a^2 k^2}}{(4+k^2)^2} dk \ . \tag{34}$$

Substituting $u = a^2(k^2+4)$, we find

$$F_{\parallel} = -V_p \frac{\gamma}{1+\gamma^2} g_p^2 \frac{1}{\pi} \left[e^{4a^2} E_1(4a^2)(1+4a^2) - 1 \right], \tag{35}$$

where $E_1(x)$ denotes the positive exponential integral. When $a \to 0$, the expression inside the bracket diverges as $-\gamma_E - 1 - \ln(4a^2)$ with γ_E begin the Euler-Mascheroni constant. It is therefore necessary to keep a finite size a.

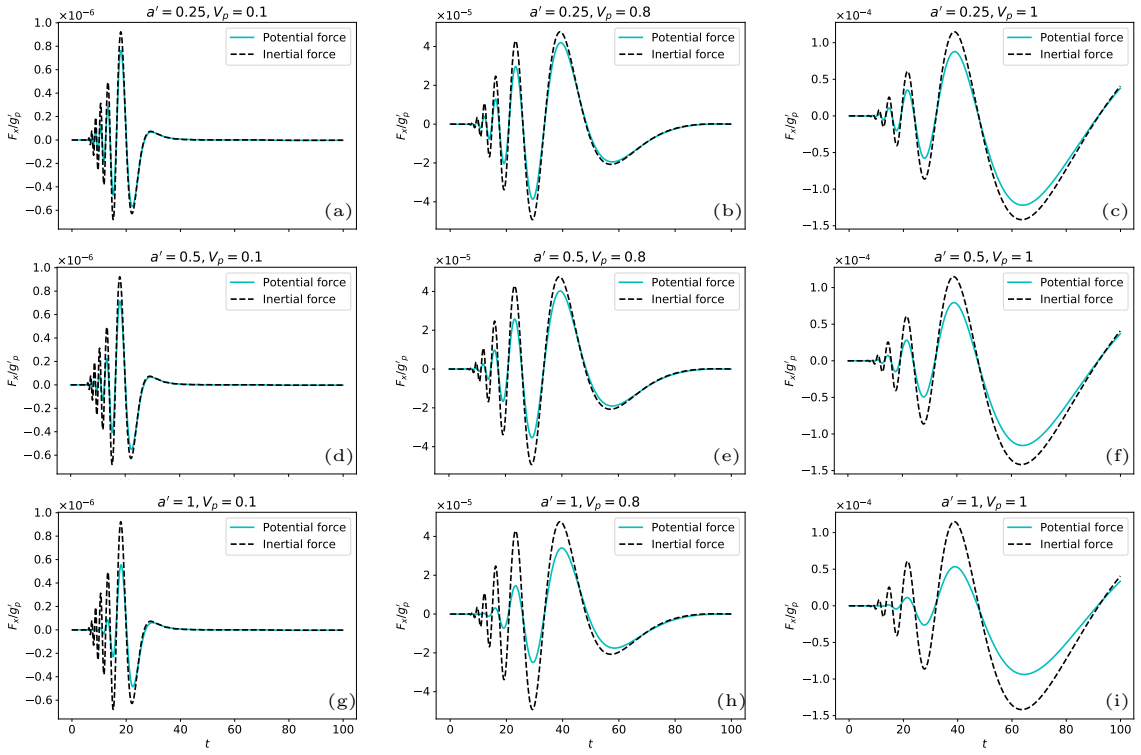

Figure 2. x component of the time-dependent force F_x/g'_p, using direct numerical simulations of the dGPE Eq. (36), on a test particle of size $a' = 0.25, 0.5, 1$ at a relative position $(\Delta x, \Delta y) = (10, 20)$ with respect to the position of the particle producing the flow perturbation. The speed of both particles is $V_p = 0.1, 0.8, 1$, and $\gamma = 0$. Cyan continuous lines correspond to the full force (x component) from the exact expression Eq. (6). They are labeled as 'potential force' because of the rather explicit appearance of the interaction potential in this formula. Black dotted lines are the predictions for the inertial force from the approximation Eq. (25) (computed in the comoving frame as explained in the text).

This drag force is akin to the viscous Stokes drag in classical fluids, but it is due to loss of energy in the condensate through its interaction with the thermal cloud. The effective drag coefficient depends on the thermal drag such that it vanishes at zero temperature. But it also depends non-trivially on the size of the impurity and it diverges in the limit of point-like particle. Faxén corrections involving derivatives of the unperturbed flow are not present here because of the decoupling between $\delta\psi_0$ and $\delta\psi_1$ arising in the perturbative approach leading to (15)-(16).

4. Numerical results

To test the analytical predictions of the inertial force and the self-induced drag deduced above from the total force expression Eq. (6), we performed numerical simulations of the dGPE. Actually, our simulations are done in the co-moving frame of the impurity moving at constant velocity $\boldsymbol{V}_p$, so that the equation we solve is (see numerical details

in the Appendix):

$$\partial_t\psi - \boldsymbol{V}_p\cdot\nabla\psi = (i+\gamma)\left[\frac{1}{2}\nabla^2\psi + \left(1 - g_p\mathcal{U}_p - |\psi|^2\right)\psi\right], \tag{36}$$

where the impurity is described by the Gaussian potential of intensity $g_p = 0.01$ and effective size $a = 1$ (in units of ξ), and is situated in the middle of the domain with the coordinates $(x, y) = (128, 64)$ (in units of ξ). As an initial condition, we start with the condensate being at rest and in equilibrium with the impurity. This is done by imaginary time integration of Eq. (36) for $V_p = 0$ and $\gamma = 0$. Then, at $t = 0$, we solve the full Eq. (36), and as a consequence, sound waves are emitted from the neighbourhood of the impurity. Their speed is determined by the dispersion relation $\omega(\boldsymbol{k})$ giving the frequency as a function of the wavenumber and can be obtained by looking for plane-wave solutions to Eq. (15). If $\gamma = 0$, $\omega(\boldsymbol{k})$ is given by the Bogoliubov dispersion relation [36] $\omega(\boldsymbol{k}) = k\sqrt{1 + k^2/4}$. Note that the smallest velocity, $c = 1$, is that of long wavelengths, and that waves of smaller wavelength travel faster. For $\gamma > 0$, the planar waves are dampened out and the dispersion relation becomes $\omega(\boldsymbol{k}) = -i\gamma(k^2/2 + 1) + \sqrt{k^2 + k^4/4 - \gamma^2}$. The damping rate is determined by γ and increases quadratically with the wavenumber. Also, in this case all waves have a group velocity faster than a minimum one that for small γ is close to $c = 1$.

When $V_p < 1$ all the waves escape the neighbourhood of the impurity (see an example in Fig. 1(a)) and are dissipated in a boundary buffer region that has large γ (see numerical details in the Appendix and Supplemental Material [37]). After a transient the condensate achieves a steady state. Fig. 1(b) shows a steady spatial configuration for $\gamma = 0$ and $V_p = 0.9$. Figs. 1(d-e) show different profiles of the condensate density along the x direction across the impurity position for V_p. The condensate density is depleted near the impurity due to the repulsive interaction, and its general shape depends on the speed V_p and thermal drag γ. If $\gamma = 0$ and $V_p \leq 1$ the density of this steady state has a rear-front symmetry with respect to the particle position (see specially Fig. 1(d)), so that under integration in Eq. (6) the net force is zero. The presence of dissipation ($\gamma > 0$) breaks this symmetry even if $V_p < 1$ so that a net drag will appear in agreement with the calculation of Sect. 3.2. When $V_p > 1$, there are waves that can not escape from the neighbourhood of the impurity, forming parabolic fringes in front of it and the Bogoliubov-Čerenkov wake behind it. (see Fig. 1(c) and 1(f) and Supplemental material [37]). The opening angle of the Čerenkov cone is determined by the dispersion relation of the waves with long-wavelength and satisfy the relation $\sin(\phi) = 1/V_p$ as shown in Fig. 1(c). It is clear that it narrows when the speed increases. The consequence is that there is a net drag induced by these fringes even when $\gamma = 0$, and that it would eventually decrease at very large velocity as the angle of the wake decreases. Similar gringes in the condensate density around an obstacle in supersonic flows has also been observed experimentally [38]. Movies showing the transient and long-time density behaviour for several values of V_p and at $\gamma = 0$ are included as Supplemental Material [37]. The fluid suddenly starts to move towards the negative x direction, and its density approaches a

steady state after the transient. Note that during all the dynamics, the density deviation with respect to the equilibrium value $\rho = 1$ is very small, justifying the perturbative approach of Sect. 3. The time evolution for $\gamma > 0$ is qualitatively similar to the $\gamma = 0$ shown in the movies, except that the waves become damped and that there is a front-rear asymmetry in the steady state.

Our numerical setup is well suited to measure the force produced by the perturbation of the impurity on the fluid, i.e. the self-induced drag. Nevertheless, in the absence of the impurity the unperturbed state is the trivial $\psi = 1$, so that $\delta\psi_0 = 0$ and the inertial force is identically zero. In order to test the accuracy of our expressions for the inertial force without the need of additional simulations under a different set-up, we still use the computed condensate density and velocity dynamics, produced by the impurity introduced in the system at $t = 0$, but we evaluate the inertial force exerted by this flow on another test particle located at a different position. In fact, there is no need to think on the flow as being produced by an impurity: it can be produced by a moving laser beam that can modelled by an external potential V_{ext} and the only impurity present in the system is the test particle on which the force is evaluated. In the following we evaluate the inertial and the self-induced drag forces on the different particles from the general expressions Eqs. (13)-(14) and from the approximate expressions of Sects. 3.1 and 3.2.

4.1. Numerical evaluation of the inertial force

We consider a test particle traveling at the same speed V_p as the impurity or laser beam producing the flow, but located at a distance of 10 coherence lengths in front of it, and 20 coherence lengths in the y direction apart from it. This distance is sufficient to avoid inclusion of $\mathcal{U}_p$ or V_{ext} in Eq. (15) for the neighborhood of the test particle. Condensate and test particle interact via a coupling constant g_p' sufficiently small so that the full force on the later, Eq. (6), is well approximated by the inertial part Eq. (13), being the perturbation the particle induces on the flow, and thus the force (14) completely negligible.

Figure (2) shows, for different values of $V_p = 0.1, 0.8, 1$ at $\gamma = 0$, the x component of the time-dependent force produced by the transient flow inhomogeneities hitting the test particle in the form of sound waves. The size of the test particle, taking several values, is called a' to distinguish it from the size a of the particle producing the flow perturbation. Blue lines are computed from the exact Eq. (6) or equivalently from Eq. (13) to which it reduces for sufficiently small g_p'. Because of the rather explicit appearance of the interaction potential in this formula, we label the blue lines in Fig. (2) as 'potential force'. High frequency waves arrive before low-frequency ones, because its larger sound speed. We also see how the frequencies become Doppler-shifted for increasing V_p. We have derived in Sect. 3.1 several approximate expressions for the inertial force. First, Eq. (21) is obtained with the sole assumption (besides g_p sufficiently small) of smallness of the unsteady and/or inhomogeneous part $\delta\psi_0$

of the wavefunction, which allows linearization. Eq. (23) assumes in addition weak inhomogeneities below scales a and ξ, and finally Eqs. (25) and (26) (equivalent under the previous linearization approximation) completely neglects such inhomogeneities (or equivalently, they correspond to $a, \xi \to 0$). We show as black lines in Fig. (2) the prediction of this last approximation, similar to the most standard classical expressions. Since we have computed the wavefunction $\psi = 1 + \delta\psi_0$ in the comoving frame from Eq. (36), we actually use expression (23) without the Faxén Laplacian terms, with $\delta\boldsymbol{\omega}^{(0)} = \nabla(\delta\psi_0 - \delta\psi_0^*)/(2i) - \boldsymbol{V}_p$, and $\dot{\boldsymbol{V}}_{\boldsymbol{p}} = 0$. Fig. (36) shows that the full force computed from Eq. (6) is well-captured by the approximate expression of the inertial force for small test-particle size a'. Accuracy progressively deteriorates for increasing a', and also for increasing V_p, but this classical expression remains a reasonable approximation until $a' \approx 1$. The accuracy can be improved by considering higher-order Faxén corrections, Eq. (23), or even better, by considering the integral form in Eq. (21). We have explicitly checked that keeping the full Gaussian integration in Eq. (21) but approximating the integrand in the Bessel integral by its value at the particle position gives a very good approximation to the exact force even for $a' = 1$.

4.2. Numerical evaluation of the drag force

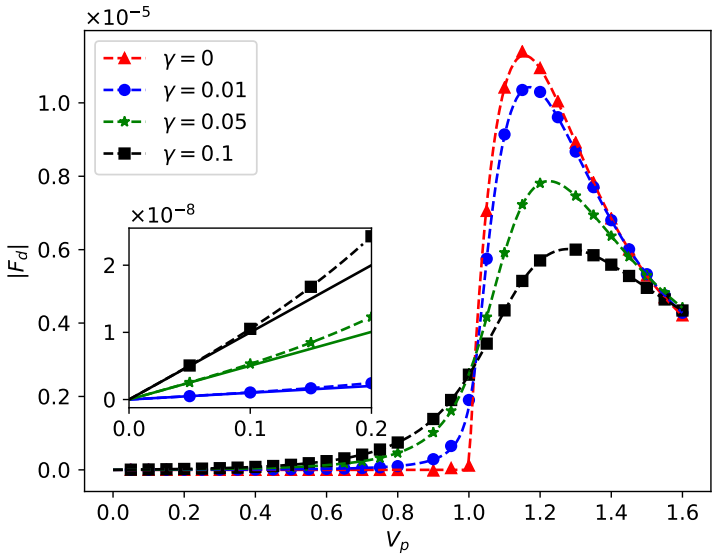

Figure 3. Self-induced drag in the steady-state regime as function of the speed V_p. Dashed lines are the analytical predictions based on Eq. (33) (for $\gamma = 0$) and Eq. (31) (for $\gamma > 0$). The symbols correspond to the numerically computed force from Eq. (6) based on direct simulations of the dGPE Eq. (36). The inset figure shows the small V_p behavior, with solid straight lines giving the linear dependence of the drag force on the speed for $\gamma > 0$, in the small-V_p approximation given by Eq. (35). We use $a = 1$ and $g_p = 0.01$.

We now return to the situation in which there is a single impurity in the system,

with size $a = \xi = 1$ and $g_p = 0.01$. It moves in the positive x direction with speed V_p producing a perturbation on the uniform and steady condensate state $\psi = 1$. We compute it in the comoving frame, in which the particle is at rest and fluid moves with speed $-V_p$, by using Eq. (36). Since in the absence of the impurity there is no inhomogeneity nor time dependence, $\delta\psi_0 = 0$ and the exact force on the impurity, Eq. (6), is also given by the self-induced drag expression given by Eq. (8). After a transient, that in analogy with the results for compressible classical fluids [39, 34] we expect to be of the order of the time needed by the sound waves to cross a region of size a or ξ, the condensate density near the particle achieves a steady state, and we then measure the steady drag on the particle. Fig. (3) shows this force, for several values of V_p and γ, as dots.

The approximate value of the drag force that is obtained under the assumption of small perturbation (small g_p) that allows linearisation is shown as dashed lines. It is computed from Eq. (33) for $\gamma = 0$ and Eq. (31) for $\gamma > 0$. The agreement is excellent. As shown in the inset figure, in the regime of small velocities, the self-induced drag is indeed linearly dependent on the speed with an effective drag coefficient that is well captured by Eq. (35). This Stokes-like drag at small speeds is due to energy dissipation through collisions between the condensate atoms and thermal atoms, quantified by the thermal drag γ. We notice that the dependence of the drag force on V_p is consistent with having a critical velocity for superfluidity even at $\gamma > 0$, in the sense that there is still a relatively abrupt change in the force (sharper for smaller γ) around a particular impurity speed. The superfluidity of BECs at finite temperature is still an open question. Recent experiments [40, 41] report superfluid below a critical velocity which is related to the onset of fringes [42]. In the dGPE, the steady state drag is always nonzero. Nonetheless, there is a critical velocity associated to the breakdown of superfluidity due to energy dissipation through acoustic excitations. This is the regime where the drag force is dominated by the interaction of the impurity with the supersonic shock waves to produce the Čerenkov wake as seen in Fig. 1(c) and observed experimentally [38]. The maximum drag force occurs near the velocity for which the cusp lines forming the wake still retain an angle close to π. With increasing speed, this angle becomes more acute (Fig. 1(f)), and this lowers the density gradient around the impurity.

5. Conclusions

We have studied, from analytic and numerical analysis of the dGPE, the hydrodynamic forces acting on a small moving impurity suspended in a 2D BEC at low temperature. In the regime of small coupling constant g_p and thermal drag γ, the force arising from the gradient of the condensate density can be decomposed onto the inertial force that is produced by the inhomogeneities and time-dependence of the condensate in the absence of the particle, and the self-induced force which is determined by the perturbation produced by the impurity on the condensate. When the unperturbed flow can be considered homogeneous on scales below the particle size and the condensate coherence

length, the classical Maxey and Riley expression [22], giving the inertial force in terms of the local or material fluid acceleration, is a good description of the force. When inhomogeneities become relevant below these scales, Faxén-type corrections arise, similar to the classical ones in the presence of a finite-size particle, but here the coherence length plays a role similar to the particle size. In addition, the condensate thermal drag enters into these expressions, at difference with the classical viscous case. We also determined the self-induced force in the steady-state regime and shown that it is non-zero at any velocity V_p of the moving impurity if $\gamma > 0$. For small V_p, this force is given as a Stokes drag which is linearly proportional to V_p with a drag coefficient dependent on the thermal drag γ. The energy dissipation associated with this drag is due to the loss of condensate atoms into the thermal cloud and is mediated by the thermal drag coefficient. In this sense, the drag on the impurity relates to the way the condensate dissipates energy at low temperature through particle exchanges with the thermal cloud. We have not considered the additional drag arising from direct interactions of impurity with the thermal cloud, since these are negligible in the low-temperature regime but maybe important at higher temperature. With increasing velocities, there are corrections to the linear drag and above a critical speed $V_c = 1$, the self-induced drag is dominated by the interactions of the impurity with the emitted shock waves.

We have checked our analytical expressions with numerical simulations in the situation in which the impurity moves at constant velocity, possibly driven by external forces different from the hydrodynamic ones analysed here. When the coupling constant g_p is sufficiently small so that only the inertial force is relevant, the equation of motion of the impurity under the sole action of the inertial force would be $m_p d\boldsymbol{V}_p(t)/dt = \boldsymbol{F}^{(0)}(t)$, with m_p the mass of the particle and $\boldsymbol{F}^{(0)}(t)$ one of the suitable approximations to the inertial force given in Sect. 3.1. For larger g_p, when the condensate becomes distorted by the impurity, we have computed the self-induced drag only in the steady case. In analogy with classical compressible flows [39, 34], we expect history-dependent forces in this unsteady situation. The dependence on the thermal drag, however, would be quite different from that of viscous classical fluids, because of the lack of viscous boundary layers in the BEC case.

In this study, we have focused on a small impurity that can only shed acoustic waves. Another interesting extension of this would be to further investigate the drag and inertial forces for larger impurity sizes, which can emit vortices, and study the effect of vortex-impurity interactions on the hydrodynamics forces. Following the recent experimental progress on testing the superfluidity in BEC at finite temperature [21], it would be interesting to test experimentally our prediction of the linear drag on the impurity due to the condensate thermal drag at small velocities by using measurements of the local heating rate. For probing the inertial force, it would be interesting to experimentally tracking the position of the impurity during non-steady superfluid flow.

Acknowledgments

We are thankful to Vidar Skogvoll, Kristian Olsen, Zakarias Laberg Hejlesen and Per Arne Rikvold for stimulating discussions. This work was partly supported by the Research Council of Norway through its centers of Excellence funding scheme, Project No. 262644, and by Spanish MINECO/AEI/FEDER through the María de Maeztu Program for Units of Excellence in R&D (MDM- 2017-0711).

Appendix: Numerical integration of dGPE

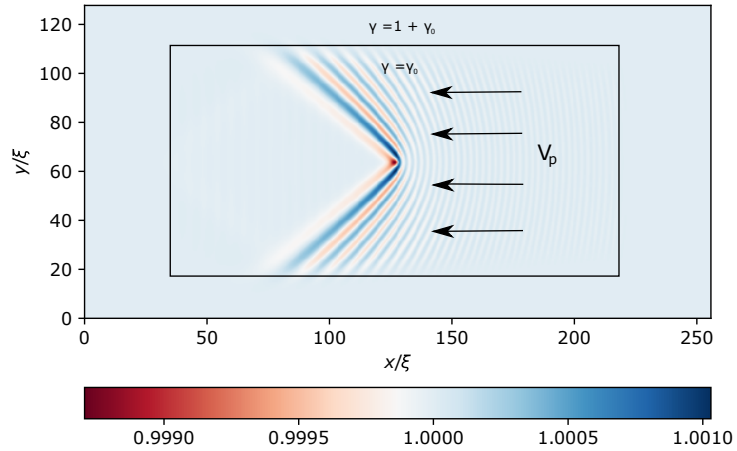

Figure 4. Simulation domain showing the buffer region, outside the main simulation region, in which thermal drag is greatly enhanced to eliminate the emitted waves sufficiently far from the moving particle (which is at $x/\xi = 128$, $y/\xi = 64$). The density shown is the steady state (in the comoving frame, hence the direction of the arrows indicating the flow velocity in this frame) for $V_p = 1.6$ and $\gamma = 0$.

Numerical simulations of dGPE Eq. (36) are run for a system size of 128×256 (in units of ξ) corresponding to the grid size $dx = 0.25\xi$, and $dt = 0.01\xi/c$. To simulate an infinite domain where the density variations emitted by the impurity do not recirculate under periodic boundary conditions, we use the fringe method from [33]. This means that we define buffer (fringe) regions around the outer rim of the computational domain (see Fig. 4) where the thermal drag γ is much larger than its value inside the domain, such that any density perturbation far from the impurity is quickly damped out and a steady inflow is maintained. The thermal drag becomes thus spatially-dependent and given by $\gamma(\boldsymbol{r}) = \max[\gamma(x), \gamma(y)]$, where

$$\gamma(x) = \frac{1}{2}\big(2 + \tanh\left[(x - x_p - w_x)/d\right] - \tanh\left[(x - x_p + w_x)/d\right]\big) + \gamma_0, \tag{37}$$

and similarly for $\gamma(y)$. Here $\boldsymbol{r}_p = (x_p, y_p) = (128\xi, 64\xi)$ is the position of the impurity and γ_0 is the constant thermal drag inside the buffer regions (bulk region). We set the fringe domain as $w_x = 100\xi$, $w_y = 50\xi$ and $d = 7\xi$ as illustrated in Figure 4.

By separating the linear and non-linear terms in Eq. (36), we can write the dGPE formally as [43]

$$\partial_t \psi = \hat{\omega}(-i\nabla)\psi + N(\boldsymbol{r}, t), \tag{38}$$

where $\hat{\omega}(-i\nabla) = i[\frac{1}{2}\nabla^2 + 1] + \boldsymbol{V}_p \cdot \nabla$ is the linear differential operator and $N(\boldsymbol{r}, t) = -(i+\gamma)(\mathcal{U}_p + |\psi|^2)\psi + \gamma\psi + \frac{1}{2}\gamma\nabla^2\psi$ is the nonlinear function including the spatially-dependent γ and $\mathcal{U}_p$. Taking the Fourier transform, we obtain ordinary differential equations for Fourier coefficients $\psi(\boldsymbol{k}, t)$ as

$$\partial_t \hat{\psi}(\boldsymbol{k}, t) = \hat{\omega}(\boldsymbol{k})\hat{\psi}(\boldsymbol{k}, t) + \hat{N}(\boldsymbol{k}, t), \tag{39}$$

which can be solved by an operator-splitting and exponential-time differentiating method [44]. It means that we exploit the fact that the linear part of Eq. (39) can be solved exactly by multiplying with the integrating factor $e^{-\hat{\omega}(\boldsymbol{k})t}$. This leads to

$$\partial_t \left(\hat{\psi}(\boldsymbol{k}, t) e^{-\hat{\omega}(\boldsymbol{k})t} \right) = e^{-\hat{\omega}(\boldsymbol{k})t} \hat{N}(\boldsymbol{k}, t). \tag{40}$$

The nonlinear term $\hat{N}(\boldsymbol{k}, t)$ is linearly approximated in time for a small time-interval $(t, t + \Delta t)$, i.e

$$\hat{N}(\boldsymbol{k}, t + \tau) = N_0 + \frac{N_1}{\Delta t}\tau \tag{41}$$

where $N_0 = \hat{N}(t)$ and $N_1 = \hat{N}(t + \Delta t) - N_0$. Inserting this into Eq. (40) and integrating from t to $t + \Delta t$ we get

$$\begin{aligned} \hat{\psi}(\boldsymbol{k}, t + \Delta t) &= \hat{\psi}(\boldsymbol{k}, t) e^{\hat{\omega}(\boldsymbol{k})\Delta t} + \frac{N_0}{\hat{\omega}(\boldsymbol{k})} \left(e^{\hat{\omega}(\boldsymbol{k})\Delta t} - 1 \right) \\ &+ \frac{N_1}{\hat{\omega}(\boldsymbol{k})} \left[\frac{1}{\hat{\omega}(\boldsymbol{k})\Delta t} (e^{\hat{\omega}(\boldsymbol{k})\Delta t} - 1) - 1 \right]. \end{aligned} \tag{42}$$

Since computing the value of N_1 requires knowledge of the state at $t + \Delta t$ before we have computed it, we start by setting it to zero and find a value for the state at $t + \Delta t$ given that $\hat{N}(t)$ is constant in the interval. We then use this state to calculate N_1, and add corrections to the value we got when assuming $N_1 = 0$.

References

[1] Winiecki T and Adams C S 2000 *EPL (Europhysics Letters)* **52** 257
[2] Wouters M and Carusotto I 2010 *Physical Review Letters* **105** 020602
[3] Astrakharchik G E and Pitaevskii L P 2004 *Physical Review A* **70** 013608
[4] Shukla V, Brachet M and Pandit R 2016 *Physical Review A* **94** 041602
[5] Pinsker F 2017 *Physica B: Condensed Matter* **521** 36–42
[6] Poole D R, Barenghi C F, Sergeev Y A and Vinen W F 2005 *Physical Review B* **71** 064514
[7] Chikkatur A P, Görlitz A, Stamper-Kurn D M, Inouye S, Gupta S and Ketterle W 2000 *Physical Review Letters* **85** 483

[8] Zipkes C, Palzer S, Sias C and Köhl M 2010 *Nature* **464** 388

[9] Balewski J B, Krupp A T, Gaj A, Peter D, Büchler H P, Löw R, Hofferberth S and Pfau T 2013 *Nature* **502** 664

[10] Jørgensen N B, Wacker L, Skalmstang K T, Parish M M, Levinsen J, Christensen R S, Bruun G M and Arlt J J 2016 *Physical Review Letters* **117** 055302

[11] Pham C T, Nore C and Brachet M E 2005 *Physica D: Nonlinear Phenomena* **210** 203 – 226" ISSN 0167-2789 URL http://www.sciencedirect.com/science/article/pii/S0167278905003167

[12] Berloff N G and Roberts P H 2000 *Phys. Rev. B* **63**(2) 024510 URL https://link.aps.org/doi/10.1103/PhysRevB.63.024510

[13] Griffin A, Stagg G W, Proukakis N P and Barenghi C F 2017 *Journal of Physics B: Atomic, Molecular and Optical Physics* **50** 115003

[14] Shukla V, Pandit R and Brachet M 2018 *Phys. Rev. A* **97**(1) 013627 URL https://link.aps.org/doi/10.1103/PhysRevA.97.013627

[15] Giuriato U and Krstulovic G 2019 *Scientific Reports* **9** 4839

[16] Roberts D C 2006 *Physical Review A* **74** 013613

[17] Roberts D C and Pomeau Y 2005 *Physical Review Letters* **95** 145303

[18] Pomeau Y and Roberts D C 2008 *Physical Review B* **77** 144508

[19] Sykes A G, Davis M J and Roberts D C 2009 *Physical Review Letters* **103** 085302

[20] Pinsker F 2017 *New Journal of Physics* **19** 113046

[21] Singh V P, Weimer W, Morgener K, Siegl J, Hueck K, Luick N, Moritz H and Mathey L 2016 *Physical Review A* **93** 023634

[22] Maxey M R and Riley J J 1983 *The Physics of Fluids* **26** 883–889

[23] Gardiner C W, Anglin J R and Fudge T I A 2002 *Journal of Physics B: Atomic, Molecular and Optical Physics* **35** 1555

[24] Rooney S J, Blakie P B and Bradley A S 2012 *Physical Review A* **86** 053634

[25] Penckwitt A A, Ballagh R J and Gardiner C W 2002 *Physical Review Letters* **89** 260402

[26] Bradley A S and Anderson B P 2012 *Physical Review X* **2** 041001

[27] Reeves M T, Billam T P, Anderson B P and Bradley A S 2013 *Physical Review Letters* **110** 104501

[28] Reeves M T, Billam T P, Anderson B P and Bradley A S 2014 *Physical Review A* **89** 053631

[29] Skaugen A and Angheluta L 2016 *Physical Review E* **93** 032106

[30] Bradley A S, Gardiner C W and Davis M J 2008 *Physical Review A* **77** 033616

[31] Billam T P, Reeves M T and Bradley A S 2015 *Physical Review A* **91** 023615

[32] Neely T W, Bradley A S, Samson E C, Rooney S J, Wright E M, Law K J H, Carretero-González R, Kevrekidis P G, Davis M J and Anderson B P 2013 *Physical Review Letters* **111** 235301

[33] Reeves M T, Billam T P, Anderson B P and Bradley A S 2015 *Physical Review Letters* **114** 155302

[34] Parmar M, Haselbacher A and Balachandar S 2012 *Journal of Fluid Mechanics* **699** 352–375

[35] Pismen L M 1999 *Vortices in nonlinear fields: From liquid crystals to superfluids, from non-equilibrium patterns to cosmic strings* vol 100 (Oxford University Press)

[36] Dalfovo F, Giorgini S, Pitaevskii L P and Stringari S 1999 *Rev. Mod. Phys.* **71**(3) 463–512 URL https://link.aps.org/doi/10.1103/RevModPhys.71.463

[37] See Supplemental Material at [URL] showing movies of the condensate density dynamics at $\gamma = 0$ and several values of V_p.

[38] Carusotto I, Hu S X, Collins L A and Smerzi A 2006 *Physical Review Letters* **97** 260403

[39] Longhorn A L 1952 *The Quarterly Journal of Mechanics and Applied Mathematics* **5** 64–81 ISSN 0033-5614

[40] Singh V P, Weimer W, Morgener K, Siegl J, Hueck K, Luick N, Moritz H and Mathey L 2016 *Phys. Rev. A* **93**(2) 023634 URL https://link.aps.org/doi/10.1103/PhysRevA.93.023634

[41] Weimer W, Morgener K, Singh V P, Siegl J, Hueck K, Luick N, Mathey L and Moritz H 2015 *Physical Review Letters* **114**(9) 095301 URL https://link.aps.org/doi/10.1103/PhysRevLett.114.095301

[42] Wouters M and Carusotto I 2010 *Physical Review Letters* **105**(2) 020602 URL

https://link.aps.org/doi/10.1103/PhysRevLett.105.020602

[43] Skaugen A 2018 *A unified perspective on two-dimensional quantum turbulence and plasticity* Ph.D. thesis University of Oslo

[44] Cox S M and Matthews P C 2002 *Journal of Computational Physics* **176** 430–455

Bibliography

[1] L.D Landau and E.M Lifshitz. *Fluid Mechanics*. Elsevier Ltd, Oxford, 2 edition, 2009.

[2] Frank M. White. *Fluid Mechanics*. McGraw-Hill Education, New York, 8 edition, 2016.

[3] I. M Khalatnikov. *Theory of Superfluidity (Frontiers in Physics)*. W. A. Benjamin, New York, 1965.

[4] Mike H Anderson, Jason R Ensher, Michael R Matthews, Carl E Wieman, and Eric A Cornell. Observation of bose-einstein condensation in a dilute atomic vapor. *science*, pages 198–201, 1995.

[5] Kendall B Davis, M-O Mewes, Michael R Andrews, Nicolaas J van Druten, Dallin S Durfee, DM Kurn, and Wolfgang Ketterle. Bose-einstein condensation in a gas of sodium atoms. *Physical review letters*, 75(22):3969, 1995.

[6] Iacopo Carusotto and Cristiano Ciuti. Quantum fluids of light. *Reviews of Modern Physics*, 85(1):299, 2013.

[7] Andrey Sokolov and Igor S Aranson. Reduction of viscosity in suspension of swimming bacteria. *Physical Review Letters*, 103(14):148101, 2009.

[8] Héctor Matías López, Jérémie Gachelin, Carine Douarche, Harold Auradou, and Eric Clément. Turning bacteria suspensions into superfluids. *Physical review letters*, 115(2):028301, 2015.

[9] David C Roberts. When superfluids are a drag. *Contemporary Physics*, 50(3):453–461, 2009.

[10] Pyotr Kapitza. Viscosity of liquid helium below the λ-point. *Nature*, 141(3558):74–74, 1938.

[11] James F. Annett. *Superconductivity, Superfluids and Condensates (Oxford Master Series in Condensed Matter Physics)*. Oxford University Press, Oxford, 2004.

[12] James P. Sethna. *Statistical Mechanics: Entropy, Order Parameters and Complexity (Oxford Master Series In Statistical, Computational, and Theoretical Physics)*. Oxford University Press, Oxford, 2012.

[13] Franco Dalfovo, Stefano Giorgini, Lev P Pitaevskii, and Sandro Stringari. Theory of bose-einstein condensation in trapped gases. *Reviews of Modern Physics*, 71(3):463, 1999.

[14] Eugene P Gross. Structure of a quantized vortex in boson systems. *Il Nuovo Cimento (1955-1965)*, 20(3):454–477, 1961.

[15] Lev P Pitaevskii. Vortex lines in an imperfect bose gas. *Sov. Phys. JETP*, 13(2):451–454, 1961.

[16] SJ Rooney, PB Blakie, and AS Bradley. Stochastic projected gross-pitaevskii equation. *Physical Review A*, 86(5):053634, 2012.

[17] Ashton S Bradley and Brian P Anderson. Energy spectra of vortex distributions in two-dimensional quantum turbulence. *Physical Review X*, 2(4):041001, 2012.

[18] CW Gardiner and MJ Davis. The stochastic gross–pitaevskii equation: Ii. *Journal of Physics B: Atomic, Molecular and Optical Physics*, 36(23):4731, 2003.

[19] Alberto Amo, Jérôme Lefrère, Simon Pigeon, Claire Adrados, Cristiano Ciuti, Iacopo Carusotto, Romuald Houdré, Elisabeth Giacobino, and Alberto Bramati. Superfluidity of polaritons in semiconductor microcavities. *Nature Physics*, 5(11):805, 2009.

[20] Wolf Weimer, Kai Morgener, Vijay Pal Singh, Jonas Siegl, Klaus Hueck, Niclas Luick, Ludwig Mathey, and Henning Moritz. Critical velocity in the bec-bcs crossover. *Physical review letters*, 114(9):095301, 2015.

[21] Christoph Zipkes, Stefan Palzer, Carlo Sias, and Michael Köhl. A trapped single ion inside a bose–einstein condensate. *Nature*, 464(7287):388–391, 2010.

[22] AP Chikkatur, A Görlitz, DM Stamper-Kurn, S Inouye, S Gupta, and W Ketterle. Suppression and enhancement of impurity scattering in a bose-einstein condensate. *Physical review letters*, 85(3):483, 2000.

[23] Jonathan B Balewski, Alexander T Krupp, Anita Gaj, David Peter, Hans Peter Büchler, Robert Löw, Sebastian Hofferberth, and Tilman Pfau. Coupling a single electron to a bose–einstein condensate. *Nature*, 502(7473):664–667, 2013.

[24] Chi-Tuong Pham, Caroline Nore, and Marc-Étienne Brachet. Boundary layers and emitted excitations in nonlinear Schrödinger superflow past a disk. *Physica D: Nonlinear Phenomena*, 210(3):203 – 226", 2005.

[25] GE Astrakharchik and LP Pitaevskii. Motion of a heavy impurity through a bose-einstein condensate. *Physical Review A*, 70(1):013608, 2004.

[26] Florian Pinsker. Gaussian impurity moving through a bose-einstein superfluid. *Physica B: Condensed Matter*, 521:36–42, 2017.

[27] Florian Pinsker. Beyond superfluidity in non-equilibrium bose–einstein condensates. *New Journal of Physics*, 19(11):113046, 2017.

[28] A Griffin, GW Stagg, NP Proukakis, and CF Barenghi. Vortex scattering by impurities in a bose–einstein condensate. *Journal of Physics B: Atomic, Molecular and Optical Physics*, 50(11):115003, 2017.

[29] Vishwanath Shukla, Rahul Pandit, and Marc Brachet. Particles and fields in superfluids: Insights from the two-dimensional gross-pitaevskii equation. *Physical Review A*, 97(1):013627, 2018.

[30] G Kälbermann. Ehrenfest theorem, galilean invariance and nonlinear schrödinger equations. *Journal of Physics A: Mathematical and General*, 37(8):2999, 2004.

[31] Andrew G Sykes, Matthew J Davis, and David C Roberts. Drag force on an impurity below the superfluid critical velocity in a quasi-one-dimensional bose-einstein condensate. *Physical review letters*, 103(8):085302, 2009.

[32] Jonas Rønning, Audun Skaugen, Emilio Hernández-García, Cristóbal López, and Luiza Angheluta. Classical analogies for the force acting on an impurity in a bose-einstein condensate. *arXiv preprint arXiv:2002.05003*, 2020.

[33] Jens O. Andersen. *Introduction to Statistical Mechanics*. Fagbokforlaget Vigmostad & Bjørke As, Bergen, 2017.

[34] Eric Cornell. Very cold indeed: The nanokelvin physics of bose-einstein condensation. *Journal of research of the National Institute of Standards and Technology*, 101(4):419, 1996.

[35] D.S. Petrov, Markus Holzmann, and G.V. Shlyapnikov. Bose-einstein condensation in quasi-2d trapped gases. *Physical Review Letters*, 84(12):2551, 2000.

[36] Nikolay Prokof'ev, Oliver Ruebenacker, and Boris Svistunov. Critical point of a weakly interacting two-dimensional bose gas. *Physical review letters*, 87(27):270402, 2001.

[37] Yu Kagan, BV Svistunov, and GV Shlyapnikov. Influence on inelastic processes of the phase transition in a weakly collisional two-dimensional bose gas. *Sov. Phys. JETP*, 66(2):314, 1987.

[38] John Michael Kosterlitz and David James Thouless. Ordering, metastability and phase transitions in two-dimensional systems. *Journal of Physics C: Solid State Physics*, 6(7):1181, 1973.

[39] Nick P. Proukakis, David W. Snoke, and Peter B. Littlewood. *Universal themes of Bose-Einstein condensation*. Cambridge University Press, Cambridge, 2017.

[40] Panayotis G Kevrekidis, Dimitri J Frantzeskakis, and Ricardo Carretero-González. *Emergent nonlinear phenomena in Bose-Einstein condensates: theory and experiment*, volume 45. Springer Science & Business Media, 2007.

[41] Audun Skaugen. *A unified perspective on two-dimensional quantum turbulence and plasticity*. PhD thesis, University of Oslo, August 2018.

[42] L.M. Pismen. *Vortices in Nonlinear Fields: From Liquid Crystals to Superfluids, From Non-Equilibrium Patterns to Cosmic Strings*. Oxford university press, Oxford, 1999.

[43] Martin R Maxey and James J Riley. Equation of motion for a small rigid sphere in a nonuniform flow. *The Physics of Fluids*, 26(4):883–889, 1983.

[44] M. Parmar, A. Haselbacher, and S. Balachandar. Equation of motion for a sphere in non-uniform compressible flows. *Journal of Fluid Mechanics*, 699:352–375, 2012.

[45] FB Tatom. The basset term as a semiderivative. *Applied Scientific Research*, 45(3):283–285, 1988.

[46] Armando Babiano, Julyan HE Cartwright, Oreste Piro, and Antonello Provenzale. Dynamics of a small neutrally buoyant sphere in a fluid and targeting in hamiltonian systems. *Physical Review Letters*, 84(25):5764, 2000.

[47] Pedro Monroy, Emilio Hernández-García, Vincent Rossi, and Cristóbal López. Modeling the dynamical sinking of biogenic particles in oceanic flow. *arXiv preprint arXiv:1612.04592*, 2016.

[48] J Peng and JO Dabiri. Transport of inertial particles by lagrangian coherent structures: application to predator–prey interaction in jellyfish feeding. *Journal of Fluid Mechanics*, 623:75–84, 2009.

[49] P.C. Hemmer. *Kvantemekanikk*. Fagbokforlaget Vigmostad & Bjørke As, Bergen, 5 edition, 2015.

[50] Erwin Kreyszig. *Advanced Engineering Mathematics (International Student Version)*. John Wiley & Sons, inc, Hoboken, 10 edition, 2011.

[51] Vijay Pal Singh, Wolf Weimer, Kai Morgener, Jonas Siegl, Klaus Hueck, Niclas Luick, Henning Moritz, and Ludwig Mathey. Probing superfluidity of bose-einstein condensates via laser stirring. *Physical Review A*, 93(2):023634, 2016.

[52] Iacopo Carusotto and Germain Rousseaux. The cerenkov effect revisited: from swimming ducks to zero modes in gravitational analogues. In *Analogue Gravity Phenomenology*, pages 109–144. Springer, 2013.

[53] CM Linton. The green's function for the two-dimensional helmholtz equation in periodic domains. *Journal of Engineering Mathematics*, 33(4):377–401, 1998.

[54] Karl Rottmann. *Matematisk Formelsamling*. Oslo, 2015.

[55] Steven M Cox and Paul C Matthews. Exponential time differencing for stiff systems. *Journal of Computational Physics*, 176(2):430–455, 2002.

[56] MT Reeves, TP Billam, Brian P Anderson, and AS Bradley. Identifying a superfluid reynolds number via dynamical similarity. *Physical review letters*, 114(15):155302, 2015.